Fall 2019

McNair Scholars Research Journal Volume XII

St. Mary's University

ST. MARY'S UNIVERSITY

One Camino Santa Maria
San Antonio, Texas 78228

www.stmarytx.edu

A Catholic and Marianist Liberal Arts Institution

The St. Mary's University
McNair Scholars Program

RESEARCH JOURNAL

Fall 2019 Volume XII

The St. Mary's University
McNair Scholars Program

RESEARCH JOURNAL

Fall 2019 Volume XII

What a long, strange summer it has been!

This summer, twenty-three McNair scholars representing the College of Arts, Humanities, and Social Sciences; the Greehey School of Business; and the School of Science, Engineering, and Technology at St. Mary's University forged a new path by completing our first-ever virtual research experience. More than any previous McNair cohort, these scholars gained important new skills as they mastered not only their individual research topics, but also a wealth of new technologies. During a typical summer, scholars are secluded together on campus, living in a community and supporting one another in frequent daily interactions in seminars and laboratories. This summer, scholars were living off campus at locations across the state, country, and internationally. The person in the next room was not another scholar, struggling with the same time constraints and tasks, but a parent, roommate, sibling, or grandparent who may not have understood what the scholars were trying to accomplish. Despite the challenges and distractions, these scholars excelled, proving themselves intelligent, motivated, creative, and resilient. Although we can hope we will never find ourselves forced into a summer like this again, the lessons and triumphs of this experience will serve our scholars well in the coming years as they confront life's unexpected challenges.

Please enjoy these fruits of a very productive, albeit very unusual, McNair Scholars Summer Research Experience.

Jennifer Zwahr-Castro, PhD
Director, McNair Scholars Program
St. Mary's University
San Antonio, Texas

TABLE OF CONTENTS

STMU-MSRJ

Academic Achievement in STEM: What Factors Influence Student Success?

Aleacia Messiah

Mentors: Mary Wagner-Krankel, Ph.D. & Anna Lurie, Ph.D.
St. Mary's University, San Antonio, TX

College is an extremely imperative transition in life, and the push for outstanding grades can seem daunting to some individuals. Nonetheless, almost everyone goes through this challenge, and it's up to us to put in the effort to achieve our desired grade in a class. The most difficult part is figuring out if we are on the right pathway to success. If there is an infallible method that can be used to determine a student's final course average, we could answer that question. This study analyzes aspects linked to success such as quizzes, midterm tests, and attendance using similar theories and techniques as previous studies. R Commander, a statistical software, is utilized to create multiple regression models and scatterplots of the first test, number of absences, and midterm grade versus final average to determine which factors or combination of factors are the most effective in predicting a student's final average. A normal probability plot and residual plot are produced to check the final regression model for any errors. It is recognized that all of these features have an influence on course grades, but midterm average and number of absences together predict final averages most accurately. Since these factors are controllable by the student, this may aid him or her in increasing the likelihood of succeeding in a college class. Additionally, this can help the professor or instructor know in advance how well a student will perform and target any weaknesses early in the course.

Key Words*: success, academic achievement, students, college, influencing factors*

1. Introduction

Millions of students attend college every year. Commuting to class, organizing study groups, and preparing for exams are a few of the activities undergraduates may do. Many of them worry about their final course grades, but is there a way to know a student's final average in a class while taking the class? Can we predict final course grades?

The primary purpose of this research study is to analyze the sources found in assessing academic achievement at a collegiate level, dealing with the question: What are good early predictors for final grades? To do this, we will determine what is success in a college course, understand if the current methods are adequate in calculating student success, locate influencing factors such as quizzes, midterm tests, and attendance, and observe if we can use these factors as predictors for scholastic achievement. The data and articles analyzed will only cover material from a traditional classroom. Online and mixed classroom data are not included due to these techniques being relatively new to the classroom environment and not enough data has been collected on them as a result.

2. Literature Review

2.1 Attendance

The first possible influence of final grades deals with the attendance rate of students. Numerous studies have concluded there is a statistically significant relationship between absences and academic performance, but some have discovered other effects attendance may have (Silvestri 2003; Lyubartseva and Mallik 2012; Kassarnig et al. 2017; Bai et al. 2018). Michael A. Clump and his colleagues (2003) discovered in their general psychology classes that there is an "importance of attending class on immediate course grades, and not just the final course grades," implying that attendance has a correlation with quizzes/tests (Clump et al. 2003, p. 223). Marcus Credé and his colleagues (2010) found through their meta-analytic review covering eighty-two years of articles and dissertations that "class attendance appears to be a better predictor of college grades than any other known predictor of college grades" (Credé et al. 2010, p. 288). Like the previous studies, the regression discontinuity classroom experiment done by Carlos Dobkin, Ricard Gil, and Justin Marion (2010) concluded that attendance affects student performance, but suggests that "attendance can be improved by instituting a mandatory attendance policy" (Dobkin et al. 2010, p. 575). Randy Moore (2003) also found that "class attendance enhances learning, which in turn improves grades, [but] attendance does not by itself guarantee higher grades" (Moore 2003, p. 370). Although this study of 140 students was conducted in Jordan, it concluded that not only attendance, but the overall student's GPA affected final course grades, demonstrating the relationship between attendance and final grades may be applicable to

educational institutions outside of the United States (Obeidat et al. 2012).

2.2 Quizzes, Tests, and Midterm Averages

Additionally, quizzes have indicated to make an impact on final grades. Quizzes given weekly have a positive correlation to tests and the final exam and "student performance in routine lecture quizzes can predict performance in the final examination and successfully completing a course" (Wambuguh and Yonn-Brown 2013, p. 1; Becerra et al. 2019). In a study focusing on pass/fail grading and weekly quizzes, Lynne S. Robins and others (1995) found that "students continued to perform well and reported greater satisfaction with the new [pass/fail] system" (Robins et al. 1995, p. 327). Joseph Nowakowski (2006) concluded in his study of early assessment and final grades at Muskingum College that "final grades do differ significantly from [early assessment grades] and that the most likely outcome is an improvement in the grade" (Nowakowski 2006, p. 558).

Midterm test grades can be impelling influences as well. Mid-semester grades positively correlate with final grades across various disciplines and "the first test/exam [is] a significant predictor for the final course grade," portraying that identifying low first test grades can help at-risk or struggling students (Connor et al. n.d.; Dambolena 2000; Ramanathan and Fernandez 2017, p. 9). Essentially, this inference can serve as an insight for students because when they realize they have control over their grades, midterms don't simply predict final grades, "[they are] a predictor that students can directly influence" (Jensen and Barron 2014, p. 88).

3. Methodology

This study will utilize similar theories and assumptions as the ones covered in the literature review, but with a different sample. The data in this study has been collected from Dr. Mary Wagner-Krankel's Introduction to Probability and Statistics classes from Spring 2012 to Spring 2016. Mainly STEM majors, specifically biology and environmental science, take this course since it was made a requirement in their degree plans by St. Mary's University. Sometimes these students do not have strong mathematical skills. The prerequisite to this course is college algebra, but biology and environmental science are quantitative in nature. There are higher demands of all students regardless of major to maintain a sufficient statistical background. Because some of the students in this course do not have satisfactory

math skills, they may need more early intervention to be successful, which explains why finding early predictors is so important. There are data from Fall 2009, Fall 2011, and Spring 2011, but the class sizes are twelve, twenty-five, and twenty-six respectively, which are relatively small compared to the double sections of the later semesters consisting of roughly twenty-five students each, so by our discretion it was determined to exclude these first three semesters from the analysis. Comparing the independent variables using various class sizes would significantly affect the results, so removing the smaller classes would make the statistics more accurate.

With the combined sections within each semester, there were fifty-two students in Spring 2012, fifty-two in Spring 2013, fifty-three in Spring 2014, thirty-seven in Spring 2015, and thirty in Spring 2016, making a total of 224 students over these five semesters. Over the course of these semesters, twenty-point quizzes, midterm averages which consist of the mean of the first three quizzes and Test 1, Test 1, Test 2, Test 3, which are 100 points each, and Final Exam grades out of 150 points, Final Averages, and attendance were collected. Each class had the same professor and textbook, similar tests, quizzes, and class times, and all were conducted in a lecture-based style. In this study, only the absences, Test 1, and midterm average data are analyzed because these were the main factors examined in the literature review articles and the results will be easier to compare to those within the previous studies above.

R Commander, a software using the R Programming language to generate statistical analyses and results, was utilized. First a multiple regression analysis was conducted between each independent variable (Test 1, midterm average, and attendance) versus the final average with Spring 2012, Spring 2013, Spring 2014, and Spring 2015 as dummy variables with Spring 2016 as a baseline for comparison to determine there are no statistically significant differences between the variables and the semesters. Next, scatterplots were made of each independent variable versus the final average to analyze for a linear correlation. Based on the literature review, it is expected that attendance should have a linear correlation with the final average, and Test 1 and midterm average should be highly correlated with the final grades. A correlation matrix, which shows linear correlations between each pair of variables, will be made to confirm or reject these assumptions. Since there is a likelihood that these independent variables are correlated with each other, there is a possibility of multicollinearity, which can alter the

results of this analysis. For those variables that portray multicollinearity, they will not be used together in the final model to predict final grades.

Finally, a normal probability plot and a residual quantile-comparison plot of the final multiple regression model will be made to verify these assumptions: the residuals are normally distributed, there is no visible pattern, and there is constant variance. Checking these assumptions makes certain there are no errors in the linear regression model.

4. Results

In the multiple regression model in Table 1 with Test 1 as the independent variable and semesters Spring 2012 (S12), Spring 2013 (S13), Spring 2014 (S14), and Spring 2015 (S15) as dummy variables compared to Spring 2016, all against the dependent variable final average, the P-value for Test 1 is statistically significant, meaning Test 1 is an appropriate predictor for final averages. The coefficient estimate for Test 1 is 0.48228, which means if the grade for Test 1 increases by one point, the final average is expected to increase by 0.48228 points, assuming the semester dummy variables remain constant. Only the P-values for Spring 2013 and 2014 are significant with Spring 2016, meaning S13 and S14 have significant differences compared to S16.

Table 1. Multiple Regression Model with Final Average versus Test 1
Regression equation: Final Average = Test 1 + S12 + S13 + S14 + S15

	Estimate	Standard Error	t value	P-value
Intercept	46.34970	2.33128	19.882	< 2e-16
Test 1	0.48228	0.02629	18.348	< 2e-16
S12	0.59435	1.05148	0.565	0.572353
S13	-4.82118	1.04942	-4.594	0.00000657
S14	-4.11661	1.06213	-3.876	0.000132
S15	0.16145	1.17791	0.137	0.891079

Residual standard error: 6.054 on 281 degrees of freedom
Multiple R-squared: 0.6112, Adjusted R-squared: 0.6043
F-statistic: 88.34 on 5 and 281 DF, p-value: < 2.2e-16

In another multiple regression model but with absences as the independent variable in Table 2, the P-value for absences was statistically significant as well, demonstrating absences is another predictor for final averages. The coefficient estimate for absences is -0.9801, which means if the number of absences increased by one, the

final average is predicted to decrease by 0.9801 points, given the semester dummy variables remain the same. However, the P-value for S12 was significant, meaning only Spring 2012 has significant differences compared to Spring 2016.

Table 2. Multiple Regression Model with Final Average versus Absences
Regression equation: Final Average = Absences + S12 + S13 + S14 + S15

	Estimate	Standard Error	t value	P-value
Intercept	86.4117	1.7160	50.356	< 2e-16
Absences	-0.9801	0.1950	-5.026	0.00000104
S12	4.3823	2.0225	2.167	0.0313
S13	-1.2771	1.9668	-0.649	0.5168
S14	-2.1101	1.9724	-1.070	0.2859
S15	3.1389	2.1116	1.486	0.1386

Residual standard error: 8.577 on 218 degrees of freedom
Multiple R-squared: 0.2405, Adjusted R-squared: 0.2231
F-statistic: 13.81 on 5 and 218 DF, p-value: 1.014e-11

The regression model in Table 3 with midterm grades displays a statistically significant P-value for midterm grades, meaning midterm grades is a predictor for final averages. The midterm grade coefficient estimate was 0.65353, which means if the midterm grade increases by one point, the final average is predicted to increase by 0.65353 points, provided that S12, S13, S14, S15 remain constant. Spring 2012, Spring 2013, and Spring 2015 have significant P-values, so these semesters have differences from Spring 2016.

Table 3. Multiple Regression Model with Final Average versus Midterm Grade
Regression equation: Final Average = Midterm Grade + S12 + S13 + S14 + S15

	Estimate	Standard Error	t value	P-value
Intercept	30.37187	2.43034	12.497	< 2e-16
Midterm Grade	0.65353	0.02816	23.211	< 2e-16
S12	3.76595	1.12230	3.356	0.000934
S13	-2.08780	1.11573	-1.871	0.062650
S14	-1.34842	1.11399	-1.210	0.227420
S15	3.29328	1.19490	2.756	0.006345

Residual standard error: 4.863 on 218 degrees of freedom
Multiple R-squared: 0.7559, Adjusted R-squared: 0.7503
F-statistic: 135 on 5 and 218 DF, p-value: < 2.2e-16

Additionally, a correlation matrix of Test 1, midterm grade, absences, and final average was created to test for multicollinearity in Table 4. As expected, Test 1 and midterm grade have high correlations with final average, 0.738977364 and 0.831802939 respectively. Absences has a low negative correlation with final average at -0.4195314. All of the correlations between the independent variables Test 1, midterm grade, and absences are low with the exception of Test 1 and midterm grade at 0.890282582. This is most likely due to the fact that Test 1 is included in the midterm grade, so a high correlation between the two is inevitable. Because these two variables are highly correlated, incorporating them in the final multiple regression model would produce inaccurate results due to redundancy, so Test 1 and midterm grade will not both be included in the model. The correlation between absences and midterm grade is -0.3554424, which is low enough to not be statistically significant, so these variables will be integrated together in the multiple regression model.

Table 4. Correlation Matrix between Test 1, Midterm Grade, Absences, and Final Average

	Absences	Final Average	Midterm Grade	Test 1
Absences	1.0000000	-0.4195314	-0.3554424	-0.3492683
Final Average	-0.4195314	1.0000000	0.8318029	0.7389774
Midterm Grade	-0.3554424	0.8318029	1.0000000	0.8902826
Test 1	-0.3492683	0.7389774	0.8902826	1.0000000

In the final multiple regression model in Table 5, midterm grade and absences were the independent variables with final average as the dependent variable. The P-values for midterm average and absences were statistically significant, meaning midterm grades and absences combined serve as a predictor of final average. The coefficient estimates for absences and midterm grade are -0.22233 and 0.63636 respectively. If the number of absences increases by one, the final average is expected to decrease by 0.22233, given that midterm grade and the semester dummy variables are held constant. If the midterm grade increases by one point, the final average is predicted to increase by 0.63636 assuming absences and the semester dummy variables are held constant. The P-values for Spring 2012, Spring 2013, and Spring 2015 were significant, so there are differences between these semesters and Spring 2016.

It is necessary to mention that a multiple regression model with final averages versus Test 1 and absences was made to observe if it is a better model than final averages versus midterm grade and absences. The model with Test 1 and absences as explanatory variables exhibits a smaller R^2 at 0.6143, which means 61.43% of variability in final average can be explained by the multiple linear regression model. This model also had a lower F-statistic at 57.61. The normal probability plot has some residuals outside of the bounds. Despite the fact that there is no pattern in the scatterplot of the residuals versus the fitted final averages, there appears to be a “funnel effect” which could exhibit non-constant variance. Because the ideal model illustrates a low standard error and a high R^2 and F-statistic, midterm grade and absences combined is a more appropriate fit for forecasting final course grades.

Table 5. Multiple Regression Model with Final Average versus Midterm Grade and Absences
Regression equation: Final Average = Absences + Midterm Grade + S12 + S13 + S14 + S15

	Estimate	Standard Error	t value	P-value
Intercept	32.55185	2.66687	12.206	< 2e-16
Midterm Grade	0.63636	0.02937	21.670	< 2e-16
Absences	-0.22233	0.11531	-1.928	0.05515
S12	3.30506	1.14070	2.897	0.00415
S13	-2.10884	1.10889	-1.902	0.05853
S14	-1.14144	1.11231	-1.026	0.30594
S15	3.15002	1.18985	2.647	0.00871

Residual standard error: 4.833 on 217 degrees of freedom
Multiple R-squared: 0.76, Adjusted R-squared: 0.7533
F-statistic: 114.5 on 6 and 217 DF, p-value: < 2.2e-16

The scatterplots of Test 1, absences, and midterm grade against final average in Figures 1, 2, and 3 showed that Test 1 and midterm grade have a positive linear correlation with final average while absences have a negative linear correlation. There are two outliers in the scatterplot between Test 1 and final average, but they are not significant enough to impact the conclusion.

Figure 1. Scatterplot of Final Average versus Test 1

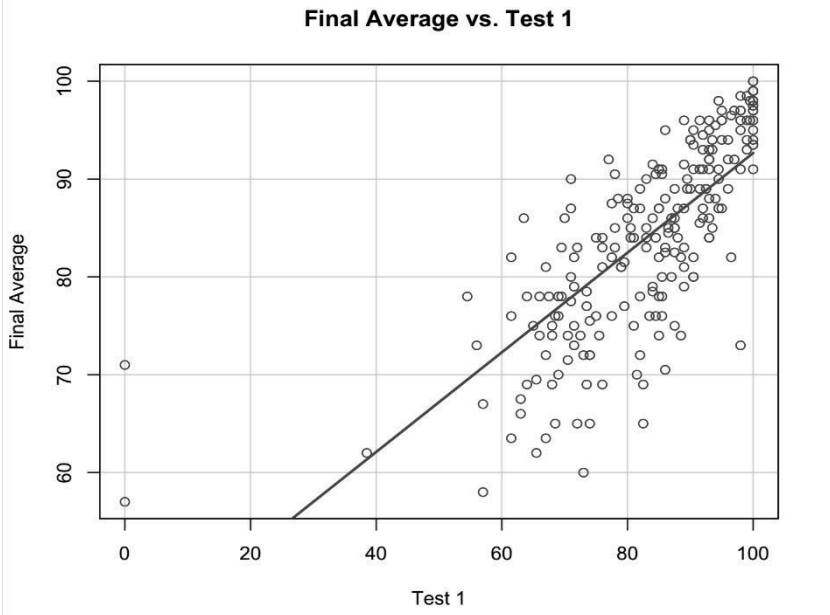

Figure 2. Scatterplot of Final Average versus Absences

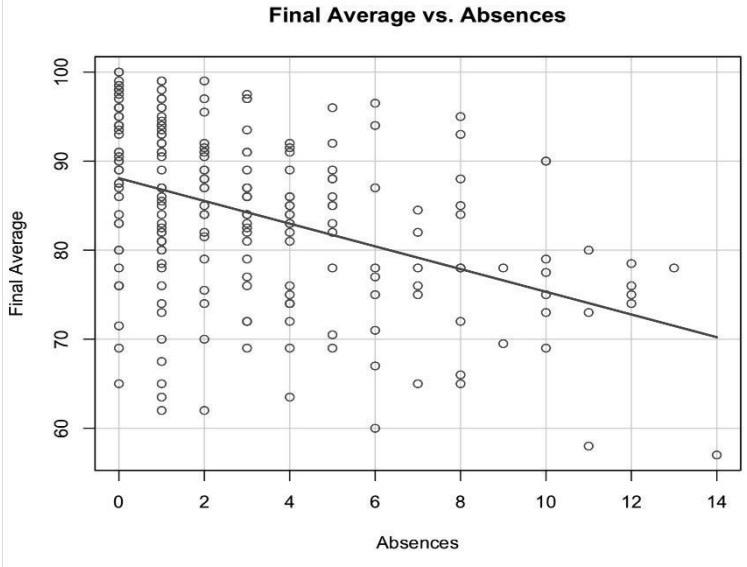

Figure 3. Scatterplot of Final Average versus Midterm Grade

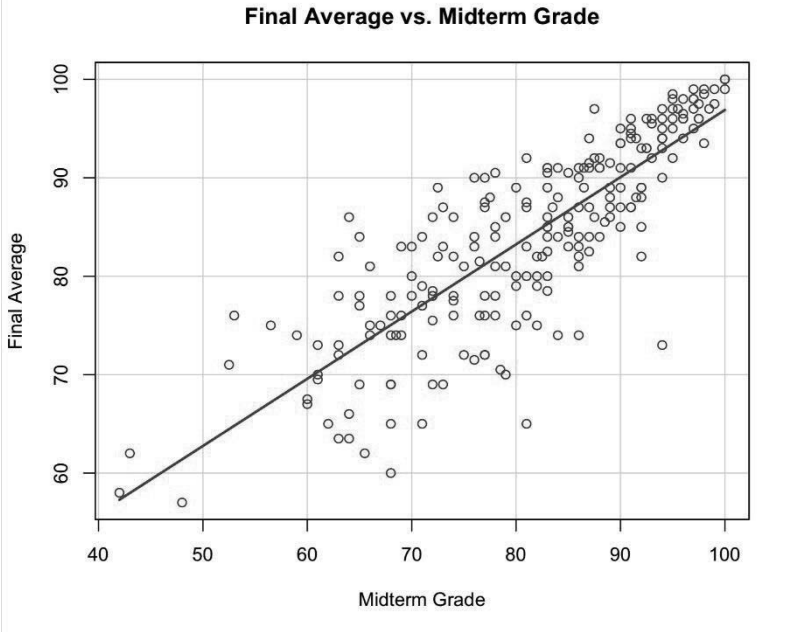

In Figures 4 and 5, the assumptions that the residuals are normally distributed, exhibit no pattern, and have constant variance are checked for the final multiple regression model of final averages versus midterm grade and absences in order to locate any potential errors. Figure 4 displays that the residuals do not portray a pattern, but do indicate a "funnel effect," implying there may be non-constant variance. Figure 5 shows the residuals are normally distributed since very few points are outside of the bounds. Despite the possible non-variance, the "funnel effect" should not influence the accuracy of the final model.

Figure 4. Scatterplot of Studentized Residuals versus Fitted Final Averages of the Final Multiple Regression Model

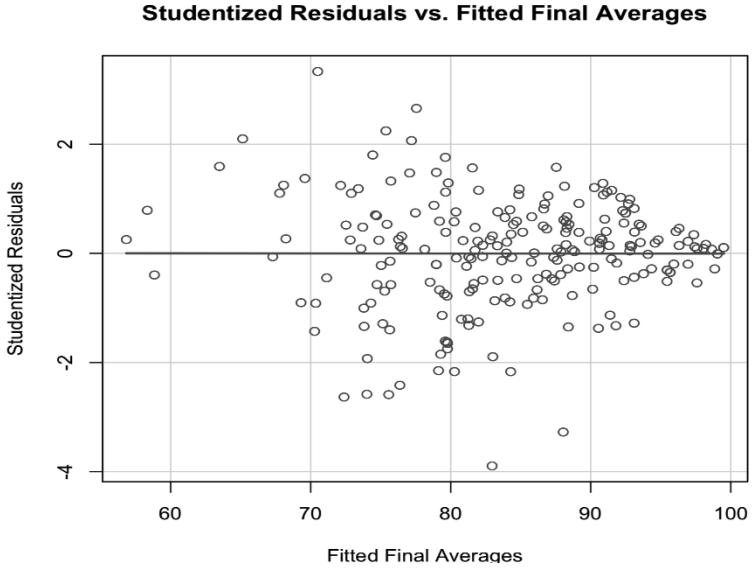

Figure 5. Normal Probability Plot of Studentized Residuals of the Final Multiple Regression Model

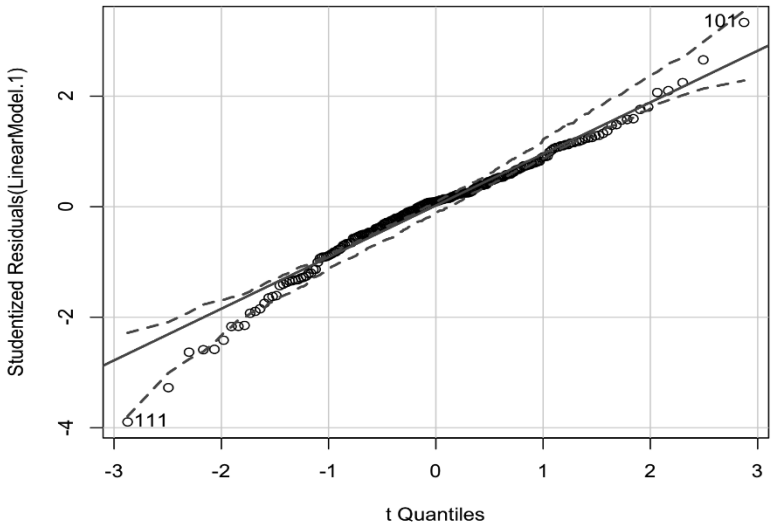

5. Discussion

In sum, there are various factors such as attendance to quizzes/exams that have a bearing on the achievement of a student. The first test proved to be a significant influence in predicting final grades, which is a valid indicator of academic success. The midterm grade is also an effective forecaster, demonstrating that assessments in the middle of a semester have an adequate outlook on how a student is performing in a course. Additionally, absenteeism is a major factor since those who missed class frequently generally did not receive high grades. Overall, the best predictor is the midterm grade and absences combined. In the future it would be beneficial to analyze studies focusing on other factors, such as study habits, personality, high school environment, and standardized test scores to create a more accurate representation of what determines student achievement. Nonetheless, the data collected will serve as a general assessment of student education in United States colleges and hopefully aid administrators and professors in guiding students to a path of success.

Acknowledgments

Miss Aleacia Messiah would like to thank her mentors Dr. Wagner-Krankel and Dr. Lurie for guiding her through her first research experience. The authors would like to thank the Ronald E. McNair Post-Baccalaureate Achievement Program at St. Mary's University for their permission to work on this study.

References

Bai, X., Ola, A., and Akkaladevi, S. (2018), "EXAMINATION OF THE RELATIONSHIP BETWEEN CLASS ATTENDANCE AND STUDENT ACADEMIC PERFORMANCE," *Issues in Information Systems*, 19, 101–109.

Becerra, D. A., Grob, M. S., Soto, R., Tricio, J., and Sabag, N. (2019), "Weekly Quizzes as a Predictive Factor of Final Academic Performance in Morphology/ Controles Semanales como Factor Predictor del Rendimiento Academico Final en Morfologia," *International Journal of Morphology*, 37, 296+.

Clump, M. A., Bauer, H., and Whiteleather Alex (2003), "To Attend or Not To Attend: Is that a Good Question?," *Journal of Instructional Psychology*, 30, 220–224.

Connor, J., Franko, J., and Wambach, C. (n.d.). "A Brief Report: The Relationship between Mid-Semester Grades and Final Grades," 1–7.

Credé, M., Roch, S. G., and Kieszczynka, U. M. (2010), "Class Attendance in College: A Meta-Analytic Review of the Relationship of Class Attendance With Grades and Student Characteristics," *Review of Educational Research* [online], 80, 272–295. Available at https://doi.org/10.3102/0034654310362998.

Dambolena, I. G. (2000), "A regression exercise: Predicting final course grades from midterm results," *Primus: Problems, Resources, and Issues in Mathematics Undergraduate Studies; Philadelphia*, 10, 351–358.

Dobkin, C., Gil, R., and Marion, J. (2010), "Skipping class in college and exam performance: Evidence from a regression discontinuity classroom experiment," *Economics of Education Review* [online], 29, 566–575. Available at https://doi.org/10.1016/j.econedurev.2009.09.004.

Jensen, P. A., and Barron, J. N. (2014), "Midterm and First-Exam Grades Predict Final Grades in Biology Courses," *Journal of College Science Teaching*, 44, 82-89.

Kassarnig, V., Bjerre-Nielsen, A., Mones, E., Lehmann, S., and Lassen, D. D. (2017), "Class attendance, peer similarity, and academic performance in a large field study," *PLoS ONE* [online], 12, 1–15. Available at https://doi.org/10.1371/journal.pone.0187078.

Lyubartseva, G., and Mallik, U. P. (2012), "Attendance and student performance in undergraduate chemistry courses," *Education*, 133, 31–34.

Moore, R. (2003), "Attendance and performance," *Journal of College Science Teaching*, 32, 367–371.

Nowakowski, J. (2006), "An Evaluation of the Relationship Between Early Assessment Grades and Final Grades," *College Student Journal*, 40, 557–561.

Obeidat, S., Bashir, A., and Jadayil, W. A. (2012), "The Importance of Class Attendance and Cumulative GPA for Academic Success in Industrial Engineering Classes," *World Academy of Science, Engineering and Technology*, 1192–1195.

Ramanathan, P., and Fernandez, E. (2017), "Can Early-Assignment Grades Predict Final Grades in IT Courses?," in *2017 ASEE Annual Conference & Exposition Proceedings* [online], Columbus, Ohio: ASEE Conferences, pp. 1–11. Available at https://doi.org/10.18260/1-2--28002.

Robins, L. S., Fantone, J. C., Oh, M. S., Alexander, G. L., Shlafer, M., and Davis, W. K. (1995), "The Effect of Pass/Fail Grading and Weekly Quizzes on First-year Students' Performances and Satisfaction," *Academic Medicine*, 70, 327–329.

Silvestri, L. (2003), "The effect of attendance on undergraduate methods course grades," *Education*, 123, 483–486.

Wambuguh, O., and Yonn-Brown, T. (2013), "Regular Lecture Quizzes Scores as Predictors of Final Examination Performance: A Test of Hypothesis Using Logistic Regression Analysis," *International Journal for the Scholarship of Teaching and Learning* [online], 7, 1–13. Available at https://doi.org/10.20429/ijsotl.2013.070107.

Aleacia Messiah
St. Mary's University
One Camino Santa Maria
San Antonio, TX 78228
amessiah@mail.stmarytx.edu

Mary Wagner-Krankel, Ph.D.
Department of Mathematics
One Camino Santa Maria
San Antonio, TX 78228
mwagnerkrankel@stmarytx.edu

Anna Lurie, Ph.D.
Department of Mathematics
St. Mary's University
One Camino Santa Maria
San Antonio, TX 78228
alurie@stmarytx.edu

Shifting Democracy: OAS Relevance and Responses to Corruption

Anthony Robledo

Mentors: Betsy L. Smith, Ph.D.
St. Mary's University, San Antonio, TX

Is the Organization of American States (OAS) losing relevance as a regional intergovernmental power? A review of OAS responses to corruption cases from 2014-2019 supports the claim that the OAS is losing relevance. This article adds to the literature by noting that the issue of high politics or low politics is a fundamental factor in the response. Most corruption cases fall under the low politics spectrum because they are non-essential to a nation's survival, but when a corruption case threatens a nations survival, The OAS is more likely to respond. The origin of the case also impacts OAS response. Corruption cases from larger states that fall under low politics are less likely to get a response. The findings from this article provides support for the shifting stances on isolation within the region and shows the potential for the loss of relevance of the OAS.

Introduction

Since the inception of the Organization of American States (OAS), Latin America has had a regional intergovernmental organization (IGO) power structure that has been the forefront of democratic continuity within the region. One major example of this democratic continuity was the handling of the Cuban Revolution and the formation of the Declaration of San Jose. This declaration reaffirmed the mission of the OAS to strengthen democracy around the region. (Herz, 2013) Over the years though, the OAS has lost credibility due to people considering it "clubs of presidents." This ideology in conjunction with the lack of funding have caused people to wonder if the OAS has lost relevance as a regional power? This article lends support to the argument that the OAS's lack of response to corruption stems from corruption being an issue of low politics. This article adds to the literature of the OAS by illustrating the responses or lack thereof, to corruption cases that have plagued Latin America. More specifically, this article adds to the post-2012 literature because of the wave of corruption that has occurred recently. The article tries

answering what the OAS has done in response to corruption, and why the OAS has taken that action.

The OAS lack of response to corruption can implicate other major IGOs when it comes to promoting cooperation among the region. If countries continue to shift priorities from multilateral cooperation, to a more unilateral mentality, then many weaker countries will have to fend for themselves and nothing would protect democracy in the west except individual countries. (Legler, Dexter, Boniface, 2007) The weakening of the OAS has already led to antidemocratic practices among countries. The biggest example is Venezuela and its withdrawal from the OAS. This was a blow to democracy in west because of the Venezuelan presidential crisis. While the OAS may have responded in an adequate matter, defending democracy in the west has become harder and will continue to remain that way without the help of IGO's like the OAS. Democracy in the west seems to be changing into a form that makes sovereign nations remain isolated, and thus protecting democracy should remain in the forefront of most regional powers.

Introducing the Crises

There are two major crises that this paper tries to look at to answer the questions of OAS response to corruption. The first is Operation Car Wash. Operation Car Wash started off as a money laundering investigation in 2014 that has now expanded to alleged corruptions done by Petrobras, a semi-public Brazilian multinational corporation in the petroleum industry headquartered in Rio de Janeiro, Brazil. The allegations state that executives from Petrobras accepted bribes in return for awarding contracts to construction firms. This corporate malfeasance caused an inflation of prices in oil. So far 11 countries have been named for their involvement and Brazilian company, Odrebrecht, has been heavily implicated. An estimated 13 Billion U.S dollars have been embezzled according to a statement by federal Brazilian police of Parana state.

The other case that this paper tries to look at is the Panama Papers. In 2016, German newspaper *Süddeutsche Zeitung (SZ),* leaked 11.5 million encrypted confidential documents that were property of Panama-based law firm Mossack Fonseca. These documents contained personal financial information of people and entities from 200 different nations. Over 214,000 tax havens were exposed from current and former world leaders, celebrities, public officials, politicians, and other business moguls. (Laila Ait Bihi Ouali, 2019) At first glance, most of the documents were considered legal offshore business with no illegal

behavior, but some malfeasance did take place including fraud, tax evasion, and the avoidance of international sanctions. The data spans from the 1970's through 2016 and has caused an uproar in the international community. Multiple Latin American politicians are being investigated including but not limited to, Argentinian President Mauricio Macri, Brazilian President of the Chamber of Deputies Eduardo Cunha, Ecuadorian General Attorney Galo Chiriboga, and Honduran former vice president Jaime Rosenthal.

Defining Corruption in Latin America

The OAS in general deserves to be to be examined because of the membership and idealistic protection of democracy. The literature for the OAS extends across defense of democracy, IGO procedures, and many other aspects, but falls short on recent corruption plaguing Latin America. Whether there is a response or not, the amount of corruption that has taken place since 2014 shows the insecurity of the regional organization. It has been over 20 years since the Inter-American Convention against Corruption (IACAC) and still a new wave of corruption hasn't been curtailed. The OAS responded to the IACAC with the Mechanism for Follow-Up on the Implementation of the Inter-American Convention against Corruption (MESICIC), but this mechanism has struggled to deal with major corruption cases.

Under the IACAC, 3 major subsets that can collude in corruption. The first is "public function", Which means any temporary or permanent, paid or honorary activity, performed by a natural person in the name of the State or in the service of the state or its institutions, at any level of its hierarchy. The second is a "public official" defined as any official or employee of the State or its agencies, including those who have been selected, appointed, or elected to perform activities or functions in the name of the State or in the service of the State, at any level of its hierarchy. The last is "property", which means assets of any kind, whether movable or immovable, tangible or intangible, and any document or legal instrument demonstrating, purporting to demonstrate, or relating to ownership or other rights pertaining to such assets. (OAS IACAC, 1996)

The IACAC vaguely describes what corruption is, so for this paper I use simple definition of corruption which means, abuse of public power for private gain. This is a law-based definition that has been used in past Latin American literature including (Casas-Zamora, 2017). In the same sense, multiple international organizations have

defined it as the misuse of public power for private benefit (Organização das Nações Unidas [ONU], 2003; World Bank, 2000).

Literature Review

Corruption crises around Latin America have proliferated at a rapid pace since the turn of the century. Multiple countries within the region are accused of some form of corruption stemming from public officials, while some countries like Brazil are implicated with more then one corruption crisis. This rapid ballooning of crises has led to many countries relying on IGO's like the OAS to respond in a democratic fashion. These democratic responses to crises through an IGO's have been subjected to scholarly probing to understand the intricacies of the responses.

One major argument is that a democratic response to crises done by any regional organization should involve sanctions. The argument keys in on that hemispheric protection of democracy should allow for strong responses that have proven to be effective. Factors including multilateral action by the U.S, support the claim that restoring democracy is easiest when regional organizations like the OAS respond collectively. (Gonzalez and Liendo, 2017) This argument is hardly seen in action in the OAS because the OAS sticks to condemnations and the use of rhetoric for responding to crises instead of relying on sanctions.

Authors like Boniface (2007) claim that the OAS responds to crises that interrupt democracy but evaluate smaller crises on a case-by-case basis. This leads to a wishy-washy history of responses because different countries get different treatments. The OAS wastes time arguing over what is and is not a threat to democracy. These arguments can deteriorate the overall impact of most responses. Authors like Arceneaux and Pion-Berlin (2007) argue about the clarity of the crisis and how the more defined the crisis is, the stronger the response is. This goes hand in hand with Boniface's argument because it shows how if the crisis is easily defined as a threat to democracy, an action is taken.

Selective Intervention on Corruption: A Theory of OAS Responses

This article argues that corruption is an issue of low politics and because of that, the crises will get a weak response from the OAS. The OAS acts only when it sees fit and follows a rule of selective intervention. Arceneaux and Pion-Berlin (2007) theory goes into detail about OAS response and demonstrates how mechanisms are in place that allow for swift responses, yet some issues receive less attention than might be expected. The literature illustrates the support for collective democracy but has gaps when explaining why support would

be expressed selectively. Applying my research question to this theory will lend support to fill the gap in the literature on selective intervention. The pure nature of the issues confronting member states can dictate how the OAS will respond. As issues change from low politic to high politic issues so do the motivations of the OAS and its members.

High Politics + OAS Response

When a corruption crisis falls under high politics, meaning that the threat of the corruption impacts the survival of the nation or some major aspect of it like the economy, The OAS is more likely to respond. (Arceneaux and Pion-Berlin 2005) At this level, the violation is more easily defined within the IACAC and the OAS Charter as a threat to democracy in the region. This makes the response easier on the OAS and fight against the arguments of sovereignty and non-interference. This issue constantly plagues the responses of the OAS because the exercise of a nations sovereignty can make the response null and void.

With a clearer identification of the violation, the MESICIC can better deal with the issue because it's a follow up mechanism for the IACAC. Under the MESICIC, 33 of the 34 Member States can review their legal framework to ensure the implementation of the IACAC and help combat the issue of sovereignty when dealing with a major crisis. The issue of selective intervention does not arise and the mechanisms that are in place allow for a swift strong response. The problem that remains is that most corruption cases fall under low politics. There is ambiguity as to when a corruption issue moves from the low politics issue to a high politics issue. The influence of high politics and OAS response can be stated as:

> H1: During corruption crises of high politics, we are more likely to see a moderate to strong response, regardless of selective intervention.

Low Politics + OAS Response

In the case of low politics, or non-essential crises, the response will get a weaker response if any because of selective intervention. Naturally, lower level threats of corruption are more difficult to address because the nature of the OAS and the agreement to uphold state sovereignty. (Arceneaux and Pion-Berlin 2007) The vague definitions under the IACAC makes it hard to determine whether lower level corruption crisis require action or should be dealt by the individual state. Non-intervention is a long-lasting pillar of the OAS and doing anything that contradicts this pillar would be detrimental to the OAS.

At this level, the individual state has control of whether a response happens. The state in question must request the assistance and if the corruption crises occurs with the executive branch of the country, an OAS response is very unlikely unless the OAS has a motive for intervening. The expected relationship between corruption crises of low politics and the response can be stated as:

H2a: During a corruption crisis of low politics, we are more likely to see a weak response from the OAS.
H2b: During a corruption crisis of low politics, we are likely to see a moderate response from the OAS, unless the OAS has motives to respond.

Conceptualization

This article argues that corruption is a low politics issue and thus does not get strong responses from the OAS. My dependent variable is OAS response and my independent variables are high/low politics and OAS motive. I argue that during a high politics issue, the OAS will have a strong response. During a low politics issue, OAS response is weak unless the OAS has a special interest in mind. The OAS acts solely for itself and its member states and follows the theory of selective intervention.

Methods

Due to the nature of the project, I use the congruence method to determine whether a relationship exist between the issue of low politics, and the OAS response. Under these methods, the relationship cannot be proven causal but does provide evidence that will strengthen the argument of selective intervention as it relates to corruption in the America's. This will hopefully encourage others to further examine the relationship between high/low politics and selective intervention within the OAS. Under this method, my hypotheses are my theory predictions and those are put to the test against actual outcomes of the case studies. This article uses two major case studies to test the expected outcome.

Case Studies

To start off, we see the initial responses to the Panama Papers. There was a response from the Secretary general in his Inaugural Speech for the VIII Summit of the America's. In this speech though, he was reluctant to bring up the Panama Papers and his word choice coincided more with "corruption scandals in the recent years." There is a push to change efforts on combating corruption, but the OAS does not have to listen to the Secretary General when it comes to formulating an

agenda. This response can be considered a weak response because of the ambiguity behind it.

The next response to the Panama papers was a report done by the Inter-American Committee on Hemispheric Security (HACIA) that was also presented at the Summit of the America's. This report addressed the Panama Papers briefly, but then backpedaled into cyber security. This wasn't a response to the issue of corruption, but more of push to avoid any more leaks in the future. While this can be seen as a more moderate response, it glosses over the corruption that actually happened. The OAS is more worried about preventing more outbreaks like the Panama Papers, instead of handling the corruption issue. This response to the OAS can be considered a motive for the OAS that triggered a response that was a bit stronger than what I hypothesized, but overall the hypothesis for no response remains.

In the Operation Car Wash case study, there has been little to no response by the OAS. We have seen presidents be impeached in brazil twice now and still the OAS remains silent. The trail of corruption is happening through the individual state and so the OAS sees no reason to respond. Not only is there a complete lack of response, the literature on the topic is bare. This case study shows that my H2a stands in this scenario. The OAS sees this as an issue of low politics and has no need to respond. The further we get into the case, the more we see a transition from low politics to high politics because of the economic implication of Operation Car Wash. If Brazil's economy continues to plummet, then way may say a strong response by the OAS.

Conclusion

How has the OAS responded to current corruption crises? This article seeks to add to the literature regarding selective intervention in the America's. We can see that responses to corruption crises from the OAS are weak because corruption is an issue of low politics. The article adds to the literature because it addresses the gap in the literature when it comes to why the OAS practices selective intervention. When a crisis is an issue of high politics, a response is more likely. When the issue one of low politics like most corruption, the response is weak unless a special interest or motive arises among the member states. This lack of response to issues of low politics like corruption can lead to the loss of relevance of the OAS. This loss of relevance could then lead to low MESICIC in place, responses to corruption should and can be handled swiftly if the OAS chooses to utilize the resources at its disposal.

References

Arceneaux, C., Pion-Berlin, D. (2007) *Issues, Threats, and Institutions: Explaining OAS Responses to Democratic Dilemmas in Latin America*. (n.d.). 32.

Arceneaux, C., Pion-Berlin, D. (2005) *Transforming Latin America: The International and Domestic Origins of Change.* Pittsburgh: University of Pittsburgh Press. 32.

Bayer, R.-C., Hodler, R., Raschky, P., & Strittmatter, A. (2018). Expropriations, Property Confiscations and New Offshore Entities: Evidence from the Panama Papers.

Casas-Zamora, K., Carter, M. (2017*) Beyond the Scandals: The Changing Context of Corruption in Latin America.* Washington D.C: Inter-American Dialouge

Gonçalves, V. B., & Andrade, D. M. (2019). A corrupção na perspectiva durkheimiana: Um estudo de caso da Operação Lava Jato. *Revista de Administração Pública*, *53*(2), 271–290.

González, M. C., & Liendo, N. A. (2017). LA DEFENSA COLECTIVA DE LA DEMOCRACIA EN AMÉRICA LATINA: ¿POR QUÉ?, ¿CÓMO?, ¿CUÁNDO? *Análisis Político*, *30*(91), 3–17.

Herz, M., (2013). *The Organization of American States (OAS).* New York: Routledge Global Institutions

Jiang, A., Pai, A., & O'Donohue, A. (n.d.). *OAS Permanent Council*. 78.

Legler, T., Lean, F.S., Boniface, S.D., *Promoting Democracy in the America's*. Baltimore: John Hopkins University Press

OAS. (1996) *Inter-American Convention Against Corruption*.

OAS. (2004) *Mechanism for Follow-Up on the Implementation of the Inter-American Convention against Corruption*

OAS. (2018) *OAS Secretary General Inaugural speech VIII Summit of the Americas*

Organização das Nações Unidas. (2003). *Convenção das Nações Unidas contra a Corrupção. Brasília*, DF: Autor.

Ouali, L. A. B. (n.d.). *Top Income Tax Evasion and Redistribution Preferences: Evidence from the Panama Papers*. 43.

Saygili, A. (2019). Concessions or Crackdown: How Regime Stability Shapes Democratic Responses to Hostage taking Terrorism. *Journal of Conflict Resolution*, *63*(2), 468–501.

World Bank. (2000) *Helping Countries Combat Corruption: The Role of the World Bank:* Washington D.C.

Indian School or HBCU? How HSIs Really Work

Brandi Loving

Mentors: Rick Sperling, Ph.D.
St. Mary's University, San Antonio, TX

Hispanic-serving Institutions (HSIs) are regarded by many as a necessary mechanism for moving Latinx students through the educational pipeline. That view, while misguided, is not entirely false quantitatively speaking. A large proportion of Latinx students spend at least some of their educational career in an HIS. Unfortunately, the academic reputation of HSIs is rather weak, which means that Latinx students who have the choice to attend a more prestigious school are left with a decision of whether to attend a PWI or earning a degree from an HSI that will not be taken as seriously by employers and graduate schools. To make matters worse, the philosophical orientation driving the structural, pedagogical, and curricular offerings at HSIs often reflects a cultural-deficit view that severely compromises the overall value of the educational experience. In this paper, I apply a critical race lens in analyzing the historical and contemporary factors that make most HSIs largely unsuccessful in living up to their supposed mission—educating Latinx students (Nelson, Bridges, Morelon-Quainoo,Williams & Holmes, 2007). My analysis concludes that HSIs in most states are likely to shortchange Latinx students while doing well to serve the interests of corporations and the White faculty and administrators that maintain employment on their hallowed grounds. I further argue that these conditions are unlikely to change so long as Latinx role models trumpet the charge for HSIs and Latinx students are content with the fruitless pursuit of Whiteness.

Indian School or HBCU?

In order for a college or university to be considered a Hispanic-serving Institution (HSI), 25 percent or more of its students must self-identify as Hispanic. Once an institution earns the HSI designation, it is immediately eligible to apply for Title V funds (Higher Education Act, as amended in 1998). These federal funds are ostensibly intended to narrow the post-secondary achievement gap between Whites and Latinx populations.

Currently, there are 492 (HACU,2018) colleges and universities in the mainland US and another 63 in Puerto Rico (HACU, 2018). Despite what sounds like a noble act on behalf of the federal government, there are no rules or regulations ensuring that the funds HSIs receive are spent specifically on Latinx students (Lacagnino, 2019). That is, grant recipients do not have to show that the money was used on activities that narrowed the achievement gap or resulted in policies and practices that emanate from a culturally-responsive framework. Consequently, HSIs are only incentivized to enroll Latinx students; they are not incentivized to respond to their needs or to educate them in a way that calls attention to the opportunity and reward gaps that make Title V funds necessary in the first place (Nora & Crisp, 2009).

Other types of minority-serving institutions operate in a radically different manner. For example, Historically Black Colleges and Universities (HBCUs) were originally designed to educate Black people, a population that, in the era during which most HBCUs were founded, had been systematically denied the opportunity to pursue higher education altogether. As such, HBCUs did not have to be retrofitted to the needs and desires of a racially different student body. They were, and for the most part continue to be, designed specifically to educate Black students, and many of them have emerged as well-respected institutions that have contributed to our nation's economic, scientific, and political leadership (Wilson, 2008).

The history of HBCUs may have allowed for a more direct path to cultural-responsiveness, but it hardly explains why HSIs have failed so miserably in comparison. As I will demonstrate in the following sections, the assimilationist mentality that permeates most HSI campuses is not a byproduct of a failure to change with the times, but rather a well-designed strategy to arrest the development of collective agency for political purposes and to maintain racial stratification in economic outcomes all the while convincing Latinx students and their families that they are better off with the type of education provided at HSIs (Garcia, 2013). Unless there is a reimagining of how HSIs are designated and a reiteration of the terms on which they may receive federal funding, there is no reason to believe that they will ambitiously pursue cultural-responsiveness or transform into sites dedicated to the radicalization of Latinx students.

The HSI as Reincarnation of the Indian Boarding School

As mentioned previously, for almost all HSIs, the federal designation occurred many years after their founding. For some, earning the title HSI was a formality, since their student body had possessed greater than 25 percent Latinx representation for many years. For others, demographic changes nationally and regionally have meant that they could earn HSI status. What both types of institutions share, however, is that almost none were originally conceptualized as being Latinx-centric, which makes them profoundly different in purpose from HBCUs. Where then might one find a suitable comparison for the HSI? I posit that one need look no further than the Indian boarding schools of the 19th and 20th centuries. Indian boarding schools were created for the expressed purpose of assimilating students sufficiently well that they could be counted on to accept the religious and economic realities being imposed upon them by Whites (Robbin et al., 2008). Students were subjected to extreme forms of behaviorism until they relented and agreed not to speak their native language, eat familiar foods, conceive of time in a culturally consistent manner, wear their hair at traditional length, or exhibit any other behavior that made their White captors feel uncomfortable or afraid. Ideally, they would also learn gendered skills and family roles that were intended to replicate those of lower-class Whites so that they could be of use as labor to White capital.

Given that the HSI designation is a contemporary idea, we can safely assume that the exact same practices are not being carried out on campuses today. However, it is less clear whether or not the same goals are driving the structure and function of modern-day HSIs. The Hispanic Association of Colleges and Universities (HACU), a highly visible non-profit organization that promotes HSIs nationwide, sees the following as its mission:

- Promoting the development of member colleges and universities
- Improving access to and the quality of post-secondary educational opportunities for Hispanic students
- Meeting the needs of business, industry, and government through the development and sharing of resources, information, and expertise.

Taken together, these statements make clear that HSIs are meant to educate Latinx students so that business, industry, and government can prosper. Needless to say, overthrowing the government, converting the economic system, and restoring Aztlán are conspicuously absent from the list.

What's more impressive is that, like the Indian boarding schools before them, HSIs tend to employ mostly White administrators whose

bidding is mostly carried out by White faculty. (Greene & Oesterreich, 2012) While it is true that there is a higher percentage of Latinx faculty at HSIs, almost no four-year HSI can claim that the majority of their faculty is Latinx. This truth extends to administration as well, where only a small fraction of university presidents have a Spanish surname (Greene & Oesterreich, 2012).

In and of itself, the racial/ethnic mismatch of students and faculty would not be a deal-breaker for Latinx students if they could be assured that the faculty they encounter were interested in, willing to, and most of all capable of educating them. However, given that there appears to be no incentive to hire or award tenure to faculty who have a background in teaching and mentoring Latinx students, there is no reason to believe that students who attend schools in which 25 percent or more of their classmates are Latinx are likely to receive any more of a culturally-responsive education than they would have had they attended a predominantly White institution (PWI). Factor in that iconic organizations like HACU fail to include identity development and consciousness-raising as part of their mission, and it seems almost inconceivable that students would find an environment much different in purpose than the Indian boarding schools one hundred years earlier.

Quality of HSIs

Latinx students might be wise to tolerate assimilation in order to gain social mobility. Granted, meritocracy in the truest sense is widely acknowledged to be a myth in serious academic circles (Solórzano et al., 2000). However, overcoming the fact that social capital is unevenly distributed in favor of White students is only possible if you have access to the types of schools that will provide the highest caliber of education and, importantly, connections with faculty who themselves are well positioned in academic networks (Contreras, Malcom, & Benjamin, 2008). Through these relationships and bolstered by the knowledge accrued through rigorous coursework and co-constructed with intellectually proficient classmates, Latinx students could begin to fight their way into positions of power and influence.

Unfortunately, HSIs are not the sites were this kind of capital can be gained. For starters, the majority of HSIs are two-year schools, which means that students are more or less limited to one or more associate degrees or professional certifications (HACU, 2018). Such credentials are meaningful if the goal is to specialize in a trade, earn a paycheck at least, and at most exert influence over minor decisions at a company, but they are not the type of credential that is likely to lead to

top positions in corporations or the government (Bradburn, 2003). However, even after putting two-year schools aside, the majority of HSIs which are also four-year institutions barely amount to the same academic achievements from their students as Predominantly White Institutions and HBCUS, who continuously outperform HSIs in graduation rate and education equity (Contreras et al., 2008). Of the 492 four-year HSIs, the overwhelming majority are considered to be "non-selective," meaning that there are essentially no admissions criteria (Lavin & Hyllegard, 1996). The question thus remains whether Latinx students are better served by attending an institution in which a larger percentage of students "look like them," or whether they are better off attending a school that confers degrees that will be seriously.

Proponents note that HSIs produce more PhD earners than do PWIs nationwide, a statistical fact intended to quell concerns about the overall quality of HSIs (Cuellar, 2014). However, presenting a raw number in this scenario is little more than a magic trick that proponents use to distract the unsophisticated from more important numerical considerations. Consider the popular idea that marijuana is a gateway drug for heroin addiction (Morral, McCaffrey & Paddock, 2002). As the arguments go, most people who end up as heroin addicts smoked marijuana before they experimented with heroin for the first time (DeSimone, 1998). On the surface, this seems like an open and shut case: smoke dope and you become a junkie. The problem lies in the difference between sampling on a large proportion to make inferences about a small proportion as opposed to sampling on a small proportion to make inferences about a larger proportion. If a very large proportion of people have smoked marijuana at some point in their lives, but only a few of those people end up addicted to heroin, the odds of predicting whether someone who smoked marijuana will end up an addict are low. If, on the other hand, very few people ever smoked marijuana and almost all of them ended up as heroin addicts, marijuana smoking would be a quite powerful predictor variable. Applying this same reasoning to HSIs, we need only consider HACUs gleeful pronouncements about the number and, more importantly, the proportion of Latinx students who matriculate at an HSI at some point in their academic careers to realize on which side of the marijuana example their predictor variable lies.

The challenge of accounting for what happens to alumni of HSIs is difficult well before a doctoral degree would even be relevant. To my knowledge, there are no data on the proportion of two-year

students who eventually make their way to any four-year school, much less a selective institution. In fact, by looking at trends in Latinx enrollment at the flagship universities in Texas and California, we can see that none of the most prestigious state schools saw a dramatic increase in Latinx enrollment after the HSI designation came to be. If two-year universities are the "gateway colleges" they are made out to be, we should have seen an explosion in Latinx enrollment over the past 25 years.

A more accurate portrayal comes from the machinations of none other than former Supreme Court Justice Antonin Scalia. In denouncing affirmative action in higher education, the obsessively right-wing justice proclaimed that Black students should not be included at the nation's most prestigious colleges and universities because they are underprepared to succeed once they get there and, equally importantly it seems, they would feel more comfortable at schools that enrolled a greater number of Black students. Ironically, proponents of HSIs, mostly left-leaning scholars who would be highly offended by someone confusing them for a Scalia ally, make the same argument when it comes to HSIs. Separate and unequal seems to play better when it comes to segregating Latinx students into substantially weaker post-secondary institutions than it does when the same logic is applied to keeping Black students out of Ivy League schools.

Critical Consciousness

Of course, it could be possible that opportunities arise within an otherwise oppressive structure that allows Latinx students to develop a healthy ethnic identity and to become more politically energized (Hubbard & Stages, 2009). For example, Latinx students would seemingly be more likely to find Latinx faculty, Chicano Studies, and other self-relevant ethnic studies programs and student organizations that would scarcely be present on more elite campuses. These identity-affirming experiences could scaffold students toward the type of intrapsychic qualities that would pay dividends as they make their way into the workforce and become enthusiastic participants in our democracy (Velasquez, 1999).

The reality is much different. Statistically speaking, a Latinx student is much more likely to find a Chicano Studies program at a top 25 university than they are at an HSI. This should come as no surprise, since the structure of the institution is not designed to promote critical consciousness. A testament to this fact can be seen in the conspicuous absence of mission statements mentioning the words Mexican,

Mexican-American, Latinx, Latino and so forth (Nelson, Bridges, Morelon-Quainoo, Williams & Holmes, 2007). Defenders of the HSI concept argue that mission statements are inert and really have no day-to-day influence on how students experience college. They see mission statements as artifacts dating back decades, sometimes over one hundred years. Changing them now, they say, would be a bureaucratic hassle that would not yield anything useful to Latinx students. Real change comes in the form of direct student support and other mechanisms to increase access to the institution.

This line of reasoning is dangerous not only because it is false, but because it promotes a narrative that is extremely corrosive to the development of a powerful HSI. It is false because organizations are tasked with manifesting their mission statement, and when convenient, administrators refer back to it to compel faculty to behave in desired ways. Artifact or not, the mission statement provides meaningful information about why the institution exists and what students can expect from it (Contreras, Malcom, & Bensimon, 2008).

It is dangerous because it plays into a corrosive narrative about the inferiority of schools attended by a critical mass of Latinx students. The general belief seems to be that changing the mission statement and advertising HSI status will be harmful in terms of recruiting non-Latinx (read White) students. Like it or not, White students are the most important recruiting targets in the eyes of White administrators because they have the economic means to keep the doors of the HSI open. Seeing that a college pays attention to Latinx students might mean that less than full, unwavering attention is paid to White students. While there may be some risk in playing into White narcissism, if economically endowed White students stop attending, the institution will not be able to carry out the business of educating economically disenfranchised Latinx students.

To a certain extent, White students should not be blamed for steering clear of schools that Latinx students attend in high numbers. The primary and secondary school system has undoubtedly sent a crystal-clear message that as the proportion of Black and Latinx students goes up, the quality and, more accurately, the prestige of the school goes down. Willfully attending an HSI when there are other options based on resources and ability to meet admissions criteria would be sheer foolhardiness.

Strangely, this logic does not stop other types of institutions from promoting their affiliations with human subgroups. For example,

all HBCUs mention the words Black or African American in their mission statements. Catholic colleges and universities also seem minimally nervous about showcasing their religious affiliation (. Administrators do not seem equally concerned that a Protestant or Buddhist student will turn away from a Catholic college or that an Asian-American will be too terrified to step foot on the grounds of an HBCU. The takeaway message, then, is that HSIs simply do not want to centralize Latinx students in the ways that Catholic colleges and HBCUs centralize their target populations (Sanford, Rudick, Nainby, Golsan, Rodriguez , & Claus, 2019).

The Department of Education plays a role in this conspiracy as well by not requiring, or for that matter, even incentivizing the Latinization of HSIs. *Excelencia in Education*, a non-profit organization focused on promoting the interests of Latinx students does take note of the ways in which HSIs address the unique needs and desires of Latinx students but being recognized by *Excelencia* does not carry with it the promise of cash. At the end of the day, administrators are driven by the bottom line, and it simply does not serve the financial interests of their institutions to scare away rich White students, just like it does not benefit their political allies and donors to radicalize a bunch of economically deprived Latinx young adults.

The Motivation for Current Status of HSIs

One might wonder why administrators, HACU, and the Department of education would be so invested in developing the HSI designation when it would seemingly be easier to ignore the plight of Latinx students altogether. The answer, I believe, can be found in critical race theory, and more specifically, in the concept of interest convergence. According to Derrick Bell, civil rights gains are rarely won, but when they are, it is usually because a policy change that benefits White people just happens to benefit a racial/ethnic minority as well (Bell, 1980). The famous *Brown v. Board* ruling that supposedly put an end to segregation in our nation's schools is often used as an illustrative example of this concept. Black students did not earn the right to attend otherwise all White schools because they were suddenly more human or more hygienically pure; they were afforded the right because allowing them to attend sent a message both domestically and internationally that the US was more morally sound than the Nazis who had just been defeated in World War II, a message that was important to secure economic and military cooperation overseas and to facilitate military recruiting efforts at home. Similarly, in the University of

Michigan Law School affirmative action case, the university won not because it was socially just to have an integrated law school or because Blacks and Latinx students were owed some form of reparations, but because it benefitted White students to be exposed to Black and Latinx classmates. In both cases, Black and Latinx people won the court case because it was determined that White people would also benefit from the decision.

The question about HSIs, then, is "What's in it for the White folks?" As mentioned previously, the HSI functions as a mechanism of assimilation. Latinx students can be subjected to additional proselytization about the sanctity of capitalism and the mythical relationship between additional years of schooling and economic might. The movement away from the liberal arts also ensures that they are unlikely to be challenged to think too hard about social or political matters, but instead can be prepared for a trade that will lock them into an inconsequential role in society as consumers rather than producers of ideology and policy. They can even be shamed into leaving behind their inferior Spanish in exchange for peninsular Spanish that is more correct than what they grew up learning (Hill, 1998). True to behaviorism, they are held accountable to these requirements lest they find themselves facing mountains of student loan debt with no degree in hand.

Those who try to resist the assimilation process can search for comrades, but they are unlikely to find student organizations or degree programs that kindle their spirits. What they are likely to find instead are White faculty who are either race-neutral or motivated to save Latinx students from the barrios and third-world countries from which they came. Even their classmates realize how the behaviorist game is played: assimilate and form the types of relationships that allow you to be tokenized once you are in graduate school or resist and forfeit research opportunities and letters of recommendation that are sorely needed in order to penetrate the next stop in the educational pipeline.

There is also a certain comfort in familiarity, so ridding the schools of Latinx cultures brings a sense of joy to many faculty and administrators. But few things bring as much joy as money. With the rising percentage of young Latinx people in the population, there is a market to be exploited by opening schools that provide a place for Latinx students, their families, and taxpayers to deposit their cash. In an otherwise tight job market, White faculty and administrators have a much higher chance of landing a job because low quality, assimilationist HSIs need them to deliver the gospel of White culture

and corporate capitalism. That they can use their position to reinforce White dominance through "scientific" methods, preparation for trade school, and the obliteration of Mexican-American Spanish is an added bonus.

The Brown Intelligentsia

A particularly humorous aspect of the HSI debate (if not for its implications) is the fact that so many proponents of HSIs are Latinx scholars. Mind you, this is not a cadre of Latinx faculty that resemble a random sample drawn from the full population. They are scholars representing some of the most prestigious universities, places like the University of California Los Angeles and The Ohio State University, and Hispanic organizations, such as HACU and *Excelencia in Education*. Of course, there are well-meaning White faculty who speak out on behalf of HSIs as well. Those faculty are also typically located at premier institutions like the University of Pennsylvania and the University of Florida. Few of the top writers in the area are employed at actual HSIs.

With such strong academic credentials, it may at first blush appear irrational and perhaps a bit irreverent to question the leading authorities on these matters. The problem, however, is that their behavior belies their argument. Each of those scholars made a decision to work at an elite college or professional institution rather than an HSI. As outsiders, we might assume that either they had a choice between a less prestigious HSI and their current workplace or that they declined to apply to HSIs in the first place because it was beneath them to do so. The answer to this question most likely varies by individual, but the fact remains that they found their way to highly selective colleges and universities, sometimes after ditching an HSI to do so.

Their behavior might seem a tad hypocritical unless we reflect on the core argument used to defend HSIs. That is, that while there may be problems with HSIs in terms of their selectivity, low retention and graduation rates, and weak portfolio of influential graduates, something is better than nothing for Latinx students who performed poorly or received an inferior K-12 education prior to applying to college. Some authors, such as Calderón Galdeano and Rodriguez have even gone so far as to use advanced statistical methods to show that HSIs are worthwhile (Rodriguez & Calderón Galdeano, 2015). Using propensity score matching, they were able to compare how well PWIs would do if they were as under-resourced as HSIs and had to educate students who were as academically bankrupt as the Latinx students enrolled at HSIs.

Their results indicated that PWIs would perform equally as poorly as HSIs in those conditions (Flores & Park, 2015).

In the eyes of the authors, it is soothing to know that PWIs would do as lousy of a job as HSIs if they were similarly situated, an outlook that clearly holds Latinx students in HSIs in exceptionally low regard. Their position also neglects to consider what could happen if the Department of Education invested in educational equity in the K-12 years rather than rewarding colleges and universities for operating as factories that churn out students who are easily swayed by assimilation rhetoric and more than eager to earn a mediocre diploma.

The "it's good for other people, but not for me and mine" position is also an excuse for more prestigious institutions to avoid full inclusion of Latinx students in terms of representation on campus, degree options, and pedagogy. As long as Latinx students have their own schools, there is no need to include them in large numbers, and as long as very few infiltrate the otherwise White space, there is no reason to change the ecology of the campus to pander to a numerical minority. Ironically, it is in those White spaces that Chicano Studies programs emerge. Rather than being dominated by Latinx students, they are typically comprised of White students who understand that there is a strategic advantage to understanding Latinx people and who have enough capital in hand that they do not need to be prepared for a trade. Like the University of Michigan law school case, foreign language requirements, and diversity requirements, this relic of Latinx culture continues to exist because it primarily serves the interests of White people.

What Can be Done?

If there is hope for HSIs it lies within the reinvention of colleges and universities in the form of HBCUs rather than Indian boarding schools. HBCUs forefront their identity, which is made possible by the deliberate acknowledgment of their purpose and their staffing around that purpose. There is no worry about keeping White students away. Ironically, the proportion of White students at HBCUs has actually risen considerably during the time that HSIs have been formally designated (Hill, 1998).

Unfortunately, this dramatic change, of course, is highly improbable. Not only do HSIs benefit White people directly through the provision of jobs to mostly non-competitive faculty and administrators and effectively subdue Latinx students into docile workers, but there is also simply no urgency among Latinx students and their families to

strive for anything different (Garcia, Okhidoi, 2015). Black students who attend HBCUs are, for the most part, unashamedly Black (Mobley, 2017). There is no confusion in their mind about whether they can pass for White or whether "playing the game" is going to land them in a second-rate managerial job where they can personally benefit from keeping other Black people down. They understand that, unlike other racial/ethnic minorities, when times get hard, they cannot console themselves by celebrating "at least I am not Black." They have accepted that they are Black and what that means in life, and they have set about trying to define themselves in healthy and productive ways in an antagonistic society.

Latinx students at HSIs emanate from a very different place. Much of what Latinx students feel is culturally relevant, such as last names and language are markers of Whiteness through their relationship with Spain. Because of the way race is practiced in places like Mexico, being Spanish carries more status than being indigenous. Therefore, the pursuit of things European conflicts with any sense of advocacy for Latinx students as racially different from Whites. In the end, there is less than full commitment to ethnic advocacy because all bets are hedged by the hope of eventually being fully accepted as White, a hope that is less widely believed among Black people.

At the same time, there is variability among Latinx students mostly based on geographic region. Some colleges and universities in California have a history of activism that still permeates the thinking of faculty and students to this day. There is some chance at those institutions that students do and will continue to demand better treatment and, maybe in time, full inclusion in the University of California system (HACU, 2018). The other state with a large share of HSIs is Texas, and that is where hope is lost (HACU, 2018). Latinx students in Texas colleges and universities have mostly bought into the promise that they can have minimally acceptable jobs that pay a fair wage if only they are willing to buy into the White way of life. For these students, the tradeoff between occupying a place in the barrio for yet another generation in order to maintain culture is not worth it. They are more than willing to put their family and neighborhood behind them if it means moving to a Whiter part of town and earning a modest living.

Reconstructing the HSI is, therefore, an ominous task. The status quo is designed to strip away culture and produce a complacent workforce that will not disrupt White claims to authority and power.

Inertia is not on the side of the revolution. Within schools, students are not encouraged to organize or to earn degrees that would promote the idea of overthrowing the state or, short of that, the HSI. They are instead rewarded for going along with whatever the White faculty and administrators put before them. More importantly, there appears to be the faintest of hope that through assimilation and inter-ethnic marriage, the Latinx student will pass as White. In comparison to the odds of exacting meaningful change at the institutional or societal levels, passing at White seems eminently doable.

Finally, and perhaps most sadly, the leaders that provide the best opportunity for role modeling are Latinx scholars who have made their careers on the backs of students at HSIs. Whether deliberately or not, these educators are policy influencers who have carved out a niche in the academic world due to their ability to write in a scholarly tone about the benefits of HSIs. They are willing to endorse the assimilationist mentality and low quality of education provided to Latinx students if it means that they can earn tenure and, if they are lucky, emigrate to a prestigious PWI. Their employment at these very elite schools, rather than being perceived as a mark of hypocrisy, is cast as evidence that assimilation pays in the long run. Against this backdrop, the perpetual mistreatment of indigenous populations plays out well into the 21st century in our newest version of the Indian school.

References

Amy Aldridge Sanford, C. Kyle Rudick, Keith Nainby, Kathryn B. Golsan, Stephanie Rollie Rodriguez & Christopher J. Claus (2019) "'I Was Gonna Go Off, but My Best Friend is White.": Hispanic Students' Co-Cultural Reasoning in a Hispanic Serving Institution, Communication Quarterly, 67:2, 158-177, DOI: 10.1080/01463373.2018.1557723

Bell, D. (1980). Brown v. Board of Education and the Interest-Convergence Dilemma. *Harvard Law Review, 93*(3), 518-533. doi:10.2307/1340546

Blake, D. (2018). Motivations and Paths to Becoming Faculty at Minority Serving Institutions. *Education Sciences*, *8*. Retrieved from http://search.ebscohost.com/login.aspx?direct=true&db=eric&AN=EJ1174994&site=ehost-live&scope=site

Bradburn, E. M. (2003). *Short-term enrollment in postsecondary education: Student background and institutional differences in reasons for early departure, 1996–98* (NCES Publication No. 2003-153). Washington, DC: U.S. Government Printing Office

Caden, B.V. (2004). Serving emerging students. In B.V. Laden (Ed.), Serving minority populations: New directions for community colleges. *San Francisco, CA: Jossey-Bass*

Cuellar, M. (2014). The Impact of Hispanic-Serving Institutions (HSIs), Emerging HSIs, and Non-HSIs on Latina/o Academic Self-Concept. *The Review of Higher Education* 37(4), 499-530. Johns Hopkins University Press. Retrieved June 27, 2019, from Project MUSE database.

Contreras,F.E., Malcom, L.E., & Benjiman, E.M. (2008). Hispanic Serving Institutions: Closeted identity and the production of equitable outcomes for Latino/a students. *In M.Gasman, B. Baez, & C.J.V. Turner (Eds.), Understanding Minority-Serving Institutions (pp. 71-90). Albany: State University of New York Press*

DeSimone, J. (1998). Is Marijuana a Gateway Drug? *Eastern Economic Journal, 24*(2), 149-164. Retrieved from http://www.jstor.org/stable/40325834

Flores, S. M., & Park, T. J. (2015). The Effect of Enrolling in a Minority-Serving Institution for Black and Hispanic Students in Texas. *Research in Higher Education*, *56*(3), 247–276. Retrieved from http://search.ebscohost.com/login.aspx?direct=true&db=eric&AN=EJ1057965&site=ehost-live&scope=site

Garcia, G.A. (2013). Challenging the Manufactured Identity of Hispanic Serving Institutions (HSIs): *Co-Constructing an Organizational Identity. UCLA.*

Garcia, G. A., & Okhidoi, O. (2015). Culturally Relevant Practices That "Serve" Students at a Hispanic Serving Institution. *Innovative Higher Education*, *40*(4), 345–357. Retrieved from

http://search.ebscohost.com/login.aspx?direct=true&db=eric&AN=EJ1068680&site=ehost-live&scope=site
Hill, J. 1998 Language, race and white public space. American Anthropologist 100 (3): 680-689. Hymes, D.1974. *Foundations in Sociolinguistics:* An Ethnographic Approach. Philadelphia PA: University of Pennsylvania

Hispanic Association of Colleges and Universities. (2018) 2018 Fact Sheet Hispanic Higher Education and HSIs [PDF file]. https://www.hacu.net/images/hacu/OPAI/2018_HSI_FactSheet.pdf

Greene, D., & Oesterreich, H. A. (2012). White Profs at Hispanic-Serving Institutions: Radical Revolutionaries or Complicit Colonists? *Journal of Latinos and Education*, *11*(3), 168–174. Retrieved from http://search.ebscohost.com/login.aspx?direct=true&db=eric&AN=EJ978532&site=ehost-live&scope=site

Higher Education Act of 1965, as amended in 1998. *Title V*, *Developing Hispanic-Serving Institutions Programs.* http://www.ed.gov/policy/highered/leg/hea98/index.html

Hubbard, S. M., & Stage, F. K. (2009). Attitudes, Perceptions, and Preferences of Faculty at Hispanic Serving and Predominantly Black Institutions. *Journal of Higher Education*, *80*(3), 270–289. Retrieved from http://search.ebscohost.com.blume.stmarytx.edu:2048/login.aspx?direct=true&db=eric&AN=EJ841999&site=ehost-live&scope=site

Lacagnino, S. N. (2019)., The Effect of Participation in a Title V Program on Latinx student success at a Community College (2019). *Seton Hall University Dissertations and Thesis (ETDs), 2642.* https://scholarship.shu.edu/dissertations/2642

Lavin, D. E., & Hyllegard, D. (1996*). Changing the odds: Open admissions and the life chances of the disadvantaged. New Haven,* CT: Yale University Press. and universities (pp.5-47). New Brunswick, NJ: Transaction

Mobley, S. D., Jr. (2017). Seeking Sanctuary: (Re)Claiming the Power of Historically Black Colleges and Universities as Places of Black

Refuge. International Journal of Qualitative Studies in Education (QSE), 30(10), 1036–1041. Retrieved from http://search.ebscohost.com/login.aspx?direct=true&db=eric&AN=EJ1160973&site=ehost-live&scope=site

Morral A. R., McCaffrey D. F., & Paddock S. M. (2002, 11 December) Reassessing the Marijuana Gateway Effect. Society for the Study of Addiction. Retrieved from: https://doi.org/10.1046/j.1360-0443.2002.00280.x

Nelson Laird, T. F., Bridges, B. K., Morelon-Quainoo, C. L., Williams, J. M., & Holmes, M. S. (2007). African American and Hispanic Student Engagement at Minority Serving and Predominantly White Institutions. Journal of College Student Development, 48(1), 39–56. Retrieved from http://search.ebscohost.com.blume.stmarytx.edu:2048/login.aspx?direct=true&db=eric&AN=EJ756183&site=ehost-live&scope=site

Nora, A., & Crisp, G. (2009) Hispanics and Higher education: An overview of research, theory, and practice. In J.C. Smart (Ed.), *Higher education: A Handbook of theory and research (pp. 321-358).* Dordrecht, Netherlands: Springer.

Rodriguez A., Calderón Galdeano E. (2015). *Hispanic Serving Institutions*. New York, NY: Routledge.

Robbins, R., Colmant, S., Dorton, J., Schultz, L., Colmant, Y., & Ciali, P. (2006). Colonial Instillations in American Indian Boarding School Students. *Educational Foundations*, *20*(3), 69–88. Retrieved from http://search.ebscohost.com/login.aspx?direct=true&db=eric&AN=EJ794733&site=ehost-live&scope=site

Santiago, D.A. (2006, March). Inventing Hispanic - Serving Institutions: *The basics. Washington, DC: Excelencia in Education.*

Solorzano, D., Ceja, M., & Yosso, T. (2000). Critical race theory, racial microaggressions, and campus racial climate: The experiences of African American College Students. *Journal of Negro Education, 64 (½), 60-73.*

Velasquez, P. (1999). *The Relationship between Cultural Development, Sense of Belonging, and Persistence among Chicanos in Higher Education: An Exploratory Study. ASHE Annual Meeting Paper*. Retrieved from http://search.ebscohost.com/login.aspx?direct=true&db=eric&AN=ED437014&site=ehost-live&scope=site

Villarreal, R.C. & Santiago, D.A. (2012). From Capacity to success: Hispanic Serving Institutions (HSIs) and Latino student success through Title V. *Washington, DC: Excelencia in Education.* www.edexcelencia.org/hispanic-serving-institutions-hsis

Wilson, V.R. (2008). The effect of attending an HBCU on persistence and graduation outcomes of African American college students. *In C.C. Betsy (Ed.), Historically black colleges.*

Investigative Study of an Anomaly at Bracken Bat Cave Preserve Using Electrical Resistivity

Cresencia Barrera

Mentors: Evelyn Mitchell, Ph.D.
St. Mary's University, San Antonio, TX

In a past resistivity survey on the Bracken Bat Cave Preserve property, an anomaly was detected on the fringes of one of the models that suggested the presence of a possibly large solution cavity. However, since the feature was on the edge of the detection limits, further study of the area was needed. An electrical resistivity survey using the dipole-dipole method was conducted to investigate the subsurface of the area for possible karst features. A two-dimensional inverted profile model was produced, revealing the existence of five small dissolution features. While the discovery was not a sizable new cave passage as previously indicated, the adjacent cave features and the small-scale voids will help in providing a clearer picture of the hydrologic properties on the preserve.

Introduction

During the Cretaceous period, the Western Interior Seaway existed, engulfing most of Texas. After the Paleogene, the shallow marine waters began to recede, exposing the seafloor's accumulated sediments, which eventually lithified. The rolling hills of the Edwards Plateau are attributed to the Miocene-age oblique normal faults of the Balcones fault system that formed during the late Oligocene and early Miocene (Clark 2018). Its fractures lie parallel to the subcrop (buried ancient eroded surfaces) of the Ouachita thrust front (Newcomb 1971). Within the fault system exists the Edwards and Trinity aquifers, with the Trinity forming the catchment area for the Edwards recharge zone (Clark 2009).

Bracken Bat Cave Preserve (Figure 1) is in the southern Comal County Bat Cave quadrangle near Garden Ridge and lies above the Edward's recharge zone. The preserve has been identified as having a savanna type vegetation where Ashe Juniper, Live Oak, Mesquite, Prickly Pear, and Texas Persimmon are prolific. Topographic elevation of the quadrangle ranges from approximately 720 feet to 1,250 feet beginning in the southeastern section and running towards the northwestern section of the quadrangle, with a total relief of 530 feet.

(Newcomb 1971). There are three small, karst features within a 250-meter radius of the anomaly, each with relatively narrow, vertical entrance passages. The caves are located on the western end of the survey line and appear to have been formed through dissolution of the exposed and permeable Kainer limestone by surface water infiltration.

Figure 1. Map of Bracken Bat Cave Preserve.

Most cave formations are in the vadose zone and are epigenic in origin. For Bracken Bat Cave, the area was once in the phreatic zone, but is presently located above the water table in the unsaturated zone and is considered an epigenic cave system. The cave developed in the Kainer Formation, with its main passage located at the boundary that separates the Upper Glen Rose Formation from the Basal Nodular Member of the Kainer Formation (also known as the Walnut Formation in older publications), along a family of parallel and evenly spaced fractures. This joint set is perpendicular to Bat Cave fault that is approximately 300 yards south of the Bracken Cave entrance. The exposed rock unit at the surface surrounding the cave is the Kainer formation of the Edwards Group. The Glen Rose Formation of the Trinity Group is not visible but is present beneath the Basal Nodular Member within the 100-foot diameter collapsed doline (sinkhole). The cave's main passage has an overall approximate height of 30 feet, with its ceiling detected at a depth of 66 feet (Newcomb 1971).

The stratigraphic units (Figure 2) of the study area are the Upper Glen Rose formation of the Trinity group, and the Basal Nodular Member of the Kainer Formation of the Edwards group. The Kainer

Formation has a thickness of 230 – 240 feet, is generally fossiliferous, with the presence of small gastropod mold masses, miliolids and oysters (Pelecypoda). It is composed of rudists bivalves' rich mudstones and wackestones, intertidal (deposited between mean high and low tide) and supratidal (deposited above mean high tide) dolomitic mudstones, indurated oosparite, pockets of pulverulent limestone, and indurated intrasparites. Also included in the formation are lenticular nodule chert, miliolid grainstone, evaporites, crystalline limestone, and dolomitic limestone with a basal nodular member (Newcomb 1971).

Figure 2. Stratigraphic column of Comal County based on Small 1997

Lower Cretaceous	Edwards Group	Pearson Formation	Cyclic and Marine Members	0-70 ft
			Leached Member & Collapsed members	30-80 ft
			Regional Dense Member	20-30 ft
		Kainer Formation	Grainstone Member	45-60 ft
			Kirschberg Evaporate Member	65-75 ft
			Dolomitic Member	110-150 ft
			Basal Nodular Member	45-60 ft
	Trinity Group	Glen Rose Formation	Upper Glen Rose	350-500 ft

The Basal Nodular Member lies at the base of the Kainer Formation and above the Upper Glen Rose Formation having an overall thickness of approximately 48 feet at this location. It is composed of pelletal biomicrite and fossiliferous pelsparite, with argillaceous and arenaceous biomicrite that is slightly glauconitic (iron potassium phyllosilicate mica). There are several small, coarsely crystalline calcite lined cavities at the lower section of the unit as well. Whole valves of Exogyra texana (Bivalvia), Trigonia (Bivalvia), Texigryphaea (Bivalvia), gastropod (mollusk) and clam mold masses, ostracods

(crustacean), oyster shell-fragments, and echinoid (sea urchin) spines are also present in the formation (Newcomb 1971).
The relatively impermeable Glen Rose formation is divided into two lithostratigraphic members by masses of Corbula harveyi internal casts (steinkerns), called the Upper Glen Rose and the Lower Glen Rose, with an approximate overall thickness of 800-900 feet. However, the lower portion of the formation is more vulnerable to solution cavies than the upper section. The Upper Glen Rose is comprised of interbedded marly biomicrite, biosparite, evaporite dolomite, crystalline dolomite, interbedded dolomitic biomicrite, fossiliferous intrasparites, limestone, and argillaceous biomicrite (Newcomb 1971).

Each year from March to October 20 million Mexican Free Tail Bats (Tadarida brasiliensis) migrate to Bracken Cave, making it the largest bat colony in the world Iskali & Zhang 2015). In 1992 Bat Conservation International initially purchased 697 acres of ranch land from the Marbach family and with the aid of the Nature Conservatory, later purchased an additional 1547 acres of surrounding land for $20.5 million, saving it from development (Nature Conservatory 2019). Apart from protecting the bat population, the preserve's unique ecosystem is inhabited by native and endangered species, including the Black-capped Vireo and the Golden Cheek Warbler.

Since the entrance into Bracken Bat Cave is a 100-foot diameter collapsed feature, BCI is interested in locating any other significant passages that might be in the area. This is partly due to their goal of protecting hydrological resources within the preserve. By becoming more informed about the caves' passages, it may help with understanding water infiltration in the area and the extent of its relationship with recharging the Edwards Aquifer. With the aid of resistivity surveys, identifying and mapping possible cave systems would also allow the agency to consider construction proposals for educational or research facilities on the property.

In an attempt to locate possible caves in the preserve, a resistivity survey (Figure 3) was performed on the property by Dr. Ron Green (2008) of the Southwest Research Institute in August 2008. In one of the models, an anomaly was detected on the fringes of the rendering, indicating a possibly large solution cavity. However, there is reasonable doubt that the feature exists since the rendering is at the end of the survey line. Because of this uncertainty, an additional electrical resistivity survey was conducted to explore the area's subsurface to validate potential karst features. The results obtained will add to the

knowledge of karst passages in the preserve and will reveal if there is an underlying relationship between the known caves near the anomaly and the possible cave at the study site.

Figure 3. Aerial photo of Bracken Bat Cave Preserve with an overlay of the previously performed resistivity study. Photo taken from Green (2008).

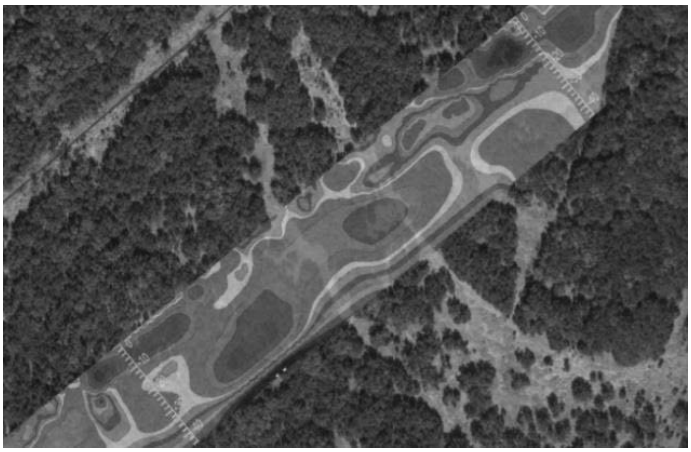

Methods

The noninvasive electrical resistivity tomography technique was used to image the subsurface geology of the study site. Attributed to the array's high sensitivity to horizontal changes in resistivity and its ability to produce detailed imagery of a target's lithology, the dipole-dipole method was chosen for the survey (El-Qady 2005). Inversion quality is directly related to image accuracy, therefore using a least-squares inversion with a smoothness regularization model was utilized to minimize model errors and data misfit (El-Quady 2006). To produce accurate resistivity models, an ideal absolute error below 10% is preferred and is achieved by completing multiple iterations of the data (Gupta 2015).

Generally, dry, nonporous dolomite and limestone host rock typically have high resistivity values, fluid-filled voids have low resistivity values, and air-filled voids are highly resistive or nonconductive causing resistivity contrast between the host rock and void (Kaufmann 2015). When highly resistive anomalies are present in a 2D inverted profile, it is typically considered a positive indication of a void (Zhu 2016).

Figure 4. Map of survey area.

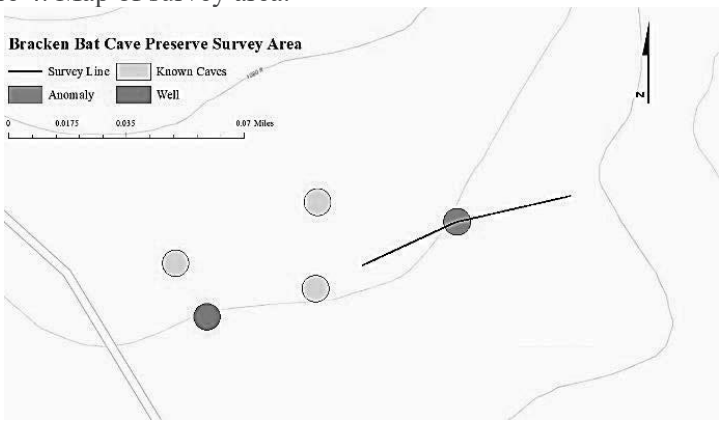

Preparation of the site involved measuring a 104-meter line for the placement of 52 electrodes at intervals of 2 meters along a linear pathway (Figure 4). After the galvanized probes were hammered into the ground, a multicore cable that was attached to the AGI SuperSting R8 electrical resistivity meter and was securely connected to each electrode. To improve conductivity of the probes, the surrounding soil was saturated with a saline solution. Prior to executing the resistivity survey, a preliminary contact resistance test was performed to ensure the retrieved data would be acceptable. During the trial, five electrodes that were near exposed bedrock or tree roots, showed high contact resistance measurements despite applying a saline solution to each problematic electrode. The survey was executed after noting which electrodes were likely to produce problematic data.

Every apparent resistivity measurement is taken at the midpoint of each current electrode pair and potential electrode pair. The results are plotted in a pseudosection that represent a colored and contoured, unrefined interpretation of the subsurface. The cross-section values were transferred onto a removeable USB and uploaded into the AGI inversion software for the apparent resistivity values to be processed, creating an approximate representation of the subsurface (Hasan 2017). For a reliable profile model to be developed, a targeted absolute error below 10% was set and accomplished by using the data misfit histogram to remove the poorly-fitted data points. The graph plots the number of collected data points to the relative data misfit error ranging from 0% to 200%. The tool allows the user to choose which data points

to remove based on its error percentage. This action is repeated until the RMS error value is below 10%.

In total, five model iterations, coupled with the removal of the noisy data points, were performed using the EarthImager tool in the AGI program. After the final iteration, a relatively accurate 2D model of the subsurface geologic features was generated. The 2D inverted resistivity profile is a replication of the subterranean lithology that is produced by comparing the measured apparent resistivity pseudosection to the calculated apparent resistivity pseudosection, where the calculated apparent resistivity directly correlates with the measured apparent resistivity.

To generate a reliable model, multiple iterations are performed until the calculated apparent resistivity matches the measured apparent resistivity and is below the targeted error percent value.

Unexpected issues sporadically occur during geotechnical investigations that may negatively impact data interpretations and renderings. One major factor contributing to these adverse effects is the failure to remove or sufficiently reduce noisy data points from the data set. The oversight will usually produce errors in the resistivity model, resulting in false or misleading interpretations of the subsurface geology. To prevent or correct these unanticipated variables, the re-examination of models, reviewing of the linear regression line, assessing the percentage error, and comparing models to cores (if available) should be conducted (Farooq 2012).

Results

Examination of the first inverted profile revealed high resistivity readings at depths of 5.8 meters at electrodes 12-18, and near the surface at electrodes 24-54 (Figure 5). When the best-fit data was reviewed, it was evident that the plotted predicted apparent resistivity and the measured apparent resistivity did not fit well along the best fit line, resulting in an RMS of 814.88% (Figure 6). To combat the error, removal of 153 (4.31%) noisy data points from a total of 3548 was necessary. The noisy data points can be attributed to the electrodes that produced high contact resistance measurements during the contact resistance test, despite saturating the soil with saline.

Figure 5. First iteration of the inverted resistivity profile.

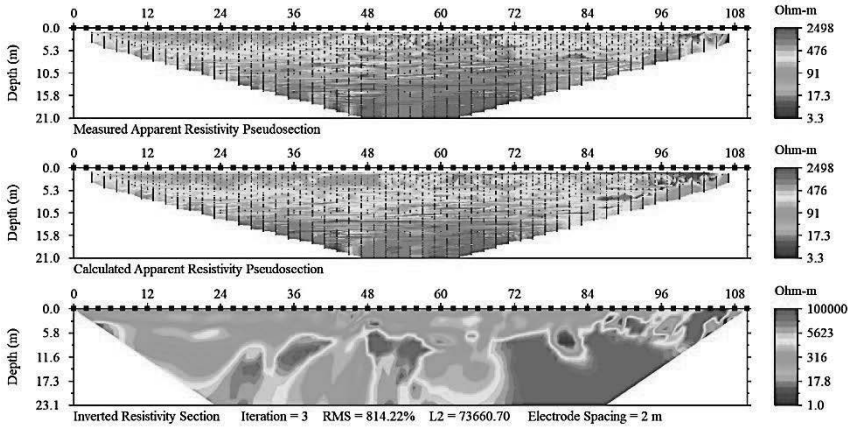

Figure 6. RMS model misfit model of first iteration.

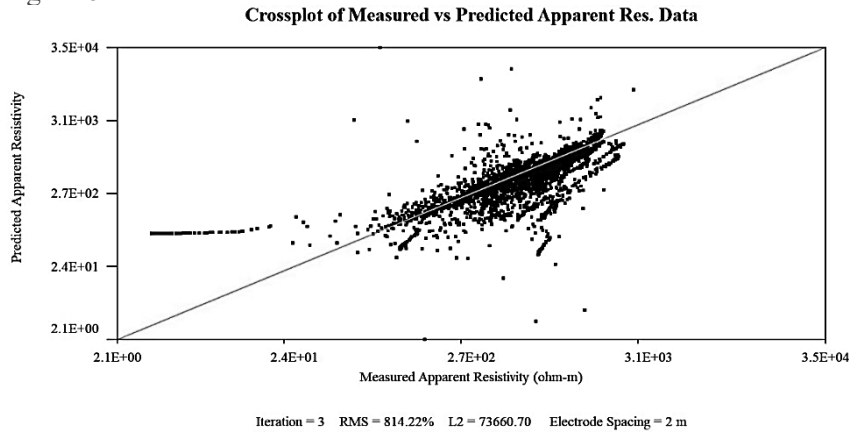

In the fifth iteration, with the removed data points, five voids were identified in the inverted resistivity profile (Figure 7) at electrodes 2-6, 18-24, and 46-53 at varying depths with an RMS of 9.88% (Figure 8). The approximate sizes of the voids in order from left to right are: 10 meters wide with a height of 2.9 meters at a depth of 2.9 meters, 22 meters wide height at a depth of 14.5 meters and continuing into the earth, 6 meters wide with a height of 8.7 meters at a depth of 2.9 meters, 6 meters wide with a height of 2.9 meters at a depth of 2.9

meters, and the final void has minimum height of 11.5 meters with a minimum width of 14 meters at a depth of 8.7 meters.

Figure 7. Fifth iteration of the inverted resistivity profile.

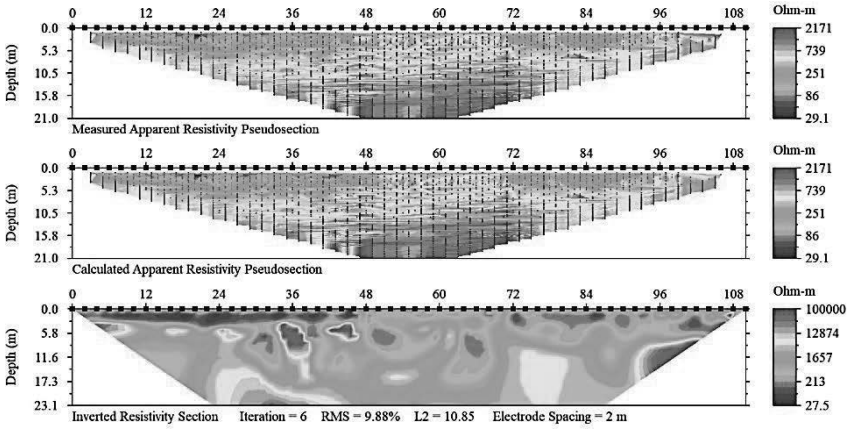

Figure 8. RMS model misfit model of the fifth iteration.

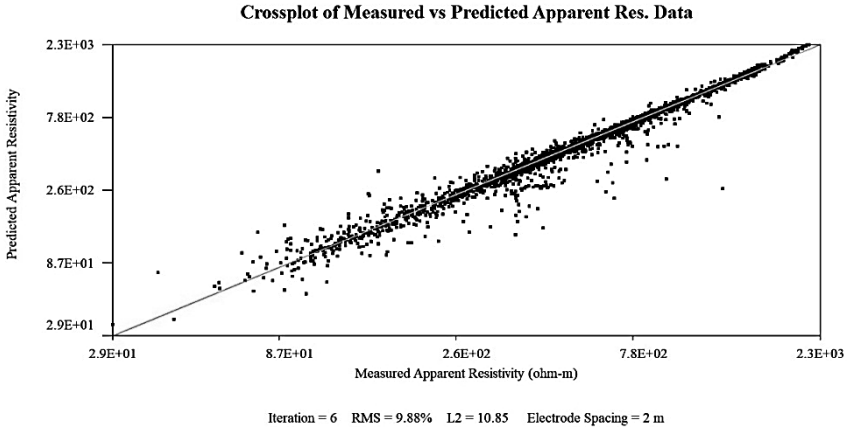

Discussion

After reviewing the location of the small-scale voids in the 2D model and knowing the lithostratigraphic units most prone to cave formation are the Upper Glen Rose Formation, the Kainer Formation, and the contact between the two units; we were unable to determine at what depth this contact exists at the survey area. However, based on the

measurements of the detected karst features, we believe the voids may be within the Kainer Formation, indicating the contact may be lower than the viewing depth of 23 meters. While the small voids that were discovered do not show connections to large cave passages, they, along with the other three cave features near the study site, are positive indications of potentially larger voids in the area.

As for the predicted dimensions of the voids, they may have been exaggerated as a concomitant of the resistivity survey, and we are unsure of their actual size. According to research performed by Mitchell & Mitchell (2017), resistivity surveys can inaccurately calculate cave volumes by a factor greater than ten when compared to LIDAR measurements. With the information provided by the survey, the ability to determine if a relationship exists between the known caves in the vicinity and the small voids detected at the study site was not established, but an association may still exist and could be investigated in a future study.

Conclusions

Although no significant cave passages were found at this location, the existence of other, sizeable cavities and features in the area show that more passages are possible. One recommendation for future work at this site is the application of resistivity surveys above the known cave features in the area to reveal if there is an underlying relationship between them and the newly discovered small-scale voids at the study site. If conducted, a broader view of the subsurface geology would provide insight into the water infiltration conditions that caused the formation of the caves and provide 2D models of the known features, aiding us in interpreting other scans more accurately.

Acknowledgements

I want to express my greatest gratitude to my mentor Dr. Evelynn Mitchell for her invaluable guidance, support, and time she has invested in me. Without your support, this project would not have been possible. I would also like to thank Fran Hutchins for allowing us access to Bracken Bat Cave Property and to Ronald Green of Southwest Research Institute for giving us permission to use and reference his resistivity models and maps.

Additionally, I would like to say thank you to John Hartnell Newcomb, and the meticulous research he conducted on the Bat Cave Quadrangle geology in 1971. His work has allowed me to successfully complete my research project, and accurately describe the geology of Bracken Bat Cave Preserve. Lastly, I want to acknowledge the McNair

Program at St. Mary's University for providing the necessary resources to conduct this investigational survey. Each of these individuals were major contributors in the realization of this study, and I am indebted to their beneficence.

References

Clark, A.K., Pedraza, D.E., Morris, R.R. 2018. Geologic Framework and Hydrostratigraphy of the Edwards and Trinity Aquifers Within Hays County, Texas. U.S. Geological Survey Scientific Investigations Map 3418. [Internet] [cited 2019 May 14] Available from: https://pubs.usgs.gov/sim/3418/sim3418_pamphlet.pdf

Clark, A.R., Blome, C.D., and Faith, J.R. 2009. Map Showing the Geology and Hydrostratigraphy of the Edwards Aquifer Catchment Area, Northern Bexar County, Southcentral Texas: U.S. Geological Survey Open-File Report 2009-1008, 24 p., 1 pl. [Internet] [cited 2019 May 20] Available from: https://pubs.usgs.gov/sir/2014/5074/downloads/Report/Selected_References/2009-1008_pamphlet.pdf

El-Qady, G. Exploration of a Geothermal Reservoir Using Geoelectrical Resistivity Inversion: Case Study at Hammam Mousa, Sinai, Egypt. Journal of Geophysics and Engineering, 2006 June 01; volume 3: issue 2, pages 114–121. [Internet] [cited 2019 March 13]. Available from: https://academic.oup.com/jge/article/3/2/114/5127604

El-Qady, G., Abdalla, M.A., Hafez, M., Ushijima, K. Imaging Subsurface Cavities Using Geoelectric Tomography and Ground-Penetrating Radar. Journal of Cave and Karst Studies, December 2005; volume 67, Issue 3, pages 174–181. [Internet] [cited 2019 February 10]. Available from: https://caves.org/pub/journal/PDF/V67/cave_67-03-fullr.pdf

Farooq, M., Samgyu, P., Young, S.S., Jung, H.K., Tariq, M., Abrallam, A.A. Subsurface Cavity Detection in a Karst Environment Using Electrical Resistivity (er): A Case Study from Yongweol-Ri, South Korea. Earth Sciences Research Journal, June 2012; volume 16: issue 1, pages 8, 75-82. [Internet] [cited 2019 March 13]. Available from: http://eds.b.ebscohost.com.blume.stmarytx.edu:2048/eds/detail/detail?vid=0&sid=f94dccc2-ae68-496b-a3fa-

0556b26855ba%40sessionmgr104&bdata=JnNpdGU9ZWRzLWxpdmUmc2NvcGU9c2l0ZQ%3d%3d#AN=78306763&db=fua

Gupta, G., Patil, J.D., Maiti, S., Erram, V.C., Pawar, N.J., Mahajan, S.H., Suryawanshi, R.A. Electrical Resistivity Imaging for Aquifer Mapping Over Chikotra Basin, Kolhapur District. Environmental Earth Sciences, 2015 June; volume 73, issue 12, pages 19, 8125-8143. [Internet] [cited 2019 March 11]. Available from: http://eds.b.ebscohost.com.blume.stmarytx.edu:2048/eds/detail/detail?vid=24&sid=098b5759-59e6-4ab0-82de-fd3c37362685%40pdc-v-sessmgr01&bdata=JnNpdGU9ZWRzLWxpdmUmc2NvcGU9c2l0ZQ%3d%3d#AN=102899432&db=edb

Hasan. 06 October 2017. Dipole-Dipole Array: Electrical Resistivity Methods, Part 3. AGI. [Internet] [cited 2019 March 13]. Available from: https://www.agiusa.com/dipole-dipole%E2%80%8B-%E2%80%8Barray%E2%80%8B

Iskali, G., Zhang, Y. Guano Subsidy and The Invertebrate Community in Bracken Cave: The World's Largest Colony Of Bats. Journal of Cave & Karst Studies, 2015; volume 77: issue 1, pages 9, 28-36. [Internet] [cited 2019 March 11]. Available from: http://eds.b.ebscohost.com/eds/detail/detail?vid=6&sid=098b5759-59e6-4ab0-82de-fd3c37362685%40pdc-v-sessmgr01&bdata=JnNpdGU9ZWRzLWxpdmUmc2NvcGU9c2l0ZQ%3d%3d#AN=120553953&db=a9h

Mitchell, E.J., Mitchell, J.N. 2017. Comparison of Shallow Geophysical Cave Detection Methods to 3D Lidar Mapping. Proceedings of the 17th International Congress of Speleology, pages 126-129. [cited 2019 June 04].

Newcomb, J.H. August 1971. Geology of Bat Cave Quadrangle, Comal and Bexar Counties, Texas. The University of Texas at Austin. [Internet] [cited 2019 May 20] Available from: https://repositories.lib.utexas.edu/handle/2152/12588

Nature Conservancy. 2019. Protecting Bracken Bat Cave. Nature Conservancy. [Internet] [cited 2019 March 11]. Available from:

https://www.nature.org/en-us/about-us/where-we-work/united-states/texas/stories-in-texas/protecting-bracken-bat-cave/

Zhu, J., O'Dell, G.A., Laudermilk, E.L., Bogosian, G., Currens, J.C., Webb, S.E. February 23, 2016. Locating a Sealed Cave in Kentucky Using Electrical Resistivity Surveys. AIMS Geosciences, 2016, 2(1): 32-44. doi: 10.3934/geosci.2016.1.32. [Internet] [cited 2019 March 11]. Available from: http://www.aimspress.com/geosciences/article/639/fulltext.html

Failure Surfaces Prediction Using Machine Learning

Gissella Lara

Mentor: Juan Ocampo De Los Rios, Ph.D.
St. Mary's University, San Antonio

In engineering and machinery, there can be many faults, such as parts not fitting correctly, incorrect usage of the machine, or different types of failures on the surface of the materials. Over time these materials can fail due to fatigue or overloading. Determining the type of failure can help identify and fix the machinery faster with less downtime. By using the new programming techniques like machine learning contained in TensorFlow, one is able to program an image detecting system that will give engineers the opportunity to take a picture of the failure surface and identify what kind of failure occurred. This new research includes two parts that will eventually correlate programming and failure surfaces, which will identify these failures faster and more accurately. Currently, many engineers have written journal articles describing the different effects of different materials, in regard to loading, temperature, and longevity. Scholars in many fields have used TensorFlow to identify areas such as bone fatigue and dental cavities, but not much information on the subject of fatigue or overload of failure surfaces. This research will provide clear information based on the image uploaded of a failure surface and the variables that caused the fatigue on that specific material. The research begins with learning how to program TensorFlow by identifying failure images to start up and train the program. Then, this data is used to examine and predict the failure by uploading new the images onto the TensorFlow program.

Keywords: Fatigue, overload, engineering, machine learning, and TensorFlow

Introduction

Physics and engineering have come hand in hand when it comes to mathematics for years. Now with the advancement of technology and how people use it in their ordinary lives, technology is coming into the mix as well. Machine learning has made a big impact on getting what used to be massive scales of engineering mathematics

and physics, into the hands of people with the basis of construction of code and algorithms. The foundation of the code of machine learning allows for images and data to be submitted, interpreted, and output a result — such as software identifying cancerous moles, cataracts, and harmful plants to digest. Machine learning can be used in a variety of ways to help people in their ordinary lives [1][2]. With the creation of the algorithm to let the system decide what is right or wrong; whether, something is an object or a person, or whatever the creator decides to predict in their system, the increase in data submitted raises the percentage of accuracy of the results over time. Machine learning allows for the development of a software model through the usage of the users, refining of the algorithm used, or implementing additional data onto the program, all done with minimal usage of complex coding. This learning machine allows for more people to get in touch with technology to develop something that can help people in their jobs, school, or daily lives.

Having machine learning be the base of what many now are using to develop their programs, a new software called TensorFlow has become known to be helpful for people to develop their own ideas for how to identify data or process images. The software TensorFlow allows researchers to download the mainframe of the program and then users complete the code to their needs. This program uses a software library, deep learning, and tensors to analyze the input information and give the result needed to the user. For my research involving failure surfaces due to fatigue and overload, TensorFlow would be very useful with respect to improving engineering designs and determining the root cause of the materials fail point. The hours of work that one must do as an engineer generally involves failure points that need to be identified with hours of calculations. The process of calculations, measurements, and time in determining whether a part failed due to fatigue or overload can lead to mistakes and cause problems during the development of an engineer's project. The development of the program for this research allows for the evolution of precise scanning of a break or failure in a material, due to many images processed and a superior algorithm, any user would then be able to take an image of the failure and in seconds be told what went wrong.

Since TensorFlow is a new program that has been recently released to the public, the literature does not have similar applications like the one attempted in this research. In relation to the software TensorFlow, one must consider the coding and how to embed images

needed to compare to the images the user inputs and the resources used to reflect them.[3][4][5] With having many different materials that engineers use on a daily basis, one must also know the information on their failures and constants to then be embedded into the program.[6][7][8][9] When retaining the articles on TensorFlow and fatigue failures they can then be combined as knowledge onto how to start the program with the inclusion of the information of the failure fatigue points.

With the ongoing advancement in machinery and technology, there will always be new things that can be created to improve an engineer's design. Trying to analyze whether the failure surface was due to fatigue or overload can be helped with this new research program of using TensorFlow to identify fatigue stress failures. Identifying how the cause of a failure on an object can take hours but taking an image and uploading it to find the information can take minutes. Both with the same result, but with a very drastic amount of time it takes to then get the result needed and implementing it into one's design, structure, or just trying to identify the root of the problem when pertaining to that critical failing surface.

Methodology

Process

Building a computational program embedded with image processing recognition requires the knowledge of machine learning, neural networks, and a coding source. For the dedicated research, Python 3.7.3 was used in order to then download the TensorFlow machine learning package. Due to the necessity of different programs involved in connecting to external file links for images or databases such as Docker, one then needs to implement those links under the Python system to be embedded. Having those embedded links and databases allows for the examples on the TensorFlow website to be executed as well as learn how the process for the insertion of new images would need to be formed. From that point the program will maintain its general aspect of input, processing, and output with more critical aspects, as shown in *Figure 1.* Having the system set up to perform the function listed in *Figure 1*, one is now able to use TensorFlow Lite on an iOS device or Android to place the code created and be able to use the camera to upload and deploy wanted images on the embedded devices. (*Figure 2*).

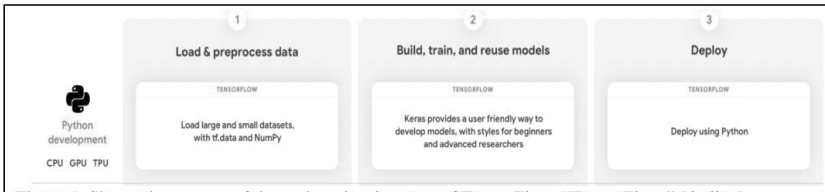

Figure 1. Shows the process of the python development of TensorFlow, "TensorFlow." [Online]. Available: https://www.tensorflow.org/learn. [Accessed: 25-Jun-2019].]

Since the process from the created computation requires to be transferred when using iOS, the use of XCode onto the device used is needed as well. With that process in place, one can embed an external database or take images of fatigue and overload to then be integrated into the image recognition system created.

Figure 2. Explains the process of the iOS development of TensorFlow, "TensorFlow". [Online]. Available: https://www.tensorflow.org/learn. [Accessed: 25-Jun-2019].

TensorFlow Explanation

TensorFlow has been designed to be a software library for high performance numerical computations. By itself, it can only be used as a tool; but, with the knowledge of neural networks and deep learning the number of algorithms for different uses is infinite. In this research, that focuses on image processing and recognition, TensorFlow allows external databases such as Docker or GitHub to retrieve images needed for said project. For this research the images would be pertaining to fatigue and overload. Having downloaded the system under Python the TensorFlow package itself is flexible in that it still allows the user to extend the program into image recognition, texts and sequences, and even estimators. Using the system as image recognition the neural network works to detect a difference for how many different outcomes you could have. Detecting from the largest commonality and minor difference, and building on that aspect to the final layer, or test, being the major developed aspect and giving an output as shown in *Figure 3*.

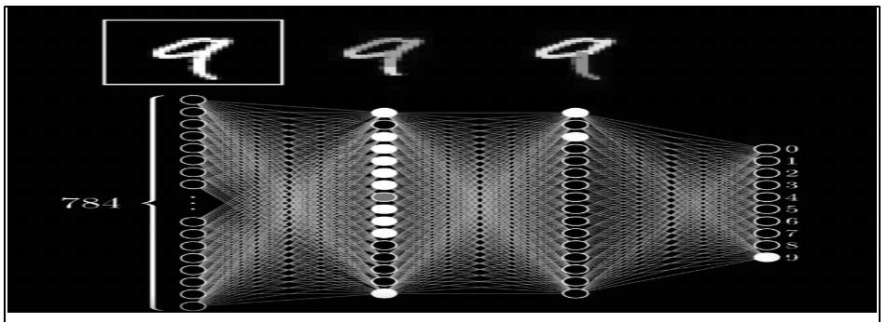

Figure 3. A visualization of the neural network layers trying to identify what the number is, Hacker Shack, *Easy Image Classification with TensorFlow*.

To expand from *Figure 3*, *Figure 4* shows what each layer of the network is considering when looking at a certain number. *Figure 4* shows how the neural network is processing each pixel of the numbers given with a designated curve-- like with the number zero-- or a line-- like with the number four. Each square with a portion of the number equaled to in *Figure 4* shows the procedure of what each layer of the neural network identifies to then assign a prediction of what that number could be. Once the last pixelated portions of the square are evaluated and assigned to a number, the final close-to-exact prediction is made to the number that it should be.

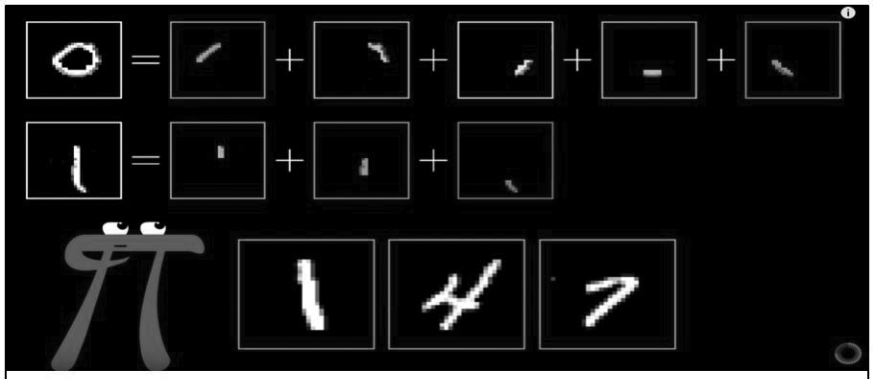

Figure 4. Shows the dissection of pieces of the numbers that each layer of the neural network identifies to then cancel out a result of other images, Hacker Shack, *Easy Image Classification with TensorFlow*.

The above example shows the understructure of the TensorFlow program when using it to add an external database with one's images or just a slight change in the code when transferring it to

TensorFlow lite for iOS mobile. Having the same foundation of the neural network, algorithm, and process, one can then enable the camera on the iOS device, and use transfer learning from a given case study on the TensorFlow website to upload or take images of fatigue, and overload to be analyzed, then given an output on what was the case of the failure surface.

Preliminary Examples

The explanation above provides the foundation for a preliminary example done to understand the software and the coding of how the image processing works. A shoe and clothing example provided on the TensorFlow website, allows the user to download the fashion MNIST dataset onto the users coding terminal that provides different twenty-eight by twenty-eight pixelated images of shoes and clothing. After downloading the example, one is able to use python commands (depending on their downloaded software) to see the first twenty images and how they are classified to then build models based on the set classification of the images (*Figure 5*). With the command in place identifying each item, one can then predict using different commands such as the prediction of the amount of an ankle boot in the first ten image sets.

Figure 5. Fashion MNIST images and the corresponding classification, "Train your first neural network: basic classification | TensorFlow Core | TensorFlow." [Online]. Available: https://www.tensorflow.org/tutorials/keras/basic_classification.

The output shows there is nine predictions that there are ankle boots. After that if the user wants to get specific on how that evaluation was conducted, then a graph is generated on how each pixel from one image is classified using a bar graph. Another graph for the user also appears, showing the image that is being evaluated, it shows where each pixel is to then correspond to what section it is in the bar graph generated (*Figure 6*). With this example downloaded, the user can also choose an image form the dataset and have it be evaluated by the program, or show all of the images from the dataset with their coordinating bar graph as to how precise or inaccurate the prediction is.

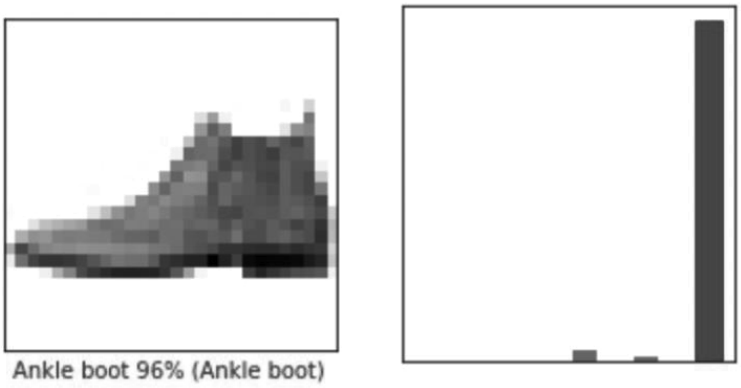

Figure 6. Shows the graphs produced by the preliminary example, "Train your first neural network: basic classification | TensorFlow Core | TensorFlow." [Online]. Available: https://www.tensorflow.org/tutorials/keras/basic_classification.

This preliminary example provides insight into the coding process using Python and the installment of image datasets using MNIST. While there are other databases for the images such as or transfer learning using iOS mobile TensorFlow, the coding process to determine each pixel in the image and for it to be classified into a category through each layer of the neural network will be conserved when using it for the categories of overload and fatigue failure surfaces.

Another preliminary example was also done but focused more on showing the development of transfer learning from originally processing the images of flowers to golden retrievers. By using Docker as an external database to store the images needed and the TensorFlow container, one is able to command on their terminal through python to download the TensorFlow container which then downloads all the images needed, in this examples case the images will be flowers. The user can then connect Docker and the computers database to the images of flowers to then create more files on describing what type of flowers. The key to good recognition when it comes to any images is more detailed files and a range of images; therefore, when connecting the Docker and the users database, one is attaching those descriptive files of already processed images so the image processing learning software integrates it into the next image that needs to be predicted. Since the user will develop this image processing for dogs, specifically golden retrievers, one can make a database of images of golden retrievers using Pixabay. Pixabay allows the user to choose images from the internet

and add then to a folder on their computer database to then attach it to their new retrained image processing software. With that folder of the images wanted in place, the code in TensorFlow for poets [18] of 'curl' is used to retrain the program for new folder attachments with the Docker container. When the code on the system is shown to be of the flower images downloaded from before the user can use the same command for prediction of which is a daisy and change the file name to the one wanting to process, in this case the golden retriever folder. With that installation in place the software is able to download each image, process them, and learn within itself how to identify if an image of a dog or any image is a golden retriever. The procedure in this example to retrain the code to substitute one image file to another using the Docker container allows for the user to then code in commands of the prediction of golden retrievers in a vaguer file of all dogs, or even all animals. This detailed operation allows for the use of image processing for any particular process by retraining the coding model given, most likely known as transfer learning. (*Figure 7*).

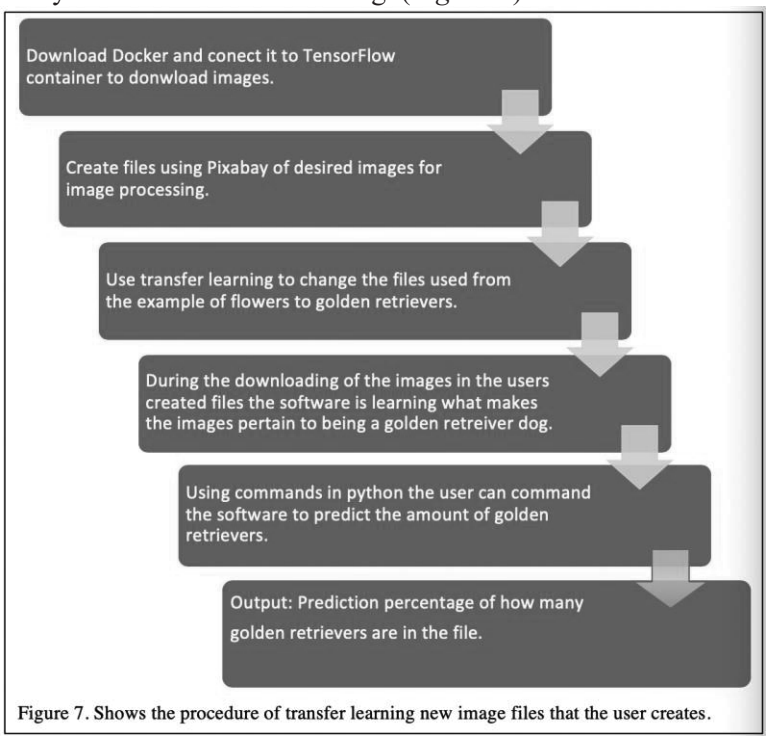

Figure 7. Shows the procedure of transfer learning new image files that the user creates.

Fatigue and Overloading Image Collection

In order to create the training dock for the TensorFlow program, different failure surfaces caused by overload (*figure 8 & 9*) and fatigue (*figure 10 & 11*) were collected. The process to collect images of fatigue and overload came down to identifying articles that discovered how a certain material failed and why, this gives the reason in what certain waves or grooves (fatigue beach marks) are an indication of what output one is looking for. Articles confirming overload failure surfaces having a sand like appearance and fatigue surfaces having visible waves throughout the entire failure platform, one can use these two main detectable differences when it comes to the neural network processing of any given uploaded image. Although overload and fatigue are just two classifications of a failure surface, the ways in which they can be seen throughout different objects or variables can result in images appearing different. Therefore, one has to make sure that the images obtained are similar so the starting of the detection using TensorFlow gets accustomed to identifying the major differences of either sand like or wave groove failure surface to then allow the output to be accurate.

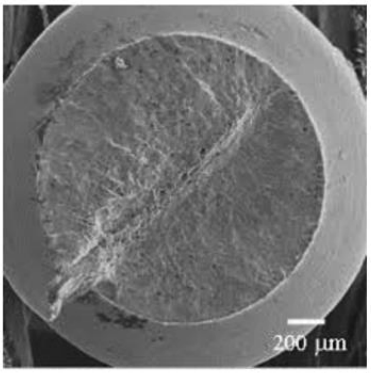

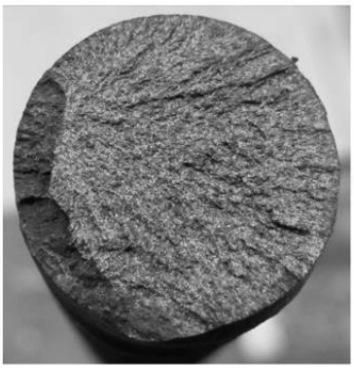

Figure 8 & 9. Sand like appearance for an overload failure surface, Susan, Don, et al. "Screw from Radar System." *Sandia National Laboratories,* 2 August 2006, www.osti.gov/servlets/purl/1264282. D. Vandermaat, S. Saydam, P. C. Hagan, and A. G. Crosky, "Examination of rockbolt stress corrosion cracking utilising full size rockbolts in a controlled mine environment," *International Journal of Rock Mechanics and Mining Sciences*, vol. 81, pp. 86–95, Jan. 2016.

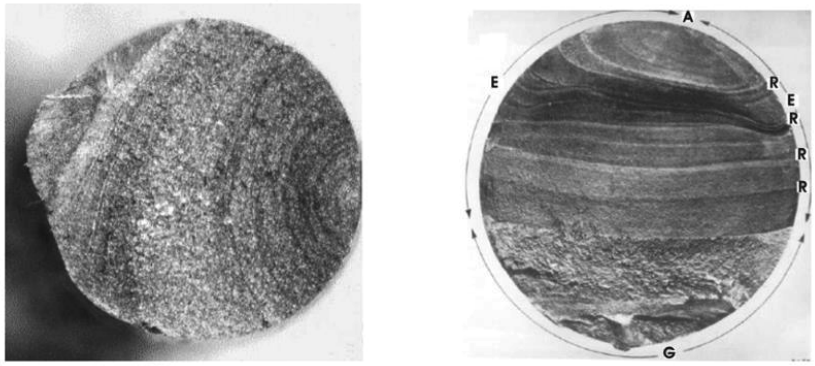

Figure 10 & 11, Wave like appearances for a fatigue failure surface, "Fatigue Striation - an overview | ScienceDirect Topics." [Online]. Available: https://www.sciencedirect.com/topics/engineering/fatigue-striation. [Accessed: 26-Jun-2019]. "Figure 2.31.: Fatigue fracture surface [39].," *ResearchGate*. [Online]. Available: https://www.researchgate.net/figure/Fatigue-fracture-surface-39_fig31_323572683. [Accessed: 26-Jun-2019].

Expected Results & Future Work

The research done this summer provides an in depth look at the TensorFlow program, neural networks, how each pixel of an image is processed within the layers of the neural network, and the determining major factor between overload and fatigue images when ready to implement it into the image processing software of TensorFlow. For future work involving research with this the development of using transfer learning or base coding with the images found of fatigue and overload will be used for the result of taking an image of a failure surface and having the software of TensorFlow determine whether the failure is due to fatigue or overload. Another development that will take place is broadening the images uploaded and used to more complex ones that could involve both fatigue and overload or even some that do not show as sand or wave like. The adaptation of different images over time allows the software to learn of different pixels and add more layers into the neural network for more of a precise output.

This research will eventually result in a program that mechanical engineers can use to take an image of a failure surface, upload it, and be told what stresses caused that failure. This development will allow for the hands-on approach into learning how a surface failed, dive in deeper into how image processing works using TensorFlow, and for a faster detection of failures in projects for engineers put on the field.

Acknowledgements

I would like to thank the McNair Scholars program for allowing me to pursue this research as well as guiding me to do more in school and with my future career. I would also like to thank Dr. Juan Ocampo De Los Rios and Dr. Amber McClung for assisting me with this research and assisting me with new complex strategies regarding machine learning.

References

[1]
J. H. Lee and K. G. Kim, "Applying Deep Learning in Medical Images: The Case of Bone Age Estimation," *Healthc Inform Res*, vol. 24, no. 1, pp. 86–92, Jan. 2018.
[2]
X. Xiao-Ling, X. Cui, and N. Bing, "Facial Expression Recognition Based on TensorFlow Platform," in *ITM Web of Conferences; Les Ulis*, Les Ulis, France, Les Ulis, 2017, vol. 12.
[3]
R. Bonnin, "Building Machine Learning Projects with TensorFlow," 2016. [Online]. Available: http://eds.a.ebscohost.com/eds/ebookviewer/ebook/bmxlYmtfXzE0MjgzMDRfX0FO0?sid=85018329-535c-41ce-9cc7-602563e8f6ea@sessionmgr4009&vid=28&format=EB&rid=2. [Accessed: 18-Mar-2019].
[4]
K. G. Dangtongdee and D. F. Kurfess, "Plant Identification Using Tensorflow," p. 17.
[5]
G. Zaccone, "Getting Started with TensorFlow," 26-Feb-2019. [Online]. Available: http://eds.b.ebscohost.com/eds/ebookviewer/ebook/bmxlYmtfXzEyOTUzNTNfX0FO0?sid=05cd2b43-5100-4d21-bc2b-2ee1e9faa629@pdc-v-sessmgr06&vid=3&format=EB&rid=1. [Accessed: 26-Feb-2019].
[6]
L. Zhang and P. Tang, "Fatigue Crack Growth : Mechanisms, Behavior, and Analysis," 2012. [Online]. Available: http://eds.b.ebscohost.com/eds/ebookviewer/ebook/bmxlYmtfXzU0MTM0MV9fQU41?sid=028db48f-2914-4f4e-814a-fed3296fb302@sessionmgr102&vid=47&format=EB&rid=1. [Accessed: 19-Mar-2019].
[7]
T. Jollivet and E. Greenhalgh, "Fractography, a Powerful Tool for Identifying and Understanding Fatigue in Composite Materials," *Procedia Engineering*, vol. 133, pp. 171–178, 2015.
[8]
S. P. Raut and L. P. Raut, "A Review of Various Techniques Used for Shaft Failure Analysis," vol. 2, no. 2, p. 13, 2014.
[9]

R. Wang and X. Zheng, “Corrosion fatigue crack propagation of an aluminum alloy under periodic overloads,” *Fatigue & Fracture of Engineering Materials & Structures*, vol. 35, no. 5, pp. 389–398, May 2012.
[10]
“TensorFlow.” [Online]. Available: https://www.tensorflow.org/learn. [Accessed: 25-Jun-2019].
[11]
Shack, Hacker, director. *Easy Image Classification with Tensorflow*. *YouTube*, YouTube, 7 July 2017, www.youtube.com/watch?v=qaQofXTxkSo.
[12]
“Train your first neural network: basic classification | TensorFlow Core | TensorFlow.” [Online]. Available: https://www.tensorflow.org/tutorials/keras/basic_classification.
[13]
Susan, Don, et al. “Screw from Radar System.” *Sandia National Laboratories,* 2 August 2006, www.osti.gov/servlets/purl/1264282.
[14]
D. Vandermaat, S. Saydam, P. C. Hagan, and A. G. Crosky, “Examination of rockbolt stress corrosion cracking utilising full size rockbolts in a controlled mine environment,” *International Journal of Rock Mechanics and Mining Sciences*, vol. 81, pp. 86–95, Jan. 2016.
[15]
“Fatigue Striation - an overview | ScienceDirect Topics.” [Online]. Available: https://www.sciencedirect.com/topics/engineering/fatigue-striation. [Accessed: 26-Jun-2019].
[16]
“Figure 2.31.: Fatigue fracture surface [39].,” *ResearchGate*. [Online]. Available: https://www.researchgate.net/figure/Fatigue-fracture-surface-39_fig31_323572683. [Accessed: 26-Jun-2019].
[17]
Hacker Shack. (n.d.). *Easy Image Classification with Tensorflow*. Retrieved from https://www.youtube.com/watch?v=qaQofXTxkSo

Social Media Influencer Perceptions: Predicting Followers on Instagram with Image Classification and Sentiment Analysis

Gabriel Reyes

Mentor: Arthur Hanna, Ph.D.
St. Mary's University, San Antonio

Instagram is a large social media application allowing users to post images with text captions. With the use of the hashtag, users can reference their favorite social media influencers. This research analyzes data from forty-three social media influencers. Posts that had images were analyzed using an image classification technique and the words associated with the image were attached to the text of each post. The text was analyzed with a sentiment analysis technique which classified the text as positive, neutral, or negative depending on the words used in the post. A neural network was then trained on the average of the sentiment analysis, the number of positive, negative, neutral posts, and a number representing the social media influencer for which the posts were related to. To predict the number of followers each social media influencer may have after the collection of approximately 60 of the most current posts available on Instagram.

Keywords: sentiment analysis, neural network, machine learning, data mining, Python, classification, Instagram

Literature Review

Instagram and Social Media

Social media produces a significant amount of data on a daily basis. Several studies have investigated the predictor power of social media (Asur & Huberman, 2010; Beck, Huang, Linder, Guo, Zhang, Helbing, & Antuloy-Fantulin, 2019; Chen, Kong, Xu, Mao, 2019; Nguyen, Shirai, 2015a; Nguyen, Shirai, 2015b; Schoen, Takis, Mustafarai, Strohmaier, & Gloor, 2013; Sun, Lachanski, & Fabozzi, 2016). Many studies have used Twitter as their primary source of social media data (Bollen Mao, & Zeng, 2011; Yang, Mo, & Liu, 2015). Twitter's primary form of media sharing is text-based posts allowing users to post a plethora of information. Although the primary source of information shared

on Twitter is text-based, Twitter also allows users to share videos and images. Instagram, in contrast to Twitter, primarily focuses on images as its main media outlet. After posting images or videos users can also caption their post using text.

Image Classification

The *ImageAI* Python library, associated with AI commons, allows developers to integrate image classification into their development. The *ResNet* Model is a pre-trained Convolutional Neural Network model available for download. *ResNet* has high performance and low complexity level. *ImageAI* using *ResNet* allows for objects in images to be labeled. Each word associated with the image has a certain probability that the word is represented in the image (Olafenwa, 2018).

Sentiment Analysis

Sentiment analysis has been used to analyze social media data. Several research projects have used sentiment analysis to make predictions using social media. Projects have investigated the predictive power of social media on cryptocurrency, the stock market, and personality (Nguyen & Shirai, 2015a; Nguyen & Shirai, 2015b; Yang et al, 2015; Skowron, Tkalčič, Ferwaerda, & Schedl, 2016; Beck et al, 2019; Bollen et al, 2011; Sun et al, 2016; Yang et al, 2015). One project analyzed the sentiment of IMBD comments categorizing each comment as positive, negative, or neutral (Agrawal, 2019). The Python library *TextBlob* was trained on the sentiment of movie reviews. *TextBlob* allows the user to assign positive, negative, and neutral to text. Nikhil Kumar contributed to *GeeksforGeeks* explaining how to run sentiment analysis on data collected from Twitter's API. Although this example was designed for Twitter, the pre-trained sentiment analysis based on the movie reviews proved useful on social media data (Kumar, 2018).

Regression Neural Network from Sklearn

Sklearn is a Python library for machine learning. *Sklearn* has *MLPRegressor*, a Multi-layer perceptron method that can be trained to approximate a non-linear function. The *MLPRegressor* method has several parameters that can be altered, best serving the program it is being implemented for. This neural network

regression model trains using backpropagation and can be trained to estimate multiple targets for output (Pedregosa, Varoquaux, Gramfort, Michel, Thirion, Grisel, & Weiss, 2011).

Urllib and BeautifulSoup

Urllib is a Python library that can pull HTML from webpages, but *urllib* does not give developers access to the websites' API (Python Software Foundation, 2019). Used with *Beautiful soup*, a Python library that parses through HTML, data from webpages can be easily collected and organized (Richardson, 2015). These libraries can only collect the most current data present in the HTML at a given time.

Hypothesis

If Instagram data comprised of images, text, and hashtags are analyzed using image classification and sentiment analysis, then a neural network trained on the results from the sentiment analysis will be able to make a prediction of the number of followers for several social media influencers that is similar to the number of individuals following each influencer at the time the analysis is run.

Method

InstagramSentimentAnalysisAndPosts.py

Data collection.

The Python program, *InstagramSentimentAnalysisAndPosts.py*, (Appendix A) collected and analyzed the Instagram data. The data was collected by pulling the HTML page from an Instagram tag page using an *urllib* request. The hashtags that the page focused on were the names of forty-three social media influencers. The names of the influencers were manually collected from the *FamousBirthdays* website. The name of each influencer was put into a read text file "Famous People.txt" (Appendix B) along with the username for each influencer proceeded by '@'. Only the influencers named in the file can be used for analysis. *Beautiful Soup* was used to parse the HTML pulling the images and text for each social media influencer hashtag. The text also contained hashtags referencing other data. For some posts, there was no text associated with the image, so an exception handler was used to proceed with the data

collection. Approximately 60 to 80 posts per social media influencer were collected each iteration of the program.

Image classification.

For the images collected by the program, each image was run through an image analysis using the *ImageAI* library. Images were retrieved from Instagram and downloaded into the same folder as the main program. Images files, saved as jpeg file, were named as the influencer and the word ‘image’, The predicted words associated with the image that had a probability of at least one percent were included and attached to the text pulled from Instagram. Punctuation was then removed (cleaned) from the posts. To save memory after an image was classified the image file was overwritten by the succeeding image. Each cleaned text post was appended in a text file named after the social media influencer and the word ‘posts’.

Sentiment analysis and followers.

The clean text, composed of only words from each post pulled from each user, was run through a sentiment analysis. The current number of followers, rounded to the nearest million, was collected at the time of the analysis. The scores for each image from the sentiment analysis were collected and an average of the scores was calculated. The information from the sentiment analysis and the number of followers was saved in a text file named using social media influencer name and the words, “followers and SA”. The data was repeatedly collected approximately every thirty minutes for three days. *InstagramSentimentAnalysisAndPosts.py* was run once, a second time in a separate folder to create the test data, in preparation for the next program. These *followers and SA* files serve as the input to the next program, *FollowerPredictionNeuralNetwork.py*.

FollowerPredictionNeuralNetwork.py

The second Python program uses the same list of influencers for analysis. A multi-layer perceptron was trained with five hidden layers each with 100 hidden nodes (Appendix C). The solver was the limited-memory Broyden-Fletcher-Goldfarb-Shanno algorithm. The *FollowerPredictionNeuralNetwork.py* (Appendix D) then pulls

the data from the *Followers and SA* files from the first folder to train the neural network. The data from the *Followers and SA* files in the second folder was used to test the neural network.

Results

A regression analysis was run to determine the effectiveness of the methodology comparing the predicted number of followers to the actual number of followers for each social media influencer (R^2=0.7045, F(1,41)=97.73, p=0.00649). The slope of the regression line was 0.56. The significance of the p-value suggests a strong correlation between the predicted number of followers and the actual number of followers. These results show that the neural network was able to make predictions that approximate the number of actual followers for each social media influencer. A representation of the regression analysis can be seen in Appendix E.

A paired samples t-test assuming equal variance was also run for the predicted number of followers (*M* = 29144649, *SD* = 31787804) comparing it to the actual number of followers per influencer (*M* = 34985300, *SD* = 47598445). Appendix F shows the actual values for predicted and actual followers and Appendix G is a bar graph that compares the actual versus predicted followers for each social media influencer. The t-test showed that the follower predictions were not significantly different from the actual followers at an alpha level of 0.05, *t*(42) = -14190867, *p* = 0.1654. The insignificant results of the t-test suggests that the predicted number of followers could be taken from the same samples as the actual number of followers for each social media influencer.

Discussion

Implications of Procedure

The procedure used for this project demonstrates the possibility of making predictions using sentiment analysis of text and images pulled from Instagram. Instagram is growing rapidly so it is possible that social media outlets like Twitter may become less popular in comparison to social media like Instagram. Using sentiment analysis of images and using the sentiment analysis

results to make predictions is a relatively unexplored field of research.

Limitations

This project was completed in less than an eight-week period and the techniques used in this project were not fully optimized. The sentiment analysis and image analysis were not trained on Instagram data which may have decreased the accuracy of the predictions made by the techniques. Data from Instagram was also limited given that only approximately 60 posts were pulled for each social media influencer for each iteration. The program also did not consider posts that may have been pulled multiple times which had the potential to bias the results of the sentiment analysis. This might decrease the accuracy of the model.

Future Directions

A future project would build on the methodology of this project. Backpropagation should be used to optimize the neural network to determine the best parameters for making accurate predictions. The future models for the image classification, sentiment analysis, and model for prediction should be trained and optimized specifically on Instagram data which includes images, captions, and hashtags. Predictions should also be tested for the future number of followers for a given social media influencer. This project tried to predict the current number of followers a given influencer had at the time of prediction. A future project could also evaluate the prediction power on multiple test cases.

Conclusion

Given social media data from Instagram, it is possible to make an approximate prediction for the number of followers for social media influencers by performing sentiment analysis on posts associated with each social media influencer. Instagram posts are composed of images, text, and hashtags which reference other relevant Instagram posts. Therefore, Instagram can be analyzed using image classification and sentiment analysis, and a neural network can be trained using the results from the sentiment

analysis to make an accurate prediction of the number of followers for a social media influencer.

References

Agrawal, S. (2019, February 18). Sentiment analysis using lstm step-by-step. Retrieved June 25, 2019, from https://towardsdatascience.com/sentiment-analysis-using-lstm-step-by-step-50d074f09948

Asur, S., & Huberman, B. A. (2010, August). Predicting the future with social media. In *Proceedings of the 2010 IEEE/WIC/ACM International Conference on Web Intelligence and Intelligent Agent Technology-Volume 01* (pp. 492-499). IEEE Computer Society.

Beck, J., Huang, R., Lindner, D., Guo, T., Zhang, C., Helbing, D., & Antulov-Fantulin, N. (2019). Sensing social media signals for cryptocurrency news. *arXiv preprint arXiv:1903.11451*.

Bollen, J., Mao, H., & Zeng, X. (2011). Twitter mood predicts the stock market. *Journal of computational science*, *2*(1), 1-8.

Chen, G., Kong, Q., Xu, N., & Mao, W. (2019). NPP: A neural popularity prediction model for social media content. *Neurocomputing*, *333*, 221-230.

Dushantha, S. (2018, July 10). Insta-dl. Retrieved June 25, 2019, from https://github.com/sdushantha/insta-dl

FamousBirthdays. (n.d.). Most popular people | famous birthdays. Retrieved from https://www.famousbirthdays.com/most-popular-people.html

Hinds, J., & Joinson, A. (2019). Human and computer personality prediction from digital footprints. *Current Directions in Psychological Science*, 0963721419827849.

Karpathy, A. (2015, May 21). The unreasonable effectiveness of recurrent neural networks. Retrieved May 17, 2019, from http://karpathy.github.io/2015/05/21/rnn-effectiveness/

Lenail, A. (n.d.). NN-SVG. Retrieved June 25, 2019, from http://alexlenail.me/NN-SVG/index.html

Matta, M., Lunesu, I., & Marchesi, M. (2015, June). Bitcoin spread prediction using social and web search media. In *UMAP Workshops* (pp. 1-10).

Moujahid, A. (2014, July 21). An introduction to text mining using twitter streaming API and python. Retrieved May 17, 2019, from http://adilmoujahid.com/posts/2014/07/twitter-analytics/

Nguyen, T. H., & Shirai, K. (2015). Topic modeling based sentiment analysis on social media for stock market prediction. In *Proceedings of the 53rd Annual Meeting of the Association for Computational Linguistics and the 7th International Joint Conference on Natural Language Processing (Volume 1: Long Papers)* (Vol. 1, pp. 1354-1364).

Nguyen, T. H., Shirai, K., & Velcin, J. (2015). Sentiment analysis on social media for stock movement prediction. *Expert Systems with Applications*, *42*(24), 9603-9611.

Olafenwa, M. (2018, April 23). Image Recognition with 10 lines of code - Moses Olafenwa. Retrieved from https://medium.com/@guymodscientist/image-prediction-with-10-lines-of-code-3266f4039c7a

Pedregosa, F., Varoquaux, G., Gramfort, A., Michel, V., Thirion, B., Grisel, O., . . . Weiss, R. (2011). Scikit-learn: Machine Learning in Python. *Journal of Machine Learning Research, 12*, 2825-2830. Retrieved June 25, 2019, from https://scikit-learn.org/stable/index.html.

Python Software Foundation. (2019, June 26). Urllib - URL handling modules. Retrieved June 26, 2019, from https://docs.python.org/3/library/urllib.html

Richardson, L. (2015). Beautiful Soup Documentation. Retrieved June 26, 2019, from https://www.crummy.com/software/BeautifulSoup/bs4/doc/

Roy, A. (2018, October 26). How to scrape instagram data using python. PromptCloud. Retrieved May 17, 2019, from https://www.promptcloud.com/blog/how-to-scrape-instagram-data-using-python/

Schoen, H., Gayo-Avello, D., Takis Metaxas, P., Mustafaraj, E., Strohmaier, M., & Gloor, P. (2013). The power of prediction with social media. *Internet Research*, *23*(5), 528-543.

Skowron, M., Tkalčič, M., Ferwerda, B., & Schedl, M. (2016, April). Fusing social media cues: personality prediction from twitter and instagram. In *Proceedings of the 25th international conference companion on world wide web* (pp. 107-108). International World Wide Web Conferences Steering Committee.

Sun, A., Lachanski, M., & Fabozzi, F. J. (2016). Trade the tweet: Social media text mining and sparse matrix factorization for stock market prediction. *International Review of Financial Analysis*, *48*, 272-281.

Kumar, N. (2018, February 07). Twitter sentiment analysis using python. Retrieved June 25, 2019, from https://www.geeksforgeeks.org/twitter-sentiment-analysis-using-python/

Yang, S. Y., Mo, S. Y. K., & Liu, A. (2015). Twitter financial community sentiment and its predictive relationship to stock market movement. *Quantitative Finance*, *15*(10), 1637-1656.

Appendix A
Code for InstagramSentimentAnalysisAndPosts.py

```
#-------------------------------------------------------------
# Gabriel Reyes
# InstagramSentimentAnalysisAndPosts.py
# Collects Instagram Posts and Images
# Runs image classification technique
# Runs a sentiment analysis
#-------------------------------------------------------------
import requests
import re
import urllib.request
import urllib.parse
import urllib.error
import ssl
import json
import os
from datetime import datetime
from imageai.Prediction import ImagePrediction
from textblob import TextBlob
from bs4 import BeautifulSoup
import numpy as np
import statistics
execution_path = os.getcwd()
prediction = ImagePrediction()
prediction.setModelTypeAsResNet()
# Alter path accordingly
prediction.setModelPath("C:/Users/Gabriel Grey Reyes/OneDrive -
St. Mary's University/Research
2019/Code/Code/resnet50_weights_tf_dim_ordering_tf_kernels.h5")
prediction.loadModel()

def ReadFamousPeople():
    fp = open("C:/Users/Gabriel Grey Reyes/OneDrive - St. Mary's
University/" +
              "Research  2019/Code/Code/Famous People.txt",'r')
    famouspeople =  fp.read().split('\n')
    for i in range(0, len(famouspeople)):
        famouspeople[i] = famouspeople[i].split('@')
    fp.close()
    return(famouspeople)

def ParseHTML(famousperson):
    obj = ssl.create_default_context()
    # pull html from url context is a context object
    html =
urllib.request.urlopen(https://www.instagram.com/explore/tags/
                                    + famousperson + "/", context =
obj)
    # parse through the html with BeautifulSoup
    soup = BeautifulSoup(html, 'html.parser')
    # find json script in html that starts with
"window._sharedData"
    script = soup.find('script', text = lambda t:
t.startswith('window._sharedData'))
```

```
    # split by first equal sign and strip ';' from the end of the
string
    page_json = script.text.split(' = ', 1)[1].rstrip(';')
    # convert data into python elements
    data = json.loads(page_json)
    return(data)

def GetPost(famousperson, data):
    i = 0
    pulled_data = []
    for post in data['entry_data']['TagPage'][0]['graphql'
        ]['hashtag']['edge_hashtag_to_media']['edges']:
        try:
            image_src =
post['node']['thumbnail_resources'][1]['src']
            text = str(post['node'][

'edge_media_to_caption']['edges'][0]['node']['text'])
            s =  famousperson + ' image.jpg'
            url = image_src
            r = requests.get(url, allow_redirects = True)
            images = open(s, 'wb')
            images.write(r.content)
            images.close()
            image_text = ImageAnalysis(s)
            # pass if CleanText(pulled_data[i]) is duplicate
            pulled_data.append(text + image_text)
            pulled_data[i] = CleanText(pulled_data[i])
            i = i + 1
        except IndexError:
            text = ""
            image_src =
post['node']['thumbnail_resources'][1]['src']
            s =  famousperson + ' image.jpg'
            url = image_src
            r = requests.get(url, allow_redirects = True)
            images = open(s, 'wb')
            images.write(r.content)
            images.close()
            image_text = ImageAnalysis(s)
            # pass if CleanText(pulled_data[i]) is duplicate
            pulled_data.append(text + image_text)
            pulled_data[i] = CleanText(pulled_data[i])
            i = i + 1
        except OSError:
            pass
        except IndexError:
            pass
    return(pulled_data)

def CleanText(Text):
    return(' '.join(re.sub("([^0-9A-Za-z \t])|(\w+:\/\/\S+)", " ",
Text).split()))

def SentimentAnalysis(pulled_data):
    pulled_data = np.asarray(pulled_data)
    sentiment_analysis = np.zeros(len(pulled_data))
```

```
    for i in range(0, len(pulled_data)):
        analysis = TextBlob(pulled_data[i])
        sentiment_analysis[i] = analysis.sentiment.polarity
    return(sentiment_analysis)

def ImageAnalysis(image):
    prediction_text = ""
    predictions, percentage_probabilities =
prediction.predictImage(image,

result_count=0)
    for index in range(len(predictions)):
        if (percentage_probabilities[index]>1): prediction_text =
prediction_text + (
           predictions[index] + ' ')
    return(prediction_text)

def GetFollowers(url):
    obj = ssl.create_default_context()
    html = urllib.request.urlopen(url, context = obj).read()
    soup = BeautifulSoup(html, 'html.parser')
    data = soup.find_all('meta', attrs={'property':
'og:description'})
    text = data[0].get('content').split()
    if ("," in text[0]): followers =
float(text[0].replace(",",""))
    if ("m" in text[0]):
        followers = float(text[0].replace("m",""))*1000000
    elif ("k" in text[0]):
        followers = float(text[0].replace("k",""))*1000
    elif ("b" in text[0]):
        followers = float(text[0].replace("b",""))*1000000000
    else:
        followers = float(text[0].replace("",""))
    return(int(followers))

def main():
    FamousPeople = ReadFamousPeople()
    for i in range(0, len(FamousPeople)):
        now = datetime.now()
        data = ParseHTML(FamousPeople[i][0].replace(" ",""))
        pulled_data = GetPost(FamousPeople[i][0].replace(" ",""),
data)
        posts = open(FamousPeople[i][0].replace(" ","") +
                     " posts.txt", 'a')
        posts.write(FamousPeople[i][0].replace(" ","") + " " +

str(datetime.fromtimestamp(datetime.timestamp(now))) + "\n")
        for j in range(0, len(pulled_data)):
            posts.write(str(pulled_data[j])+'\n')
        posts.close()
        SA = SentimentAnalysis(pulled_data)
        follower_file = open(FamousPeople[i][0].replace(" ","") +
                             " followers and SA.txt", 'a')
        follower_file.write(FamousPeople[i][0].replace(" ","") + "
" +
```

```
str(datetime.fromtimestamp(datetime.timestamp(now))) +
                "\n")
        follower_file.write("P : " + str(len(SA[SA > 0])) + "\n")
        follower_file.write("N : " + str(len(SA[SA < 0])) + "\n")
        follower_file.write("Z : " + str(len(SA[SA == 0])) + "\n")
        follower_file.write("A : " + str(statistics.mean(SA)) +
"\n")
        followers =  GetFollowers(https://www.instagram.com/
                                  +FamousPeople[i][1].replace("
","")
                                  +"/?hl=en")
        follower_file.write("F : " + str(followers) + "\n")
        follower_file.close()
        print(FamousPeople[i][0])

print(str(str(datetime.fromtimestamp(datetime.timestamp(now)))),
          "Done")


if __name__ == "__main__":
    main()
```

Appendix B
Famous People.txt

```
Annie LeBlanc @annieleblanc
Ariana Grande @arianagrande
Asher Angel @asherangel
Baby Ariel @babyariel
Beyonce @beyonce
Billie Eilish @billieeilish
Cameron Dallas @camerondallas
Cardi B @iamcardib
Cash Baker @cash.baker
Colleen Ballinger @colleen
Danielle Cohn @daniellecohn
David Dobrik @daviddobrik
Drake @champagnepapi
Emma Chamberlain @_emmachamberlain
Ethan Dolan @ethandolan
Grayson Dolan @graysondolan
Hayden Summerall @haydensummerall
Hayley LeBlanc @hayley.leblanc
Jacob Sartorius @jacobsartorius
Jake Paul @jakepaul
James Charles @jamescharles
Johnny Orlando @johnnyorlando
Jojo Siwa @itsjojosiwa
Justin Bieber @justinbieber
Kim Kardashian @kimkardashian
Kylie Jenner @kyliejenner
Lele Pons @lelepons
Lil Pump @lilpump
Liza Koshy @lizakoshy
Logan Paul @loganpaul
Loren Gray @loren
Maddie Ziegler @maddieziegler
MattyB @mattybraps
Maverick Baker @maverickbaker
Millie Bobby Brown @milliebobbybrown
PewDiePie @pewdiepie
Piper Rockelle @piperrockelle
RiceGum @rice
Selena Gomez @selenagomez
Shane Dawson @shanedawson
Shawn Mendes @shawnmendes
Taylor Swift @taylorswift
Zendaya @zendaya
```

Appendix C

MLPRegression Neural Network Representation

This image is a representation of the MLPRegressor neural network used to analyze the sentiment analysis to make a prediction of the number of followers each social media influencer has. This image was created using the neural network generator created by Alex Lenail for the purposes of publication (Lenail, n.d.). This perceptron shows four input nodes for the number of positive, negative, neutral posts, and the average score of all the posts from the sentiment analysis. The image shows a representation of the five hidden layers comprised of 100 hidden nodes each, and a single output node for the number of followers this model predicts.

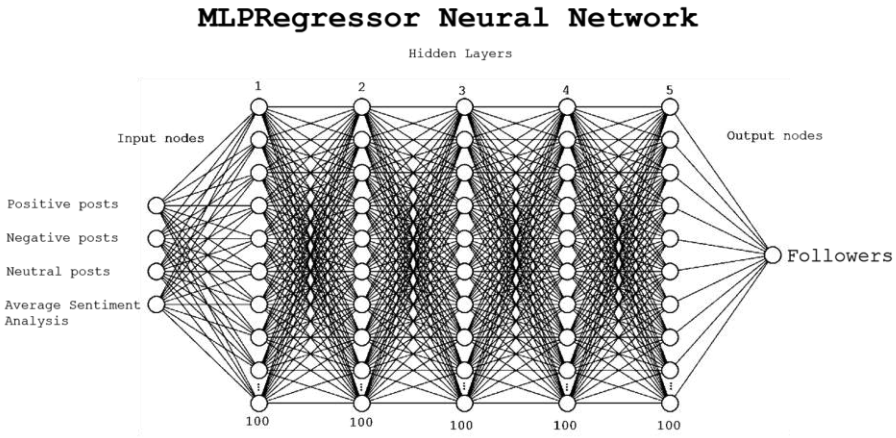

Appendix D
Code for FollowerPredictionNeuralNetwork.py

```
#-------------------------------------------------------------
# Gabriel Reyes
# FollowerPredictionNeuralNetwork.py
# Collects output from InstagramSentimentAnalysisAndPosts.py
# Trains regression Neural Network
#-------------------------------------------------------------
from sklearn.neural_network import MLPRegressor
import numpy as np

# read famous people.txt
famousp = open("famous people.txt")
X = famousp.read().split("\n")
famousp.close()

# clean famous people.txt
for i in range(0, len(X)):
    X[i] = X[i].split("@")

for i in range(0, len(X)):
    X[i][0] = X[i][0].replace(" ","")

# Collect Data from {famous person} followers and SA.txt
A = []
UserID = []
for i in range(0, len(X)):
    file = open(X[i][0] + " followers and SA.txt", "r")
    A.append(file.read())
    A[i] = A[i].split("\n")
    UserID.append(i)
    file.close()

# Clean data from followers and SA.txt
X = []
for i in range(0, 43):
    for j in range(0, len(A[i])):
        if(A[i][j] == ""): continue
        if (" : " in A[i][j]):
            X.append(float(A[i][j].split(" ")[2]))
        else:
            X.append(i)

# Train Neural Network
X = np.asarray(X).reshape(int(len(X)/6),6)
y = X[:,5]
X = X[:,0:5]
reg = MLPRegressor(hidden_layer_sizes=(100, 100, 100, 100, 100, ),
alpha=0.0, solver='lbfgs')
reg.fit(X, y.reshape(len(X),1))
# testdata
famousp = open("famous people.txt")
X_test = famousp.read().split("\n")
famousp.close()

for i in range(0, len(X_test)):
```

```
    X_test[i] = X_test[i].split("@")

for i in range(0, len(X_test)):
    X_test[i][0] = X_test[i][0].replace(" ","")

test_folder = "C:\\Users\\Gabriel Grey Reyes\\OneDrive - St.
Mary's University\\Research 2019\\Code\\Test\\"
A_test = []
UserID_test = []
for i in range(0, len(X_test)):
    file = open(test_folder + X_test[i][0] + " followers and
SA.txt", "r")
    A_test.append(file.read())
    A_test[i] = A_test[i].split("\n")
    UserID_test.append(i)
    file.close()

X_test = []
for i in range(0, 43):
    for j in range(0, len(A_test[i])):
        if(A_test[i][j] == ""): continue
        if (" : " in A_test[i][j]):
            X_test.append(float(A[i][j].split(" ")[2]))
        else:
            X_test.append(i)

X_test = np.asarray(X_test).reshape(int(len(X_test)/6),6)

y_actual = X_test[:,5]
X_test = X_test[:,0:5]

y_test = reg.predict(X_test)
```

Appendix E
Multiple Regression Analysis

This graph represents the regression analysis estimating the relationship between the value of predicted followers and actual followers. This graph shows a strong positive correlation between the two values indicating some accuracy in the predictions of the model.

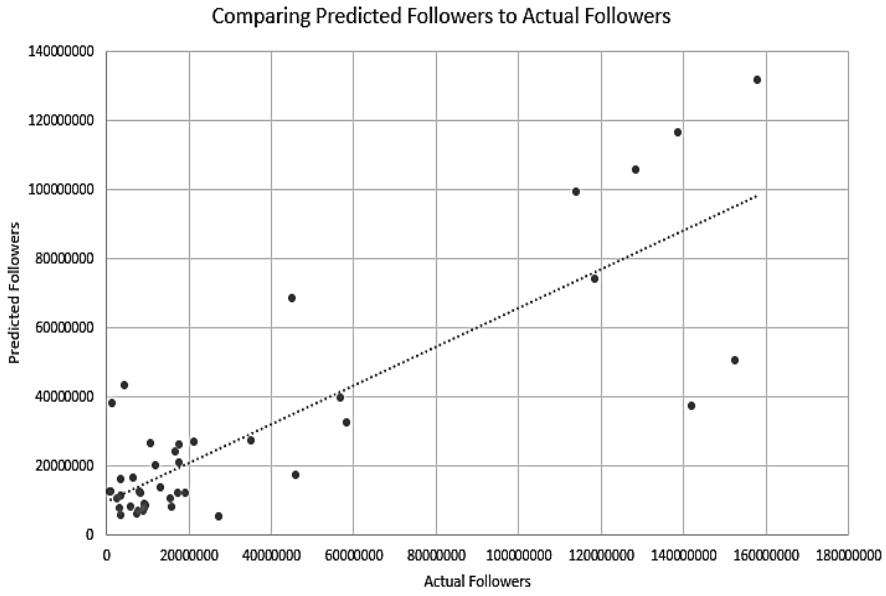

Appendix F
Social Media Influencer Follower Table

Social Media Influencer Table

Social Media Influencer	Instagram Username	Predicted Followers	Actual Followers
Annie LeBlanc	annieleblanc	5783088.979	7600000
Ariana Grande	arianagrande	131794749.9	157900000
Asher Angel	asherangel	5664892.438	3500000
Baby Ariel	babyariel	7510336.913	9400000
Beyonce	beyonce	105606453.7	128600000
Billie Eilish	billieeilish	5259568.79	27200000
Cameron Dallas	camerondallas	26651793.56	21200000
Cardi B	iamcardib	17041308.95	46000000
Cash Baker	cash.baker	12171645.88	1000000
Colleen Ballinger	colleen	16380518.96	6700000
Danielle Cohn	daniellecohn	15777286.18	3500000
David dobrik	daviddobrik	12205114.67	8000000
Drake	champagnepapi	32567982.12	58300000
Emma Chamverlain	_emmachamberlain	6863845.833	7700000
Ethan Dolan	ethandolan	8782155.243	9200000
Grayson Dolan	graysondolan	8269378.145	9500000
Hayden Summerall	haydensummerall	10169068.29	2700000
Hayley LeBlanc	hayley.leblanc	7632193.682	3200000
Jacob Sartorius	jacobsartorius	6742256.688	8900000
Jake Paul	jakepaul	19793334.02	12000000
James Charles	jamescharles	10385633.09	15500000
Johnny Orlando	johnnyorlando	8010378.147	5900000
Jojo Siwa	itsjojosiwa	12021943.54	8400000
Justin Bieber	justinbieber	99160576.11	114200000
Kim Kardashian	kimkardashian	37297060.56	142200000
Kylie Jenner	kyliejenner	116458001.6	138700000
Lele Pons	lelepons	27271864.17	35100000
Lil Pump	lilpump	25910188.26	17800000
Liza Koshy	lizakoshy	20799231.9	17800000
Logan Paul	loganpaul	7906266.762	15900000
Loren Gray	loren	24158055.48	16700000
Maddie Ziegler	maddieziegler	13692397.24	13100000
MattyB	mattybraps	11198036.2	3600000
Maverick Baker	maverickbaker	12173640.47	867900
Millie Bobby Brown	milliebobbybrown	12004021.3	19100000
PewDiePie	pewdiepie	11973951.08	17300000
Piper Rockelle	piperrockelle	38082121.93	1600000
RiceGum	rice	43363853.26	4500000
Selena Gomez	selenagomez	50517395.98	152500000
Shane Dawson	shanedawson	26211494.89	10700000
Shawn Mendes	shawnmendes	68448749.71	45200000
Taylor Swift	taylorswift	73819123.43	118700000
Zendaya	zendaya	39688957.47	56900000

Appendix G
Followers Per Social Media Influencer

The following graph is a comparison of actual followers each social media influencer has compared to the prediction made by the model. The number of followers is on the vertical axis and each influencer is listed on the horizontal axis. The predicted number of followers are in orange, and the actual values are in blue.

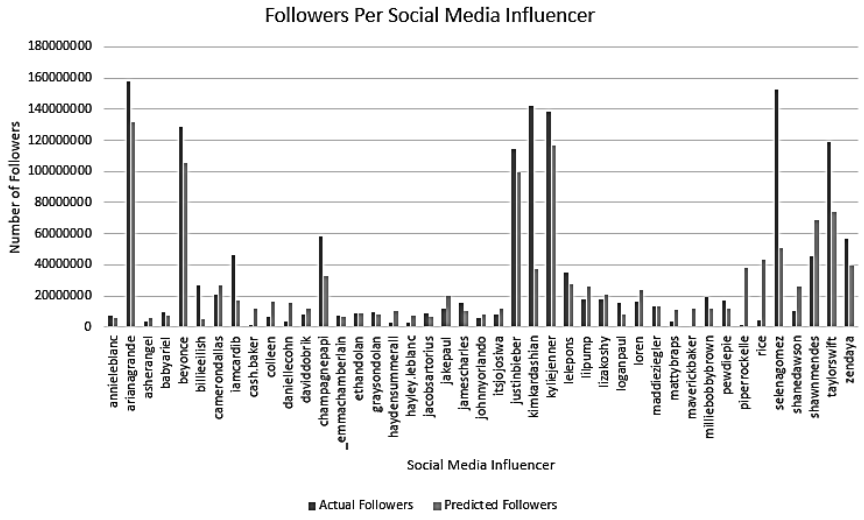

An Extension of the Independent Samples t-test for Pre-test/Post-test Data: The Case of MNAR

Jessica Márquez-Muñoz

Mentor: Rick Sperling, Ph.D.
St. Mary's University, San Antonio

Research suggests that students in the Rio Grande Valley that are of low socio-economic status (SES) have a high rate of mobility (U.S. Census, 2018) This is important because students are more likely to experience curricular inconvenience, language barriers, and therefore, resulting in lower achievement when compared to stable students. In fact, according to Voight, Shinn, and Nation (2012), student mobility has a greater impact than poverty when predicting high school dropout rates. Student mobility and dropout rates cause an additional problem when it comes to measuring student achievement due to high rates of missing data, creating social justice issues such as equal opportunity for education. Missing data arise from attrition, data entry errors, participants' failure to respond, and other reasons. Schools want to measure the effects of the curricula, but missing data obfuscates interpretation of results. This study explores one method of managing missing data that is accessible to teachers and other non-statistically-minded stakeholders. Specifically, I compare the use of independent samples t-tests and paired sample t tests at varying levels of missingness and correlation when data is missing not at random (MNAR). Results support earlier findings on the utility of the independent samples t-test in situations where missingness is high and the pre-test/post-test correlation is low by demonstrating that non-normality does not adversely impact conclusions drawn from statistical hypotheses testing.

Keywords: student mobility, missing cases, statistical power, Type I and II errors

Practitioners seeking to measure the effectiveness of their interventions often find that a fraction of their participants opt out of the study before all their data can be collected. Another situation is that some participants may intentionally, or unintentionally skip questions due to sensitive topics and uncertainty with the content of the question (Sulis & Porcu, 2017). There has been significant research done on the effects of missing data demonstrating that not only will the power of the statistical test be affected, but would also lead to inflated standard errors and biased estimates (Schafer & Graham, 2002), leaving practitioners at a crossroads.

What is the best way to handle missing data? Often practitioners who come across missing data are not trained in identifying types of missingness or even handling the missing data in a responsible fashion. The most common practice that practitioners move towards is listwise deletion (LD), in which means that any case with missing data is thrown out of the dataset. One of the advantages of LD is the ease of simply disposing of data. The cost, of course, is that there is a reduction in sample size and increased risk of bias if the type of missingness is not taken into consideration.

Missing data can be categorized into missing at random (MAR), missing not at random (MNAR), and missing completely at random (MCAR). Data that are MNAR are dependent on the values that are observable, even when the practitioner cannot identify the model that predicts the missingness. Whether the researcher can detect MNAR or not, data that are MNAR cannot be subjected to LD due to the heightened chance of producing biased estimates (Olinsky, Chen & Harlow, 2013)

The present study extends that of Cruz et al. (2017) who proposed the use of an independent samples t-test rather than a dependent samples t-test for pre-test/post-test scenarios in which the correlation between measurement points was low and missingne ss was high. This is especially impo1iant since in real world applications MNAR data is a common occurrence, especially in areas where student mobility is high.

According to the U.S. Census, around I 0.2% of children ages 5-1, that identified as Hispanics or Latinx, were considered highly mobile, whereas children, ages five to seventeen that identified as White , had a lower rate of mobility (U.S. Census, 2018). According to Voight et al., student mobility is more predictive of high school drop-out rates than socio-economic status (SES). However, SES is still a high predictor of student mobility, which is most common in families that have a lower SES (2012). For example , the Rio Grande Valley, has a higher representation of Latinx or Hispanics as compared to other ethnicities. Residents of the Rio Grande Valley area have high rates of Latinx/Hispanic student s that can be classified as English Language Learners (ELL) or are enrolled in English as a Second Language (ESL) programs.

Schools that have ELL or ESL programs are likely to be labeled low-performing institutions (Elizondo, 2014). Elizondo, also states that Hispanic ELL student s are the lowest scoring group on the Texas state test, which, like most standardized state tests, is geared towards English native speakers (2014). It follows that results for students whose first language is not English, will not be representative due to the language ba1Tier and other barriers such as changes in scheduling and trouble transitioning into different schooling environments, also known as curricular incoherence (Rumberger, 1999).

In situations such as this, measuring student outcomes becomes difficult due to students moving in and out of school and language barriers. When pre and post tests are conducted, the results will have high rates of missing data for schools with a high rate of mobility. In areas of low SES and high student turnover, measuring student outcomes in an effective manner has proven to be difficult. With students moving from different districts constantly, the outcomes measured from interventions may not be representative of the population. Meanwhile, in areas of high SES and low student mobility, the ability to measure student outcomes

becomes a much simpler task and adjusting certain interventions to serve students is easier.

This then brings us to the question of how do we as researchers identify methods that teachers and other educators can use to handle missing data that are MNAR Missing data has always been a topic of interest for statisticians and R hobbyists, though in real world application missing data is a common occurrence and to properly measure student outcomes it is important to explore simple statistical methods in capturing the whole student experience as to best serve the student. While missing data might seem to be a minor issue at first, missing data can lower the power of statistical analyses as well as introduce bias, leading to flawed conclusions (Enders, 2011; Graham, 2009).

Results

Results indicate the independent-samples t-test exhibited a lower than nominal Type-I error rate when there was no difference in pre-test/post-test means (see Table 1). Additionally, the independent sample t-test approach showed a modest advantage over the paired-samples t- test with listwise deletion at small, moderate, and large differences in means between the two administrations. Taken together, the results extend Sperling, Cruz & Zwahr-Castro's (2017) original conclusion that the independent-samples t-test is a powerful method of detecting mean differences when high missingness is a problem to include situations in which post-test data are MNAR.

Discussion

I agree with Cruz, Zwahr-Castro, & Sperling's (2017) assertion that most practitioners are unlikely to feel comfortable attempting sophisticated imputation methods for handling missing cases, and we applaud them for calling attention to the possibility of using the independent samples t-test approach to address the problem of high missingness. The results provided reinforce their recommendation and should allow teachers and other practitioners seeking to assess individual-level change to use accessible calculators, such as GraphPad, to perform their own

statistical analyses, even when challenged with high student turnover. Though this study cannot go without some limitations due to it being a simulation study produced in R, to further understand the consequences of MNAR data in a pre/post-test design it would be wise to observe the effects a skewed distribution has on results as well as violations of assumptions.

Furthermore, the study was challenged by ceiling effects at high levels of power. it would be wise to observe the effects a skewed distribution has on results as well as violations of assumptions. Furthermore, the study was a bootstrapped simulation in R, therefore observing ceiling effects and looking at variations in sample size would also be open to further study.

References

Cheema, J.R. (2014). A review of missing data handling methods in education research. Review of Educational Research, 84. doi: 10.3102/0034654314532697

Elizondo, A. (2014). Factors that contribute to Hispanic English Language Learners' high academic performance in high school science in the Rio Grande Valley of Texas: A multicase study. ProQuest Dissertations and Theses, 3642182 doi: https://search.proquest.com/openview/caeed93bl 8733d7ca6d54968d4b4ea38/I?pq-origsite=gscholar&cbl=18750&diss=y

Enders, C. K. (2011). Missing not at random models for latent growth curve analyses. Psychological Methods, 16, 1-16. doi: 10.1037/a0022640

Graham, J. W. (2009). Missing data analysis: Making it work in the real world. Annual Review of Psychology, 60, 549-576. doi: 58.110405.085530

Olinsky, A., Chen, S., & Harlow, L. (2003). The comparative efficacy of imputation methods for missing data in structural equation modeling. European Journal of Operational Research, 151(1), 53-79. https://doi.org/10.1016/S0377-2217(02)00578-7

Rumberger, R. (2003). The Causes and Consequences of Student Mobility. The Journal o,/ Negro Education. 72(I), 6-21. doi: l 0.2307 /3211287

Schafer, J. L., Graham, J. W. (2002). Missing data: Our view of the state of the art. Psychological Methods, 7 147-177. doi: I0.1037//1082-989X.7.2.147

Sperling, R., Cruz, F., & Zwahr-Castro, J. (May, 2017). The (dis)advantage of paired samples t- test with high missing data: Addressing a perennial problem in our K-12 schools. Poster presented at the 29th Annual Association for Psychological Science Conference, Boston, MA.

U.S. Department of Commerce, Economics and Statistics Administration, U.S. Census Bureau (2018). Geographical Mobility: 2017 to 2018. (U.S. Census Publication No. Retrieved from https://www.census.gov/data/tables/2018/demo/geographic-mobility/cps-2018.html

Table 1

Type I error

	Unique	Shared	Total	+/- Nominal
No Missing Data	18	32	60	+0.01
Paired Samples	44	32	76	+0.16

Power: 0.5 sd difference

	Unique	Shared	Total	+/-
No Missing Data	310	272	582	N/A
Paired Samples	4	272	276	-0.31

Power: 1 sd difference

	Unique	Shared	Total	+/-
No Missing Data	83	898	981	N/A
Paired Samples	0	898	898	-0.08

Type I error

	Unique	Shared	Total	+/- Nominal
No Missing Data	17	15	32	-0.18
Independent Samples	9	15	24	-0.26

Power: 0.5 sd difference

	Unique	Shared	Total	+/- Nominal
No Missing Data	141	423	564	N/A
Independent Samples	41	423	464	-0.10

Power: 1 sd difference

	Unique	Shared	Total	+/- Nominal
No Missing Data	20	961	981	N/A
Independent Samples	2	961	963	-0.02

Note. Independent samples t-test shows lower than nominal type-I error rates when there was no difference in pre-test/post-test means. It also shows advantages over the paired-samples t- test with listwise deletion at small, moderate, and large differences in means between the two administrations

Mama's Boy: A Pilot Study of Contact in Killer Whales (Orcinus orca) in Tw Mother-Calf Pairs

Kimberly Salazar

Mentor: Heather Hill, Ph.D.
St. Mary's University, San Antonio, TX

The role of contact as an affiliative behavior has been studied in cetaceans such as bottlenose dolphins (Tursiops truncatus) and beluga whales (Delphinapterus leucas). However, little is known about this same behavior in killer whales (Orcinus orca). Based on previous research, it is expected that contact will occur mostly between mother-calf pairs. The purpose of this study was to analyze the frequency of contact (e.g., touches) and the receiver of the contact in two mother-calf pairs. As a pilot study, the researchers utilized data collected from Marineland of Canada from the year 2000. Observations occurred in 9-minute focal follows using continuous and instantaneous sampling for two mother-calf pairs. Results suggested that calves initiated a significant majority of the contact with their mothers. The mothers however, initiated a more diverse range of behaviors with their calves. This suggests that calves are initiating many of the same behaviors with their mothers as a source of social and physical development. These data suggest that mothers demonstrated a more diverse set of behaviors because they were more knowledgeable of their bodies and environment. As a pilot study, the results should be interpreted with caution. Ultimately, the role and frequency of contact in killer whales should continue to be examined.
Keywords: Orcinus orca, contact, touches, cetaceans

Killer Whales (*Orcinus orca*) have fascinated researchers for many years, yet the majority of research conducted thus far has been on the topics of health/physiology and

foraging/predation with very little on social behavior (Hill, Guarino, Dietrich, & St Leger, 2016). Killer whales in their natural habitat are separated into ecotypes based on their geography, dispersion patterns, and foraging habits. The two best known ecotypes are residents and transients, which differ in diet, vocalizations, and dorsal fin shape. Resident killer whales travel in stable groups that include many maternal lineages, while transient killer whales engage in social dispersal and leave their maternal groups (Mann, Connor, Tyack, & Whitehead, 2000). Although behaviors such as foraging and vocalizations have been studied, much less is known about killer whale social interactions and the role of contact in those interactions.

One of the most important bonds is the bond between mother and calf. Recent research has even shown that this bond is instrumental in survival of adult male offspring. Also known as the grandmother hypothesis, adult female killer whales in menopausal age have been observed to lead their sons and likely increase their fitness and overall survival rate (Brent et al., 2015). This long-lasting bond begins at birth when neonates initiate contact with their mother's mammary area, usually a few hours after birth (Asper, Young, & Walsh, 1988). This initial contact after birth is important in establishing both nursing behaviors and social relationship between mothers and calves. The mother-calf bond continues to strengthen postnatally. Research on the sleeping patterns of killer whales and their calves suggest that the preferential sleeping partner for the calves is with their mothers (Hill, Guarino, Geraci, Sigman, & Noonan, 2017). This research also demonstrated that in the first month of life, killer whale calves typically engage in swims with their mothers in either in echelon or infant position the majority of their time, suggesting that maintaining proximity to their mothers is important for the calves' physical and social development. Calves also display a spatial laterality and side preference when swimming with their mothers, which appear to be dependent on the presence of a possible threat or predator (Karenina, Giljov, Ivkovich, Burdin, & Malashichev, 2013). After the first year of life, killer whale

calves engage in more solitary swimming, playing with objects and others, and other motor play activities (Guarino, Hill, & Sigman, 2016).

One aspect of social interactions that has been neglected in most research involving cetaceans is the function of tactile communication. While many researchers speculate on the importance of tactile communication for cetaceans, citing skin sensitivity, close swimming, and the frequency with which touching occurs during various social interactions, few have studied its frequency and functions systematically. Of the cetaceans studied, bottlenose dolphins (*Tursiops truncatus*) have been the most frequently observed in terms of touch. Pryor (1990) suggested that dolphins were especially sensitive to touch as training could be performed using only touch as reinforcement for their behaviors (Pryor, 1990). Moreover, dolphins, like many other cetaceans, are thought to maintain their position and judge both "water flow and movement" through skin stimulation (Pryor, 1990).

Contact behavior in delphinids appears to occur frequently in wild and captive populations. In a population of Atlantic spotted dolphins (*Stenella frontalis*), Dudzinski (1998) identified seven different contact behaviors utilized as a form of tactile communication. Using a "video/acoustic array," Dudzinski was able to pair behavior with acoustics along with determining the identity of each dolphin. This information enabled Dudzinski to establish the relationship between age and sex on the frequency of contact behavior within each social group studied. Specifically, dyads identified as a mother and calf, contributed to the calves initiating and receiving the most contact with adults over any other age category (Dudzinski, 1998). Additional research has suggested that pectoral fin contact occurs in several species of dolphins both captive and wild, including the Indo-Pacific bottlenose dolphin (*Tursiops aduncus*), the Atlantic spotted dolphins (*Stenella frontalis*), and a captive population of bottlenose dolphins (*Tursiops truncatus*) (Dudzinski, Gregg, Paulos, & Kuczaj, 2010; Dudzinski, Gregg, Ribic, & Kuczaj,

2009). The function of contact for these animals has been suggested to serve as a social bonding or to facilitate hygienic behaviors.

Both dolphins and killer whales belong to the family of delphnidae in the taxonomic hierarchy, which suggests that these to delphinids should share some characteristics despite slightly different social structures. Behavioral similarities include similar post-natal mother-calf proximity and the appearance of independent behaviors (Mann & Smuts, 1999; Guarino, Hill, & Sigman, 2016). Some other hunting strategies, such as beach-feeding or intentional stranding, has been observed in both bottlenose dolphins and killer whales (Silber & Fertl, 1995). Research on delphinid and cetacean communication also suggests that bottlenose dolphins and killer whales have similarities in their use of echolocation (Tyack & Clark, 2000).

Although little is known about the frequency or function of touch in killer whales, tactile contact has been observed and reported for a variety of contexts. For example, killer whales off the coast of Argentina push their young on to the beach towards prey. The use of contact to intentionally strand their young demonstrates teaching by providing their young with the experience of capturing prey on the beach (Rendell & Whitehead, 2001). In this teaching behavior, contact appears to serve a practical or survival function. Contact between killer whales and inanimate objects has also been demonstrated through beach-rubbing behavior. Killer whales off of the coast of Vancouver Island have been observed to utilize two different gravel beaches to rub themselves (Williams, Lusseau, & Hammond, 2009). The function of beach-rubbing behavior is unknown; however, it has been suggested to be utilized as a hygienic or socializing activity (Ford, Ellis, & Balcomb, 1996). In both the beaching and beach-rubbing behaviors, contact is seen as the means by which these behaviors are performed.

Contact between mothers and calves is often observed during stereotyped swim positions such as infant position (Gubbins et al., 1999). It has been documented that calves will

start to separate from their mother at around 8 weeks old and may even engage in contact with killer whales other than their mother (Asper et al., 1988). However, the role of contact during affiliative rubs and interactions is less well known. Analyzing the specificities in which contact occurs could provide more knowledge regarding the development of killer whales.

Overall, the lack of information concerning the frequency and type of contact in killer whales is apparent. The purpose of the current study is to address this gap by analyzing the frequency of contact (e. g., touches) and the receiver of the contact for two mother-calf pairs as a pilot study on the role of contact in calf development. Recent research on the role of contact as a social behavior in captive beluga whales (*Delphinapterus leucas*) suggested that out of all social groups present, more than half of contact occurred between bonded mother-calf pairs (Hill, Alvarez, Dietrich, & Lacy, 2016). It was also found that, apart from the mother-calf contacts, two immature belugas initiated all other contact between two belugas, which corroborates research on dolphin calves initiating most of the pectoral fin contact (Dudzinski, 1998). Since the current study only involves two killer whale mother-calf pairs, it can be expected that the two killer whale calves will initiate a majority of the contact, likely with their own mothers. Furthermore, since killer whale calves were observed to engage in more independent behaviors as they mature (Guarino, Hill, & Sigman, 2016), it can be expected that most of the contact behavior initiated by the two male calves will occur in the first six months of the observation period.

Method

Subjects

The current study was conducted with four captive killer whales, two adult females and their male calves. $Calf_1$ was approximately 1.5 years old and $calf_2$ was 6 months old at the beginning of observations. All killer whales were housed in the captive facility, Marineland of Canada.

Sample

The data utilized for the current study were collected by researchers at Marineland Canada during the year 2000. Continuous event sampling was performed, and a database of over 12,000 events involving physical contact was created. This database was organized by initiator and receiver to evaluate the frequency and nature of the contact events between mothers and calves and their companion animals.

Procedure

Data were collected utilizing 9-minute focal follows, using continuous and instantaneous sampling. Two different social groupings were recorded, one with the adult male present with the two mother-calf pairs and one without the adult male present. Data were initially coded using the Observer program and was then transferred into text files to be used in Excel. Once the data were in Excel, the researcher organized the data to be processed in SPSS. Rates of behavior (total frequency of behavior/total seconds observed) were calculated for each killer whale for the behavior of touches.

Results

An independent samples *t*-test was conducted to compare the rate of behavior in calves ($M = 0.003$ behaviors/sec, $SD = 0.0051$) and adults ($M = 0.0007$ behaviors/sec, $SD = 0.00068$). Results showed a significant difference, $t(45.584) = 2.335$, $p = 0.024$. As expected from previous studies, calves (83%, $n = 10{,}167$) demonstrated a higher rate of behavior than adults (17%, $n = 2{,}114$) calves.

A Pearson Chi-Square test was conducted to examine the relationship between the age of the killer whales (adults and calves) and type of behavior. The type of behavior was dependent on the age class initiating the behavior, $\chi^2(9, N = 12{,}219) = 2{,}931.2$, $p < .001$. As demonstrated in Figure 1, calves engaged in head touches significantly more than expected compared to all other touch behaviors observed. Calf head touches accounted for 63.7% ($n = 6{,}454$) of all calf touch behavior and 52.8% of all total behavior. Figure 1 also shows

that the rate of mouth touches was a common behavior, accounting for 19.7% (n = 1,998) out of all calf behavior.

Figure 1. Frequency of calves' behavior.

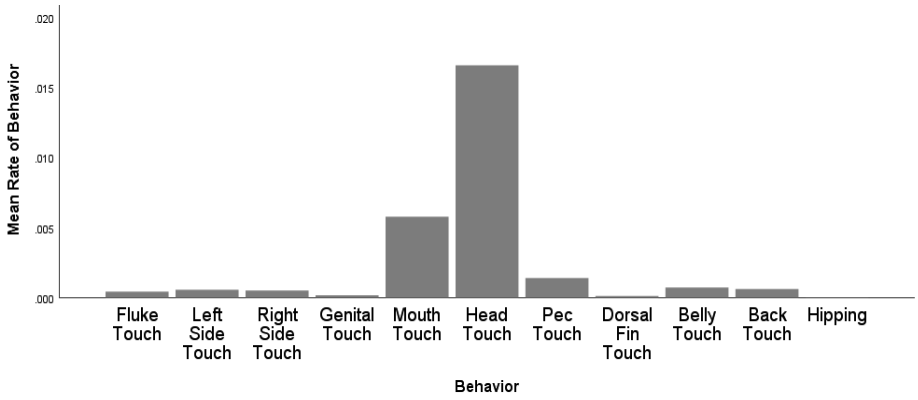

In contrast to the calves, adult touch behaviors were more evenly distributed and displayed more diversity in total rates (Figure 2). Pectoral fin touch behavior was the most frequent among the adults, accounting for 31.5% (n = 660) of the total of all adult behaviors. The second most frequent behavior for the adults was the mouth touch, accounting for 20.1% (n = 420) out of all adult behaviors.

Figure 2. Frequency of adults' behavior

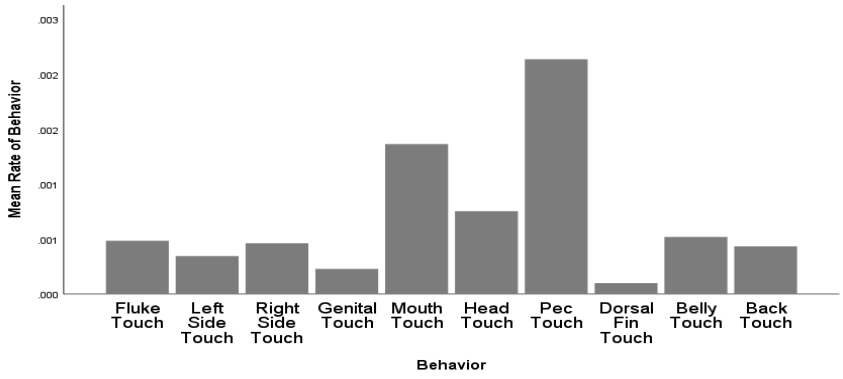

When the relationship between behavior types and receiver was examined for each calf, the same pattern was found. For $calf_1$, 79% (n = 4399) of the behavior was directed towards his mother ($adult_1$). Out of all total behaviors directed towards $adult_1$, $calf_1$ initiated 78% (n = 3,433) head touches towards his mother. Similarly, $calf_2$ also showed 79% (n = 3,634) of his behaviors were directed towards his mother ($adult_2$), and 73% (n = 2,654) of total behaviors were head touches.

Within the first six months of the observation period, $calf_1$ (aged 1.5 years old) engaged in 93% (n = 5,158) of all behavior for the entire observation year. During the first six months, 94% (n = 3,449) of the behavior were head touches. $Calf_2$, however, engaged in a little over half (52%, n = 2,368) for the first six months of observation, and the other half (48%, n = 2,224). Head touches for $calf_2$ directed towards $adult_2$occurred 50% (n = 1,385) within the first six months and 50% (n = 1,401) within the second six months.

Discussion

The purpose of the current study was to analyze the frequency of contact (e.g., touches) and the receiver of the contact in two mother-calf pairs. The skin sensitivity of cetaceans and rate in which it occurs in both captive and wild population demonstrates that contact serves as a function of social development and a method of teaching (Pryor, 1990; Dudzinski, Paulos, & Kuczaj, 2010; Hoppitt, Brown, Kendal, Rendell, Thornton, Webster, & Laland, 2008). Therefore, it is important to understand the context of contact and explore the function of contact, especially between mothers and calves in order to fully understand the development of cetacean behaviors.

Calves Initiate Contact

Based on previous research it was expected that the killer whale calves would initiate the majority of the contact compared to the rate to which adults initiated the contact. This hypothesis was supported with the data, with the calves initiating over 80% of the total behavior. Calf initiation of behavior with a mother is corroborated by research on contact between captive beluga

whales (Hill et al., 2016) and several populations of wild and captive dolphins (Dudzinski, 1998). The frequency in which $calf_1$ (aged 1.5 years old) engaged in contact with his mother was likely the result of his age. By this time, $calf_1$ was knowledgeable of his body and his surroundings. However, he still needed contact with his mother for the purposes of social bonding and nutrition (Asper et al., 1988; Guarino et al., 2017). $Calf_2$ also initiated a significant amount of contact with his mother, which was less than $calf_1$ who was approximately one year older, and more knowledgeable of his surroundings.

Mothers Matter for Young Calves

Along with the calves initiating a majority of the contact behavior, it was expected that killer whale calves would initiate the majority of this contact with their own mothers. Due to the limited sample size, inferential statistics were not possible and descriptives are reported. The results indicated that both mother-calf pairs in this sample contacted their mothers almost 80% of the events. This pattern for mother-calf contact has also been observed with belugas in captivity (Hill et al., 2016). Similarly, mother-calf synchrony may facilitate future synchronized actions and possible imitation in bottlenose dolphins and other delphinids (Fellner, Bauer, & Harley, 2006).

Contact between mothers and calves has been suggested to be important in the development of specific skills, such as social learning, feeding, and hunting behaviors in the wild (Guinet, 1991). The significance and function in mother-calf contact in captivity likely corroborates the function of contact in wild populations, namely facilitating social learning. Teaching and observational learning have been demonstrated in killer whales, who have been observed to teach their young to intentionally beach themselves to capture prey on the beach (Hoppitt, Brown, Kendal, Rendell, Thornton, Webster, & Laland, 2008). In captivity, experimental evidence exists from a study assessing the capabilities of killer whales to imitate both familiar and novel behaviors on command found that killer whales learned the imitate command and successfully imitated their conspecific's

behavior quite quickly (Abramson, Hernandez-Lloreda, Call, & Colmenares, 2013). Together, these findings suggest that social learning, such as imitation, is likely developed through mother-calf interactions, which often include contact.

Timing Matters

Lastly, based on research assessing the development of mother-calf relationship behaviors (Hill et al., 2017), it was expected that a majority of calf contact would occur in the first six months of the observation year. This pattern also corresponds to killer whale calf development of independent behaviors (Guarino et al., 2016). Frequencies for $calf_1$ indicated that 93% of his total behavior was performed within the first six months of the observation year. $Calf_2$ also demonstrated a little over half (52%) of total behaviors in the first six months of the observation period, supporting the hypothesis. As any animal develops and matures, the dependency on the mother for teaching and survival decreases. Killer whales travel in matrilineal social groups, and both transient and resident killer whales retain a long-term social bond with their mothers (Bigg, Olesiuk, & Ellis, 1990). Therefore, while contact between killer whale mother and calf will decrease as the calf matures, neither the social bond nor contact should disappear.

Future research should continue to investigate contact with a larger sample size of killer whales, with a more diverse social composition. Once the trends of contact are established with a larger sample size, a formal comparison of the nature and function of contact for killer whales, beluga whales and dolphins can be conducted. Overall, this pilot study revealed some trends in contact for killer whale mother-calf pairs. However, due to the limited power and small sample size, results should be interpreted with caution. Contact research in killer whales and other related animals should be continued in order to fully understand the relationship between contact and developmental patterns. Beside from humans, killer whales are the most far-reaching carnivore and is the predator for almost every marine mammal (Pitman, Balance, Mesnick, & Chivers, 2001). Therefore, killer whale

behavioral research is fundamental in understanding the complexities of the animals that affect the behavior of several different marine and land animals.

Acknowledgements

Thanks to Dr. Michael Noonan for the use of his data, and his input on this project. Also, thanks to the McNair Scholar Program at St. Mary's University for providing funding and s support for this project.

References

Abramson, J. Z., Hernández-Lloreda, V., Call, J., & Colmenares, F. (2013). Experimental evidence for action imitation in killer whales (Orcinus orca). *Animal cognition*, *16*(1), 11-22.

Asper, E. D., Young, W. G., & Walsh, M. T. (1988). Observations on the birth and development of a captive-born Killer whale Orcinus orca. *International Zoo Yearbook*, *27*(1), 295-304.

Bigg, M. A., Olesiuk, P. F., Ellis, G. M., Ford, J. K. B., & Balcomb, K. C. (1990). Social organization and genealogy of resident killer whales (Orcinus orca) in the coastal waters of British Columbia and Washington State. *Report of the International Whaling Commission*, *12*, 383-405.

Brent, L. J., Franks, D. W., Foster, E. A., Balcomb, K. C., Cant, M. A., & Croft, D. P. (2015). Ecological knowledge, leadership, and the evolution of menopause in killer whales. *Current Biology*, *25*(6), 746-750.

Dudzinski, K. M. (1998). Contact behavior and signal exchange in Atlantic spotted dolphins (Stenella frontalis). *Aquatic Mammals*, *24*, 129-142.

Dudzinski, K. M., Gregg, J. D., Paulos, R. D., & Kuczaj II, S. A. (2010). A comparison of pectoral fin contact behaviour for three distinct dolphin populations. *Behavioural Processes*, *84*(2), 559-567.

Dudzinski, K. M., Gregg, J. D., Ribic, C. A., & Kuczaj, S. A. (2009). A comparison of pectoral fin contact between two different wild dolphin populations. *Behavioural Processes*, *80*(2), 182-190.

Fellner, W., Bauer, G. B., & Harley, H. E. (2006). Cognitive implications of synchrony in dolphins: A review. *Aquatic Mammals*, *32*(4), 511.

Ford, J. K., Ellis, G. M., & Balcomb, K. C. (1996). Killer whales: the natural history and genealogy of Orcinus orca in British Columbia and Washington. *UBC press*.

Guinet, C. (1991). Intentional stranding apprenticeship and social play in killer whales (Orcinus orca). *Canadian Journal of Zoology*, *69*(11), 2712-2716.

Guarino, S., Hill, H. M., & Sigman, J. (2017). Development of sociality and emergence of independence in a killer whale (Orcinus orca) calf from birth to 36 months. *Zoo Biology*, *36*(1), 11-20.

Gubbins, C., Mcowan, B., Lynn, S. K., Hooper, S., & Reiss, D. (1999). Mother-infant spatial relations in captive bottlenose dolphins, Tursiops truncatus. *Marine Mammal Science*, *15*(3), 751-765.

Hill, H. M., Alvarez, C. J., Dietrich, S., & Lacy, K. (2016). Preliminary findings in Beluga (Delphinapterus leucas) tactile interactions. *Aquatic Mammals*, *42*(3).

Hill, H. M., Guarino, S., Dietrich, S., & St Leger, J. (2016). An inventory of peer-reviewed articles on killer whales (Orcinus orca) with a comparison to bottlenose dolphins (Tursiops truncatus). *Animal Behavior and Cognition*, *3*(3), 135-149.

Hill, H. M., Guarino, S., Geraci, C., Sigman, J., & Noonan, M. (2017). Developmental changes in the resting strategies of killer whale mothers and their calves in managed care from birth to 36 months. *Behaviour*, *154*(4), 435-466.

Hoppitt, W. J., Brown, G. R., Kendal, R., Rendell, L., Thornton, A., Webster, M. M., & Laland, K. N. (2008). Lessons from animal teaching. *Trends in ecology & evolution*, *23*(9), 486-493.

Karenina, K., Giljov, A., Ivkovich, T., Burdin, A., & Malashichev, Y. (2013). Lateralization of spatial relationships between wild mother and infant orcas, Orcinus orca. *Animal behaviour*, *86*(6), 1225-1231.

Mann, J., & Smuts, B. (1999). Behavioral development in wild bottlenose dolphin newborns (Tursiops sp.). *Behaviour*, *136*, 529-566.

Mann, J., Connor, R. C., Tyack, P. L., & Whitehead, H. (Eds.). (2000). Cetacean societies: field studies of dolphins and whales. *University of Chicago Press*.

Pryor, K. W. (1990). Non-acoustic communication in small cetaceans: glance, touch, position, gesture, and bubbles. In *Sensory abilities of cetaceans* (pp. 537-544). Springer, Boston, MA.

Rendell, L., & Whitehead, H. (2001). Culture in whales and dolphins. *Behavioral and Brain Sciences*, *24*(2), 309-324.

Pitman, R. L., Ballance, L. T., Mesnick, S. I., & Chivers, S. J. (2001). Killer whale predation on sperm whales: observations and implications. *Marine mammal science*, *17*(3), 494-507.

Silber, G. K., & Fertl, D. (1995). Intentional beaching by bottlenose dolphins (Tursiops truncatus) in the Colorado River Delta, Mexico. *Aquatic Mammals*, *21*, 183-186.

Tyack, P. L., & Clark, C. W. (2000). Communication and acoustic behavior of dolphins and whales. In *Hearing by whales and dolphins* (pp. 156-224). Springer, New York, NY.

Williams, R., Lusseau, D., & Hammond, P. S. (2009). The role of social aggregations and protected areas in killer whale conservation: the mixed blessing of critical habitat. *Biological Conservation*, *142*(4), 709-719.

Assessment of Ground Penetrating Radar as a Tool for Surveying World Newt Cave

Miguel Valdes

Mentor: Evelynn J. Mitchell, Ph.D.
St. Mary's University, San Antonio, TX

Techniques for shallow geophysical survey have advanced far and broadly in recent years. While their technologies have become more sophisticated and accurate for locating shallow features, a question remains about how accurate these methods actually are. A previous study found ground penetrating radar (GPR) to render a more accurate passage size in Cricket Cave, when compared to LIDAR data, than resistivity measurements. By surveying World Newt Cave, a feature on a property in the far west side of San Antonio, Texas, USA, this study aimed to prove whether this conclusion was still true when adding a second dimension to GPR data by surveying a grid, rather than a single two-dimensional scan. An analysis was performed comparing GPR to LIDAR as the example for accurate data. The LIDAR system used was unable to properly read certain remote parts of the survey area but did generate accurate data for the main part of the passages. Comparisons between models demonstrate the accuracy of GPR given the task of cave passage detection.

As techniques for mapping near-surface geology advance, so does the need for their evaluation as efficient and accurate survey systems. In areas under urban development, the need for accurately mapping nearby caves and karst features becomes more important to property owners and contractors. The systems of ground penetrating radar (GPR) and LIDAR are common techniques for documenting subsurface geophysical features.

Most GPR systems are portable and do not require researchers to enter a feature of interest to conduct a geophysical survey. The instruments required for GPR are relatively obtainable and do less harm than alternative methods, such as

borehole logging (Yeboah-Forson et al. 2014). LIDAR, however, does require surveyors to enter a feature of interest and demands sufficient visibility to provide a full rendering of said feature. Developments in this technology have granted surveyors increased mobility with LIDAR systems while allowing for heavily detailed maps of caves, requiring little training (Zlot and Bosse 2014).

Because of the precision of LIDAR systems, they yield high-quality, detailed, data for a precise model to be developed from. A previous study has found GPR to render more accurate scans of features than resistivity (Mitchell and Mitchell 2017) when compared to LIDAR scans. This study will conduct a more detailed study of World Newt Cave using GPR to better gauge the accuracy of the instrument. The earlier study obtained a single GPR scan of Cricket Cave to compare to LIDAR data. This study will include a grid survey and an individual 2D scan of an area near the entrance of World Newt Cave. The added samples of data will generate a better perception of GPR's accuracy when compared to LIDAR.

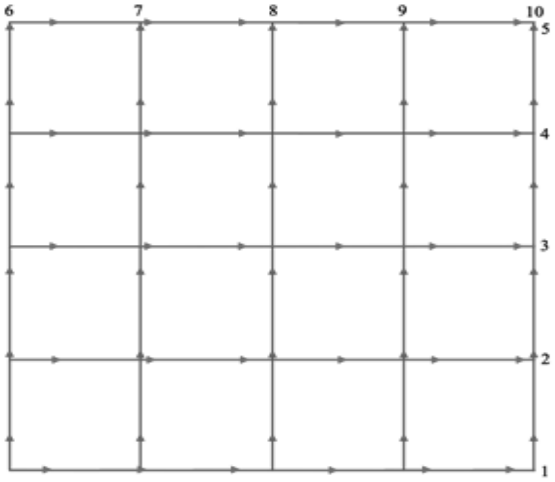

***Figure 1**: Depiction of 4*4 m grid with lines numbered after their order of scanning. (Red indicating y-axis; Blue indicating x-axis.)*

World Newt Cave, and its three sister caves, are in a geologic feature known as Austin Chalk. This geologic layer is known for yielding small to moderate quantities of water, given its properties as a chalky limestone. The limestone's conductive capacity comes from its ability of dissolution from water of good to poor quality, increasing its water storage capacity. In this region Austin Chalk is found above the Eagle Ford Shale, a confining layer known for being a poor conductor of water (Arnow 1963). This confining layer generally limits the conductive capacity of features in Austin Chalk, due to restricted dissolution below. While there are examples of Austin Chalk features having hydraulic connection with the Edwards Aquifer, there is no indication that any features on the property are hydrologically significant (Thoene 2014).

METHODS

For the application of the GPR method, the determined survey area was first cleared of any objects large enough to obstruct the system. A square grid of 4 meters by 4 meters was then constructed. Five flag markers were afterward placed, one every meter, along the y-axes of the grid (Figure 1). Another 5 were placed on the opposite side of the grid, one mirroring each marker on the y-axes. This was primarily to guide the driver of the GPR system. Once all 5 paths were scanned, the same process was done for the x-axes of the grid. When the survey was finished, the data were taken from the GPR system and downloaded to a flash-drive. The data were afterwards processed using the GSSI RADAN 7 software to create individual slices through the grid and a more defined image. By using the easy processing tools in the software, noise was removed, and a clearer image was developed. These tools allowed for the data to be corrected by informing the software of where the horizon line was located, adjusting for the feedback observed by the system and making anomaly detection more distinguishable from the background data. Lastly, potential void features observed were

measured frame-by-frame to compare slices of the data to LIDAR. The resulting model was an outlined version of what the cave is interpreted to look like. An additional scan was made across a line parallel to line 1 to obtain a scan near the entrance of the known passage of the cave. This scan will be known as “line 11.” Line 11 was processed and compared to LIDAR data just as the other scans were.

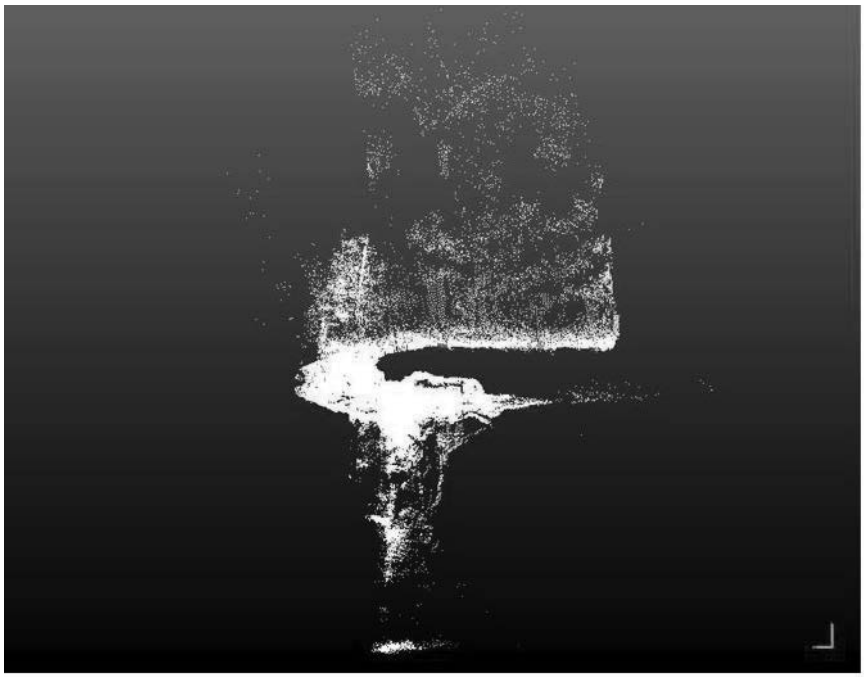

Figure 2: *Full extent of the LIDAR data mapping the cave. The data representing the surface above the feature are the points that make up the solid white line with many floating points above it. Points below this line are data representing the caves feature.*

The LIDAR system used to scan World Newt Cave was the Caveatron, a portable tool designed specifically for cave survey and mapping (Mitchell 2017). While scanning in motion, the Caveatron positionally references scans made to a retroreflective card so the system can make a correct registration of distance and direction. This card was required to be visible at every station for the system to make a valid scan. The coordinates recorded in the point cloud register stations to create a

meaningful shape or feature. These coordinates are on a digital line plot with X, Y, and Z axes. The coordinates and the data were input to the CloudCompare processing software to create a visual model (Figure 2). Slices from the full model were created at a 1-meter spacing at a width of 0.2 meters to align with the locations of the GPR scans. Afterwards, points from the LIDAR model were compared to data from the GPR survey lines to observe similarities and differences in their dimensions.

Once potential features were identified, they were measured according to what was speculated. Slices of the LIDAR data were isolated to compare with the GPR data. The features were measured by width, height (tallest point from the bottom of the void), and depth (closest point to the surface). An error percent was calculated for each feature observed in each scanned line using the equation ABS((GPR-LIDAR)/LIDAR)*100. The end result was a percentage that indicated how well the GPR data aligned with LIDAR data.

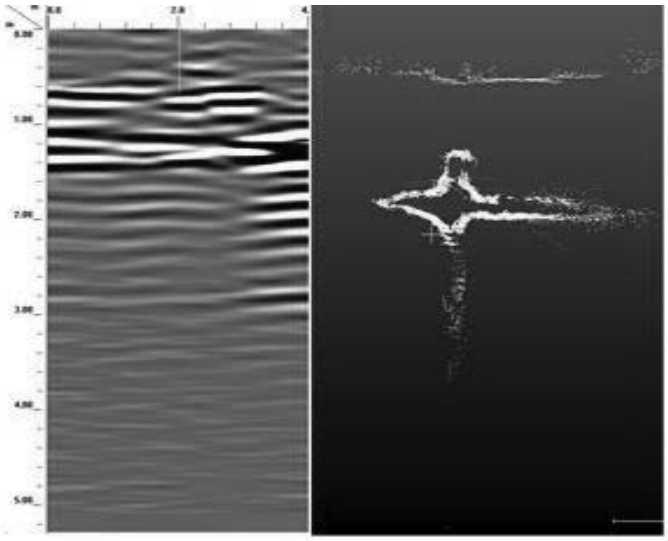

Figure 3: *Scans of line 1 using LIDAR and GPR. (Left, GPR: Right, LIDAR)*

RESULT

The LIDAR survey created an incomplete scan, containing multiple gaps in the data, particularly in the known pit feature. However, the LIDAR survey did still create an image that makes out most of the cave's known features.

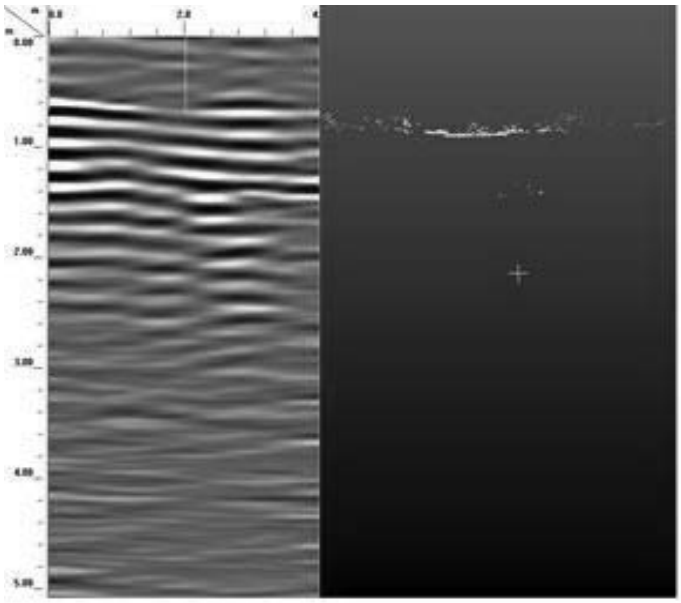

Figure 4: *Scans of line 4 using LIDAR and GPR. (Left, GPR; Right, LIDAR)*

The full extent of the LIDAR data presents World Newt Cave as an at most 8 m deep and 8 m long feature. Figure 3, line 1, shows a 7.66 m pit drop and a passage that extends 3.2 m. The extent of the GPR survey did not cover as much area as that of LIDAR. As a result, more data was generated through the utilization of LIDAR than when GPR was used. Similarly, the GPR scans included multiple features that had data where LIDAR seemingly did not. In figure 4, a distinguishable image can be observed by the GPR image while LIDAR data for the same area only shows several points below the surface data. This data was not enough to make any measurements from or to compare with

GPR data. Lines 5, 6, 7, and 8 all had this same issue. Line 8 did have enough data to draw an image from but contained very little information within the range of the GPR survey. This made it insufficient for comparing to the GPR scan.

Figures 3 and 6 show LIDAR data picking up the anomaly of a known pit inside the cave in that area. Figure 3 also shows the GPR scan to have found similar data to that slice of the LIDAR data. The error percentages for the measurements on line 1 were similar to the average errors for all scans. With an average error for depth of 244%, the GPR system was least successful when accurately defining the extent of the bottom of a feature. The GPR scan for line 10 (Figure 5) was much closer to defining the same features as in LIDAR but generated the highest amount of error in proportion to the size of the feature. Figure 6 shows how GPR and LIDAR generated completely different images.

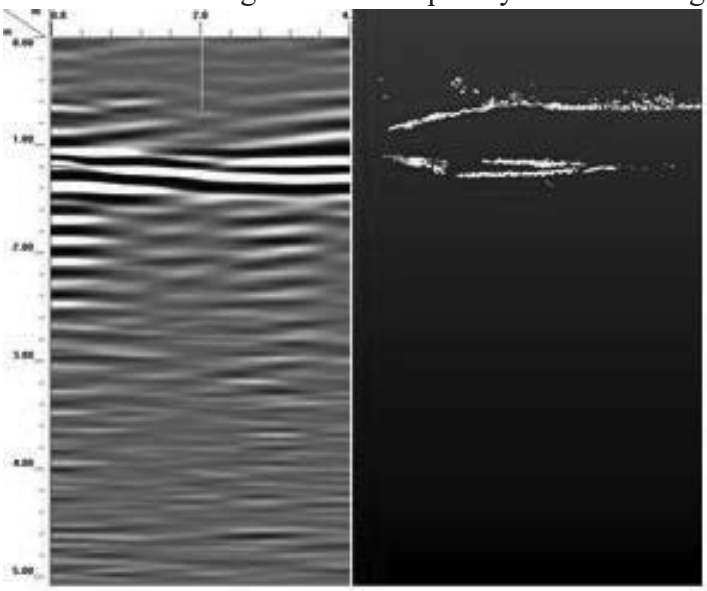

Figure 5: *Scans of line 10 using LIDAR and GPR. (Left, GPR; Right, LIDAR)*

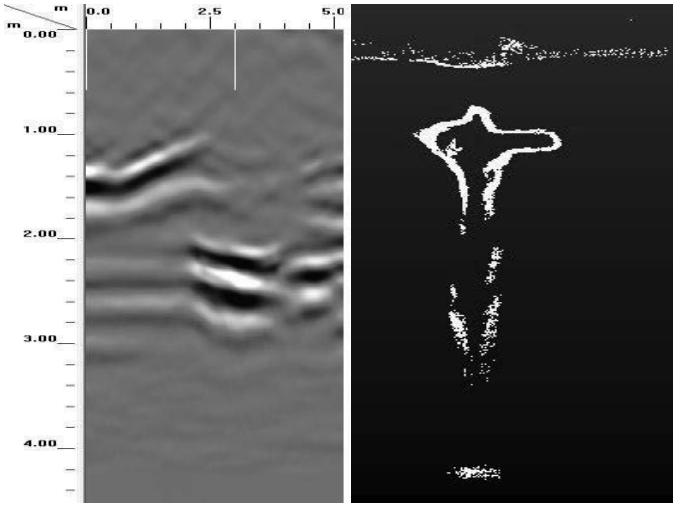

Figure 6: *Scans of line 11 using LIDAR and GPR. (Left, GPR; Right, LIDAR)*

While neither method created a full model of the cave, in this study, GPR failed to accurately portray the width, height, and depth of the features by on average 158%, 52%, and 245% respectively. GPR data contained a large amount of noise and made findings not recorded in known information about this area; the validity of which will need to be addressed in the future.

DISCUSSION

The GPR grid was most successful when recording known features of the cave. The measurements of GPR scans were generally not in line with what LIDAR data indicated. A radar scan on line 10 measured at a depth of 2.2 m when the LIDAR scan for line 10 measured .6 m. This may be due to using a low dielectric constant when processing the data. The correction of this may reduce the error associated with the dimensions of observed features. The detection of features at various depths using GPR did not vary as much as was the case with the LIDAR survey. The radar scans generated images that seemed to show features that may have been features not yet connected with the

main passage (Figure 4), which would be why LIDAR was not able to register them. The images could have also been the result of other materials in the area such as water-saturated rock.

CONCLUSION

While data retrieved using ground penetrating radar did not yield the same results as LIDAR, it did display its viability in detecting shallow features. LIDAR also proved its own weakness by displaying that not all surfaces are detectable in an area with features that are not humanly passable. Ground penetrating radar may not be as accurate a method as LIDAR, but it does have capabilities in detecting features impenetrable to light.

It should be acknowledged that precise GPS equipment was not available for this study. If it were available, the location of the GPR scans would have been easier to compare to LIDAR data. It is possible that the lines of data derived from the LIDAR survey do not match the actual location of the GPR grid. This likely could have contributed to the differences in results between the two surveys. Future work should include detailed GPS information and observe full 3D models for a deeper assessment of the accuracy of GPR.

ACKNOWLEDGEMENTS

Thanks to Joseph N. Mitchell for conducting the LIDAR survey and organizing the CloudCompare files for observation. The authors would like to include additional thanks to the U.S. Department of Education Ronald E. McNair Postbaccalaureate Achievement Program for sponsoring this research.

REFERENCES

Arnos T, 1963. Ground-water geology of Bexar County, Texas. Washington, U.S. Govt. Print. Off., 1963, p. 1–40.

Mitchell, Evelynn J., and Joseph N. Mitchell. Comparison of Shallow Geophysical Cave Detection Methods to 3D LIDAR Mapping. Proceedings of the 17th International Congress of Speleology, July 2017, p. 126-129.

Mitchell J, 2017. Caveatron – Description. [accessed 2 June 2019]. http://caveatron.com/description.html

Thoene A, Kennedy J, 2014. Draft Management Plan for Rolling Oaks Cave Preserve, Bexar County, Texas. 4–26.

Yeboah-Forson A, Comas X, Whitman D, 2014. Integration of electrical resistivity imaging and ground penetrating radar to investigate solution features in the Biscayne Aquifer. J. Hydrol. 515, 129–138.

Zlot R, Bosse M, 2014. Three-dimensional mobile mapping of caves. J. Cave Karst Stud. 76, 191–206

Analyzing 3-D Printed Commercial PLA Properties Using a Baseline Impact Testing Trial

Nicolas Fabbri

Mentor: Amber McClung, Ph.D.
St. Mary's University, San Antonio, TX

With 3-D printing technologies becoming ever more relevant in the improvements of modern manufacturing and technologies, the research necessary to continue improving those technologies must advance as well. A number of different areas of study are necessary when it comes to 3-D printing as the process involves many different steps. On one end of the process, the printing machines themselves are being studied. Mechanical efficiency, temperature control, and speed are all performance parameters those interested in the technology wish to improve. Before the printing process even begins, the materials used in the machines are even more of a concern. One such material, Polylactic Acid (PLA), is taking the spotlight for its cost efficiency, its availability, and its biodegradable nature. While PLA has many apparent positives, one major negative prevents it from reaching the efficiency many researchers want. At the temperatures required for 3-D printing, PLA has a tendency to break down and lose as much as 20% of its integrity as the chemical bonds collapse. Carbon, cellulose, copper and many other types of materials are candidate additives to enhance the material properties. The long-term focus of this research is to test how the addition of copper flakes affects the mechanical properties of 3-D printed objects printed using PLA. The short-term focus of this paper is to establish the baseline properties of pure PLA filament. This will establish a much-needed benchmark for measuring the long-term effectiveness of adding copper flakes to the PLA.

In recent years, 3-D printing has become one of the most promising areas in production technologies. Although this spotlight has paved the way for a large amount of investment, regulations are still relatively preliminary, and research still focuses on areas that have been defined in other manufacturing methods for a long time. In fact, several studies featured in "Rapid Prototyping" and "Procedia Manufacturing" choose to define analytical and experimental approaches of further research instead of going into specific detail of actual research [1] [2]. A few things from those articles do focus on actual experimentation, among these are the Taguchi Method and ANOVA. The Taguchi Method is a departure from the traditional experimental approach and uses a system of matrix analysis to lower the overall number of experiments needed to gather significant data. ANOVA stands for Analysis of Variance and is essentially the numerical analysis of the different sections of data obtained from the Taguchi Method.

One of the main focuses of a lot of newer research is the material that 3-D printing machines use during the printing process. The most prominent materials include Acrylonitrile Butadiene Styrene (ABS), Polylactic Acid (PLA), Polyvinyl Alcohol (PVA), and Nylon. Of these PLA is of the most interest in the current study because of its low cost, environmental friendliness, and the fact that it has incredible mechanical properties when compared to several of the other candidates. One downside, however, is the fact that PLA has relatively poor resistance to higher temperatures. Most, if not all, 3-D printing processes heat the filament substance to temperatures of somewhere around 200 degrees. At this temperature, reductions of up to 20% of the mass of PLA have been observed. Another area of recent research is the addition of "nanofillers" to pure PLA, in order to increase its heat resistance while retaining many of the properties that has made PLA an area of study to begin with. Several types of nanofillers have been explored. An article

in the “Journal of Nanomaterials” attempted to carry further with PLA’s bio-friendliness by adding a type of nanocrystal formed from farming by-product [3]. An article in “Polymers” detailed the addition of several types of carbon additives that made astounding strides with as little as 1% of additive to the original PLA [4]. Another article by Gianluca Cicala et. All focused-on poly/lignin blends in traditional manufacturing which is essentially woodchip additive [5]. Each of those articles found similar results, in that adding the substances in a particular amount tended to increase the resistance to stress by amounts of up to 60%, but if too much of the substance was added, a sharp decline in mechanical properties was observed.

The third major area of research tends to focus primarily on the mechanical properties of the products of 3-D manufacturing instead of the experiment techniques or the substance being experimented with. Another article from the “Rapid Prototyping Journal” details specifically how important print orientation is to the overall integrity of the printed product [6]. They noted that a rotation of 45 degrees could mean the difference between almost double the integrity. An article from “PloS ONE” submerged 3-D printed parts in water and pumped air through them. Imperfections existed that could not be seen by the naked eye but could have easily been solved by the rate at which filament was extruded [7]. A final presentation from a conference in Greenville, SC noted the effects of heat during the printing process [8]. Ductility and brittleness could be heavily affected by the temperature at which the processes were carried out.

Our area of research falls more closely to the third category. While it is of long-term interest to us the actual composition of the filaments, this paper focuses on establishing a proper baseline of mechanical properties of 3D printed PLA. Many of the articles mentioned previously zeroed in on several

common types of tests such as fatigue and tensile tests. Our focus will be the amount of energy standard PLA samples can absorb.

Methodology

Figure 1 shows the overall flow of the research conducted in this paper. Impact samples were 3D printed, and from there, were taken to the impact machine in the lab, which output the results as the tests occurred.

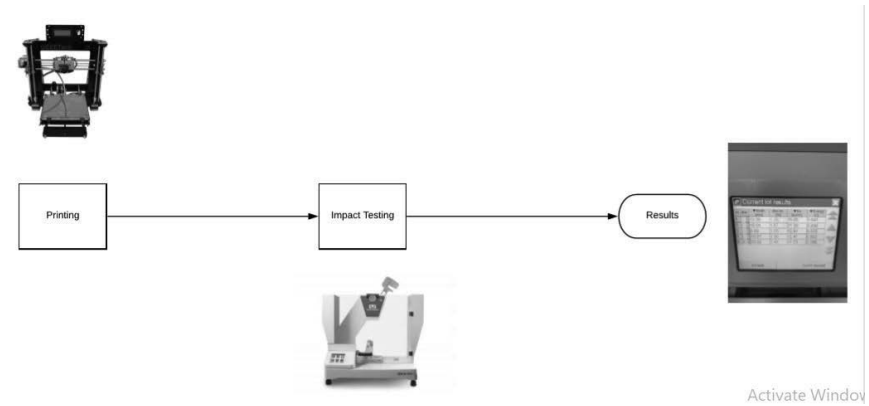

Figure 1: Flow Chart of Experimental Steps

Impact testing is conducted on an Instron CEAST 9050 Pendulum Impact System following ISO 179-1. ISO 179-1 details the standard procedures for Charpy Impact Testing of normal composite materials [9]. Subsection 1.5 reinforces that notched samples are not normally used with rigid cellular materials, long-fiber reinforced materials, or thermotropic liquid crystal polymers. Since the 3D printing process creates a material with voids similar to a cellular structure, notches are not used in this study. Specimens are to be 80mm in length, 10mm wide, and 4mm thick. Two different orientations are generally used in Charpy Impact testing. The two styles are edgewise, and flatwise. Flatwise impact occurs along the width of the specimen (10mm), while edgewise impact occurs along the height of the specimen (4mm). For our purposes, flatwise impact will be used for every

test. The standard also calls for a minimum of 10 specimens to be tested at a time, for a consistent range of data.

The material printed is a 1.75mm diameter PLA (Polylactic Acid) filament manufactured by K-Camel. The samples required for testing were all printed using a Geeetech Prusa I3 model. This model printer uses Fused Filament Fabrication. Layer resolution ranges from 0.1-0.3mm, filament diameter is 1.75mm, and the two nozzle diameters are 0.3 and 0.35mm. The first set of samples used for control purposes was printed at printer defaults. The samples were set at an infill speed of 30mm/s and an infill percentage of 100%. The experimental samples were printed at varying speeds above 30mm/s, ranging from 40mm/s to 70mm/s. Infill percentages for each speed ranged from 0% to 75%, filling in the complete range of the printer's capabilities. The printer is capable of printing using several types of material, including PLA, ABS, Wood-Polymer, and Nylon. Of all the mechanical properties of printed PLA parts, the one that this experiment is most interested in, is toughness. Toughness is defined as the measure of a materials ability to absorb energy. To obtain values for the parameters in question, a Charpy Impact Test will be performed. The main differences in the types of impact tests, is the orientation of the specimen. The Charpy method requires the specimen to be supported like a horizontal beam.

Impact testing was performed using an Instron CEAST 9050 Pendulum Impact System. The system requires both a power input and that of an airline for pneumatic operation of the impact hammer. When starting the system, it is recommended the airline safety switch be thrown, and then the power switch. When powering down the system, the steps are to be done in reverse order. If the machine was powered down correctly, it is likely the emergency stop switch will be thrown. Turn the button roughly one quarter rotation to disengage the safety and allow proper use. Using the touchscreen display, maneuver from the main screen to

the calibration menu, which should be the option in the top left corner of the screen. Calibration is necessary to allow the machine to identify which hammer is currently installed and allow the machine to zero itself accordingly. After calibration has occurred, it might be necessary to outline the set of parameters used in upcoming tests. The parameters section of the display is the bottom left corner of the main screen. The parameters section is where specimen size is defined, as well as other things. After parameters are established, testing can occur. The operations section of the display can be found on the main screen in the top middle position of the main screen. A parameter set must be selected for the testing to actually occur, otherwise the instrument will give an error message. Once a parameter set is selected, the start button will begin the experiment. All safety measures must be in place, and all other previous steps must have taken place, otherwise error messages may appear. The results of each test will be calculated by the impact testing machine based on several formulas listed below. The instrument will provide percentage of the energy absorbed by the specimen, the actual energy absorbed by the specimen, and the resistance value of the specimen.

Equations

Impact energy is the amount of energy the sample is able to absorb before it breaks. It is the main value our experiments are concerned with.

$$A_cU = \frac{E_c}{h*b} * 10^3 \qquad \left(\frac{kJ}{m^2}\right)$$

A_cU = Impact energy absorbed in breaking an unnotched specimen.

E_c = the corrected energy, in joules, absorbed by breaking the test specimen

h = thickness, in millimeters, of the specimen

b = is the width, in millimeters, of the test specimen.

E_d stands for the energy lost during any one individual test do to forces acting on the machine, such as friction. Energy lost is generally calculated prior to any tests during the calibration process and follows the equation.

$$E_d = \frac{E_m}{1 - \cos(\alpha_n)} * \cos(\alpha_f) - \cos(\alpha_i))/(N_{cicli}) * 2$$

E_m = nominal potential energy of the hammer (directly derived by the hammer list during recognition).
α_n = nominal release angle (derived as well from the hammer list).
N_{cicli} = the number of oscillations to measure the lost energy set by the operator in the setup menu.
α_i = the recovery angle after release, thus related to the first oscillation.
α_f = the recovery angle of the last oscillation.

Data and Analysis

Several preliminary tests have been run so far, including the control group (printed at 40mm/s) with the isolated variable being infill percentage and another baseline group of infill percentage with varying print speed. For the infill percentage baseline shown in Figure 2, the behavior followed the expected trend, as the printer printed the samples with less and less material (lower infill percentage), the energy each sample was able to absorb decreased. For the samples printed at the varying rates (Figure 3 to 5), the trends followed those found in the 40 mm/s; as the infill increases, the energy absorbed also increases.

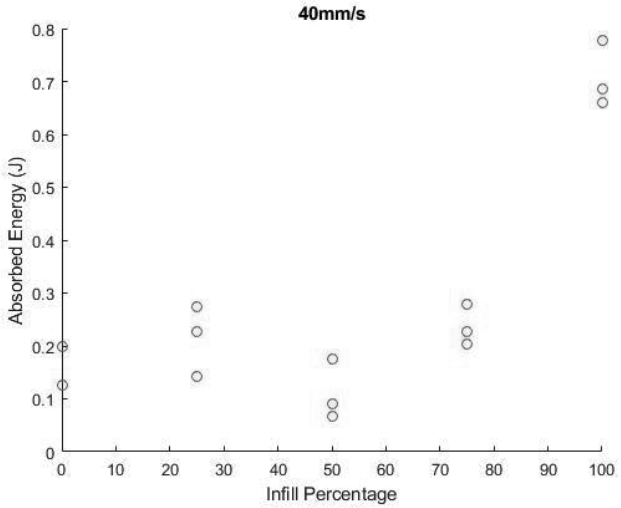

Figure 2: Absorbed Energy at a Print Speed of 40mm/s at Varying Percentages of Infill

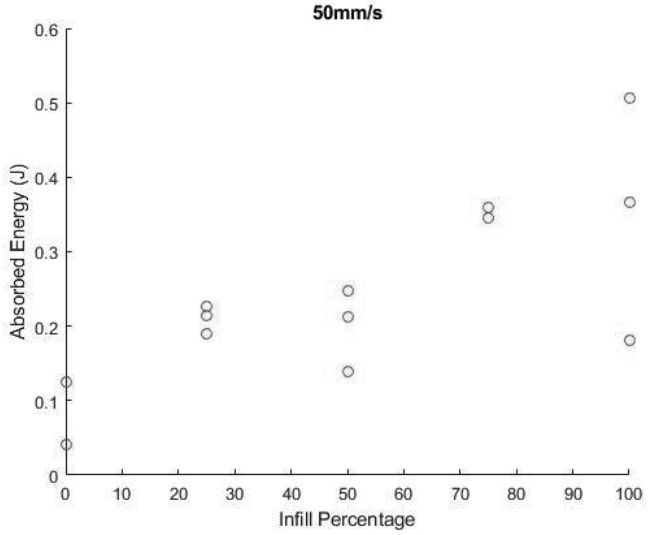

Figure 3: Absorbed Energy at a Print Speed of 50mm/s at Varying Percentages of Infill

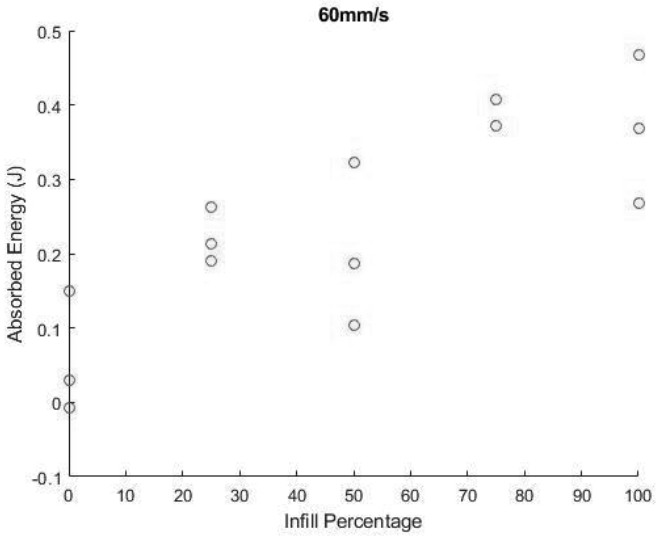

Figure 4: Absorbed Energy at a Print Speed of 60mm/s at Varying Percentages of Infill

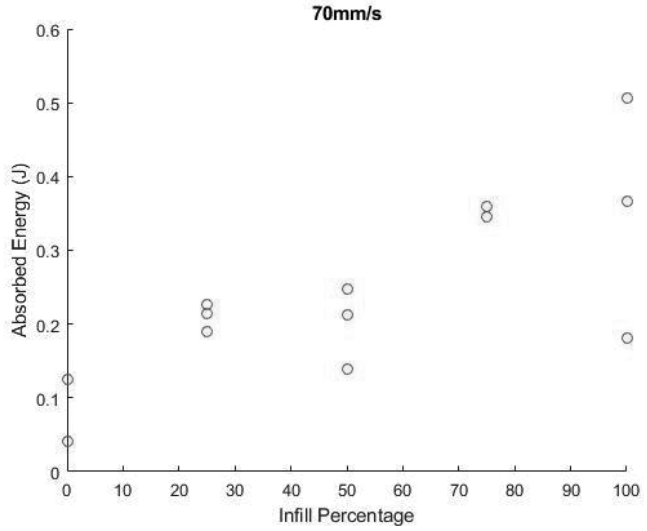

Figure 5: Absorbed Energy at a Print Speed of 70mm/s at Varying Percentages of Infill

As for the comparison tests of energy versus speed, the results were rather interesting. As the speed at which the samples were

printed increased, so did the average energy the samples were able to absorb. From the information in figure six, the samples printed at 60mm/s showed the highest values, even when compared with those at 70mm/s, which means there is a theoretical cap for printing speed, at which point mechanical properties will decrease from that speed and higher. Infill percentage showed the same trend in the comparison tests as it did in the baseline tests, absorbed energy increased with greater infill percentage. Looking at information presented in all of figures 2-6, the samples printed with 100% infill and at 40mm/s showed the highest absorbed energy of all the samples across all the tests, but the averages of the remaining infill percentages at 40mm/s were lower than expected. At 60mm/s each of the lower infill percentages showed greater averages than the same averages at different speeds. While the greatest absorbed energy values occurred at the larger infill percentages, the range of absorbed values across all speeds was the smallest at 75%, meaning that at this infill percentage, the printer was the most consistent. At both 0% and 50%, the absorbed energy samples across all speeds were lower than compared with 25%, 75%, and 100%.

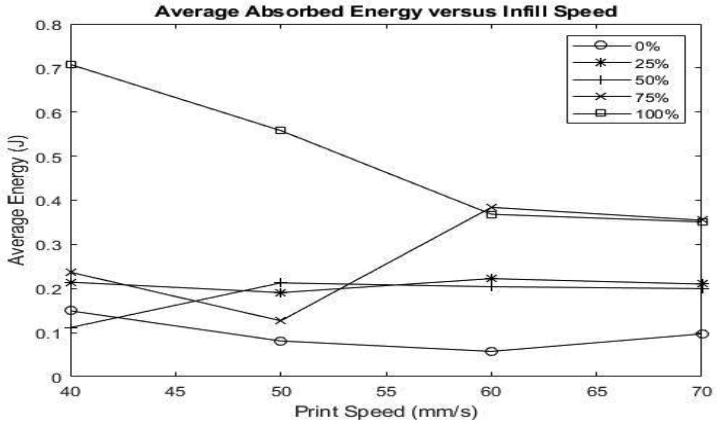

Figure 6: Energy vs. Speed

Conclusions

For the maximum values for impact resistance, 100% infill density should be used, and speed values of roughly 60mm/s appear to be optimal. Further testing to narrow down print speeds even further will be conducted, but the rough estimates the samples have provided so far give an estimated starting point. The tests conducted so far provide a decent outlook on how tests involving the copper-infused PLA should proceed. Experimental methods have been narrowed down through some preliminary investigations, and it looks like the optimal method for combining PLA with the copper flakes will be to use some sort of grinder to resolve both compounds to fine particulate.

References

[1] J.Torres, M.Cole, A.Owji, Z.DeMastry and a. A. Gordon, An approach for mechanical property optimization of fused deposition modeling with polylactic acid via design of experiments, Rapid Prototyping, vol.22, 2016.

[2] R. Jerez-Mesa, J. T. Rodriguez, J. L. Fuentes, G. Gomez-Gras and a. D. Puig, Fatigue lifespan study of PLA parts obtained by additive maunfacturing, Procedia Manufacturing, 2017.

[3] J. Orellana, J. Wichart and a. C. Kitchens, Mechanical and Optical Properties of Polylactic Acid Films Containing Surfactant-Modified Cellulose Nanocrystals, Journal of Nanomaterials, 2018.

[4] D. U. Acocella, G. M.R. Guerra, V. Iozzino, F. De Santis and R. and Pantani, PLA melt stabilization by High-Surface-Area-Graphite and Carbon Black, Polymers, 2018.

[5] G. Cicala, G. Saccullo, I. Blanco, S. Samal, S. Battiato, S. Dattilo and a. B. Saake, Polylactide/lignin blends: effects of processing conditions on structure and thermo-mechanical properties, J Therm Anal Calorim, 2017.

[6] J. T. Cantrell, S. Rohde, D. Damiani, R. Gurnani and L. DiSandro, Experimental characterization of the mechanical properties of 3-D printed ABS and polycarbonate parts, Rapid Prototyping Vol. 23, 2017.

[7] E. Gordeev, A. Galushko and a. V. Ananikov, Improvement of quality of 3D printed objects by elmination of microscopic structural defects in fused deposition modeling, PLoS One Vol. 13, 2018.

[8] J. Torres, O. Onwuzurike, A. J.W McClung and J.D Ocampo, Influence of an extreme on the tensile mechanical properties of a 3D printed thermoplastic polymer, Greenville SC, 2018.

[9] International Standards Organization, ISO 179-1, 2015.

Fatigue Characterization of Polyatic Acids

Roberto Enrique Vargas

Mentor: Juan Ocampo, Ph.D.
St. Mary's University, San Antonio, TX

This paper investigates the fatigue life behavior of 3-D printed polymethyl methacrylate (PMMA) to construct stress-life curves to accurately predict the failure of PMMA under a given stress application. A combination of various U-shape notch diameters, spin frequencies and loads were tested to determine ideal testing geometry when utilizing a rotating fatigue machine. A notch sensitivity analysis was preformed to determine which of these combinations greatly reduces or increases fatigue life and which of these have very little impact on fatigue life. Fatigue life was measured on a rotating fatigue machine rather than the traditional servo hydraulic testing machine. Experiments run with forced convection proved to have superior fatigue strength to samples run without forced convection. The superior fatigue strength was attributed to a lower modulus of elasticity when the sample was kept at lower temperatures rather than when the sample was allowed to warm up due to friction. Results showed that samples run at lower frequencies had an increased fatigue life. All results were reported, and prediction work based on current work was proposed for future work.
Keywords—PMMA, 3D printed plastics, Fatigue life, Rotating Fatigue Machine, S-N Curve

Introduction

PMMA (Polymethyl methacrylate) is an acrylic transparent thermoplastic used in a variety of applications like lighting, automotive and numerous electronics due to its impact resistance, strength and transmittance. This paper is focused on the analysis of fatigue and prediction of failure of PMMA at different loads and cycle rates to determine the ideal geometry

which should be used to create and predict life expectancy of PMMA. The specimen being tested will have a U-shaped notch at the midpoint which will create a localized stress concentration to generate crack initiation at that location.

Similar fatigue tests were conducted by Aifeng Huang et. al. [1] using a servo hydraulic testing machine. Testing was conducted a 27°C and the max stress applied varied from 33 to 44 MPa while the frequency varied from .03 to .5 Hz. Results from their experiments concluded that fatigue life increases as cyclic frequency increases. This method was previously performed with more precautions to ensure consistent results by D. HOEY and D. TAYLOR. [2] They analyzed the fatigue of PMMA by using dog bone specimens cut from a sheet. Each specimen was sanded using 320 grit silicone carbide paper to ensure all sides were finished similarly. Samples were created in a vacuum to ensure they were pore free. Testing was done using an Instron servo hydraulic testing machine at 3Hz with a stress ratio of 0.1. Fatigue testing was conducted in a water bath at 37°C. The estimated fatigue strength was 105 cycles to failure. Jeremy L. Gilbert et. al. [3] conducted similar experiments by three-point flexural fatigue tests using an electrohydraulic mechanical test system. Experiments were conducted at room temperature using a frequency of 5Hz and a stress ratio of 0.1. They concluded form their results that “there is loglog linear relationship between damage energy and number of cycles to failure.”

The difference between other analyses of fatigue on PMMA and ours is that we will be using a rotating fatigue machine rather than a Servo hydraulic or electrohydraulic machine. This type of analysis has not been readily examined on PMMA due to sensitivity to temperature and its flexibility. This machine will treat the specimen like a cantilever beam with a load at one end creating an infinite amount of alternating stresses. The goal is to determine the most effective geometry of the round specimen and use this geometry to effectively calculate the

fatigue life of PMMA at 103,104,105 and 106 to plot the stress vs life diagram (S-N curve) in order to predict the life of a given sample. The PMMA being used will be printed on a Stratasys Objet260 Connex3. Testing will be done according to standard E739 [1] (Standard Practice for Statistical Analysis of Linear or Linearized Stress-Life (S-N) and Strain-Life (e-N) Fatigue Data. Overall, this paper describes a method for predicting failure of a PMMA in order replace components before failure is reached.

Methodology

To determine which sample geometry and type will be most effective in determining the fatigue life, we will conduct a series of fatigue tests using a rotatory fatigue machine described in the equipment section. All samples will be designed in SolidWorks and printed on a Stratasys connex3 object260 3D printer. The printer's characteristics and print settings will be described in the equipment section. The different sample configurations will have a circular geometry with an outer diameter of 9mm. The U-Shape Notch will have a varying diameter until the appropriate diameter is found.

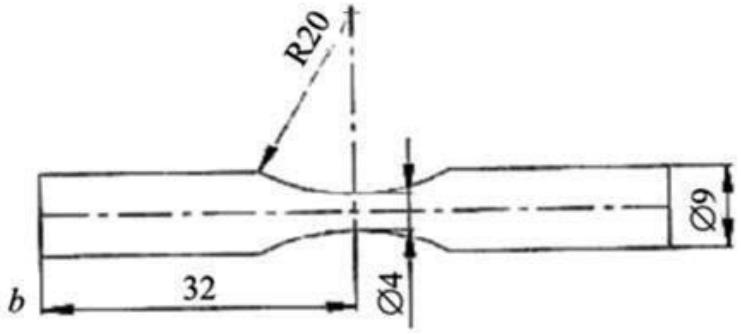

Fig. 1 First 3D printed PMMA specimen design iteration.

The first set of specimens will be printed horizontally using high quality printing. High quality printings have a 16-micron (0.0006 in.) resolution. Next, we will determine whether a

Glossy, matte or sanded finish will be used for that sample trial. Tested samples will be printed from VEROPUREWHITE RGD837, VEROGRAY RGD850, VEROBLACKPLUS RGD875, VEROWHITEPLUS RGD835, or. VEROMAGENTA RGD851. Once printed, the free end of the samples will be sanded using 220 grit sandpaper if needed to smoothly fit into the machine bearing.

Initial test results showed that as the machine spins, friction heat began to slowly warm up the specimen causing it to become more elastic and allowing it to bend. This tricked the break sensor into believing the sample has broken. In order to counteract this, we decided to add a fan which caused forced convection to cool down the specimen while the machine was running in order to extend its spin time and obtain more precise data. The sm1090s safety cover was by-passed by using a magnet allowing the forced convection to reach the sample.

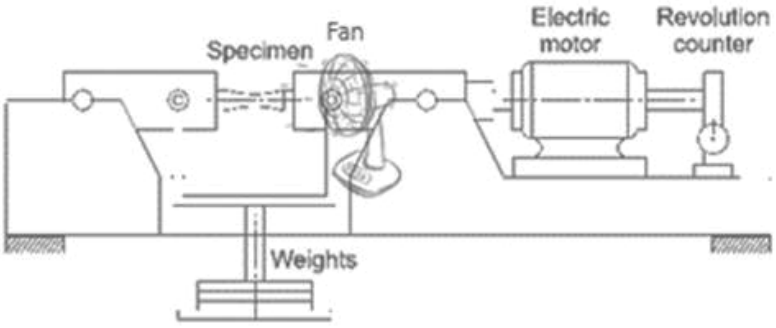

Fig. 2 Representation portraying experimental setup

Experiments were started using samples with a U-shape notch 4mm in diameter. Fatigue results from these samples will determine whether the notch thickness should be increased or decreased. Using the new-found thickness, the sample will be reanalyzed using the techniques mentioned above. Each trial will be run in three different configurations at least three times to ensure consistency of results. Samples will be run under loads from 1N to 20N. The specimens will be run at both low and high

frequency to determine which produces better results. Below is a flowchart representing the process followed to determine the ideal testing geometry for PMMA.

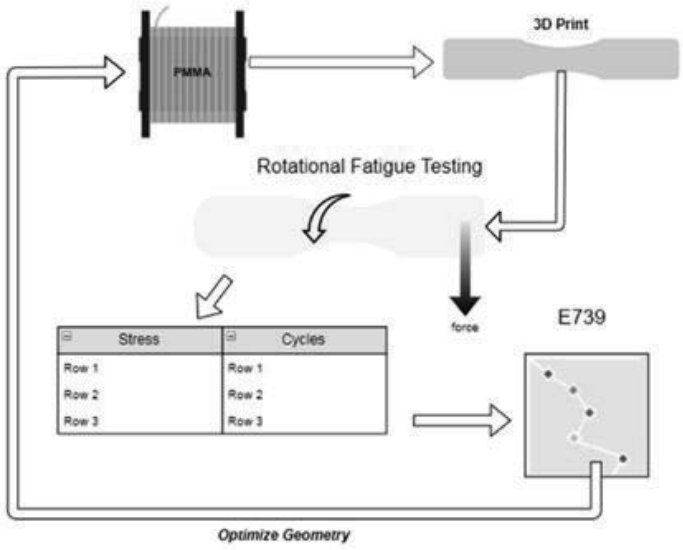

Fig. 3 Flowchart depicting the process used to consolidate down the ideal geometry to use for fatigue analysis of 3D printed PMMA

Equations

The stress on the sample will be measured using equation 1:

$$\sigma = Mc/I \quad (1)$$

where M is the moment which is equal to the load value times the distance from the load to the fulcrum. c is the radius of the specimen and I is the moment of inertia. To find the life of a sample at a given stress, we will be using standard E739 [1] as stated above. The stress-life equation used will be equation 2:

$$\text{Log } N = A + B(S) \quad (2)$$

where N denotes the life cycles of at a given cyclic stress. The S is the max value of constant amplitude applied cyclic stress. The value for A is given by equation 3:

$\hat{A}=\bar{Y}-\hat{B}\bar{X}$ (3)

where $\bar{y}$ is the average of the log(Ni).

$\bar{Y}=\sum_{i=1}^{k}[Y_i/K]$ (4)

The log(Ni) is the life values computed in life cycles. $\bar{X}$ is the average of the life values and k is the total number of tests specimens being analyzed.

$\bar{Y}=\sum_{i=1}^{k}[X_i/K]$ (5)

The B parameter is given by equation 6

$\hat{B}=(\sum_{i=1}^{k}[(X_i-\bar{X})(Y_i-\bar{Y})])/(\sum_{i=1}^{k}(X_i-\bar{X})^2)$ (6)

where $Y_i=Log(N_i)$ and $X_i=\sigma_i$ .Once the stress vs cycles table is built, we can use it to plot the stress vs life diagram. From here, we can determine whether or not the values follow a regular distribution. The geometry will then be optimized to produce better results.

Equipment

The equipment being used are a Stratasys connex3 object260 3D printer and a Tecquipment sm1090 rotating fatigue machine. The sm1090 simulates a cylindrical cantilever beam with a designated force at its free end.

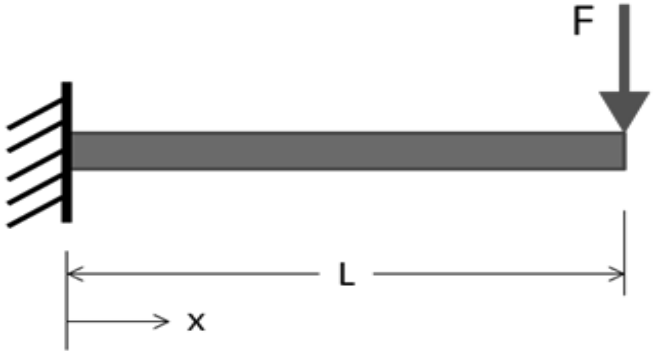

Fig. 4 Cantilever beam representation where F is the magnitude of the load measured in Newtons, x is the distance from the fulcrum to the point where the deflection is being measured L is the length of the sample

The machine allows for variable speed and load at which the object is analyzed. The sm1090 measures the cycles and load at which the object is run until the specimen breaks, tripping a switch to turn off the motor which is spinning the sample. All data is recorded in accurate real time. The 3d printer being utilized has a build resolution for each axis of -axis: 600 dpi; Y-axis: 600 dpi; Z-axis: 1600 dp with an accuracy of up to 200 microns for full size rigid material model. This depends on geometry, model orientation and build parameters.

Printing properties

The Stratasys printer uses two main heads and eight smaller printing heads to print 3d materials. Temperatures of the main heads and smaller adjacent heads will vary depending on the material being printed. For the Vero white material, the 3d printer started printing once the two main heads reached or surpassed 73 degrees Celsius and the smaller heads were all hotter than 66 degrees Celsius. The main temperature is the temperature at which the main manifold feeds the main printer heads. The final temperature reached for the printer heads was 75 degrees Celsius for the main heads and 70 degrees Celsius for the smaller heads.

Experimental Conditions

Fatigue tests were run by applying alternating stresses at the free end of a fixed, spinning specimen. Tests were run using constant load on a tecquipment sm1090 rotating fatigue machine per trial with an environment-controlled temperature of 72 degrees Fahrenheit. All trials were run at a frequency range of 22Hz through 63Hz, and loads for each trial were run in the range of 0.4N through 11.8N. Cycles were measured using the tecquipment sm1090 control unit.

Discussions

The main goal of this paper was to determine the ideal geometry to use with 3D printed PMMA on a rotating fatigue Machine. This machine was originally only designed to run with

metal specimens. This caused a problem within the first few trials of testing. Metal specimens came from the manufacturer with a U-shaped notch and round diameter of 4mm; therefore.as a base trial we started with the exact same dimensions for our PMMA specimen to begin testing. Within a few trials, it was determined that the round 4mm diameter was too thin for our material. The samples would fracture within a few seconds of spinning on the machine. Most of the time, the fracture would occur before the machine was at full speed when ran at frequencies over 30Hz. Due to these fractures, we decided to increase the diameter to 5mm.

A 5mm diameter proved to yield much better results with a few outliers that were due to mounting error. The problem with the 5mm round diameter samples is that they could not run for enough time to successfully build a S-N curve. The highest life cycle reached was 180k, and our S-N life bounds were between 103 and 106 thus we were too far away from our upper boundary. We also had a few specimens which cracked partially and other specimens which either bowed up or down. We originally believed increasing the diameter to 6mm would remedy both of these problems but later discovered it actually increased the severity of them. 95% of the 6mm specimens did not break and instead were extremely bowed up or down with no signs of cracking. However, this allowed us to uncover the fact that the specimens were becoming bowed because of friction heat generated by the moving parts. As the frequency was increased, samples would run for less time before becoming extremely bowed. They would trip the break sensor and trick the machine into believing a failure had occurred. To combat this problem, we decided to add forced convection with a fan to help keep the samples at a cooler temperature while running. We immediately saw a drastic change in life expectancy of the samples and even had samples run significantly longer than our upper limit. With

this newly discovered information, we decided to lower the specimen notch area back down to 5mm.

With the addition of forced convection, the 5mm diameter specimens would break at reasonably timed cycles, except we had many samples that once again exceeded the upper limit of our limit. Some of these samples would run for over 72 hours without any sign of failure occurring anytime in the near future. Considering the fact that we were closing in on our diameter size, we decided to drop the specimen diameter by 0.5mm. This small change in diameter caused our specimens to run within our lower and upper bounds successfully. The only problem we encountered was that the range and precision of forces we could use was extremely limited. This was due to the design of the machine and its original purpose: to be run with metal samples. We addressed this issue by adding free weights to increase the precision allotted by the machine restrictions. This allowed us to increase our precision but was not a permanent fix as it is not recommended to add free weights to the machine. In future work, we will investigate how to add a safe way of adding precision to our machine while following the standard set in place by industry.

Results and Conclusions

The final results from our trials, run at 44hz with a 4.5mm diameter, proved consistent enough to build a stress life according to industry standards. The S-N curve built included any outliers found during testing. Most of the actual data points appear to follow the predicted curve. The S-N curve below only applies to 3D printed PMMA which is under forced convection at approximately the same ambient conditions due to the variability in elasticity at different temperatures.

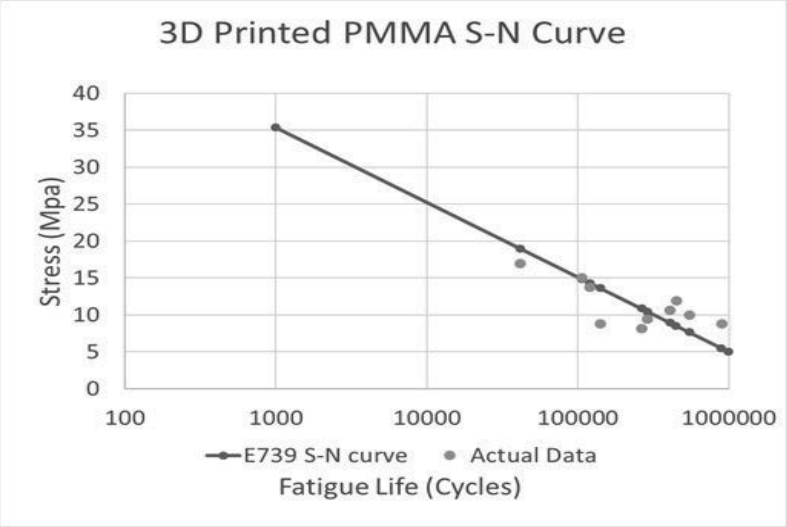

Fig. 5 S-N Curve made from Standard E739 and after solving for values A and B equation 2 becomes Log N = 6.49 $^{-0.098(S)}$

Future work

Our model exhibits good characteristics to successfully predict the life cycles to failure when given a certain stress or vice versa at a mid-range frequency with forced convection when using a rotating fatigue machine to produce fatigue. However, future work will be performing sensitivity analysis on the variables involved to determine which variables account for a majority of the change in the results and which variables, if changed, have little or no effect. Additionally, we would like to investigate a better solution to keep samples cool when running at higher frequencies and a new way to fine tune the force applied on the specimens due to the small range of forces values available to us with this machine combination. We will also investigate if there is any variation in tensile strength of 3D printed PMMA when printed with different colors.

Acknowledgment
This paper was supported in part by a US Department of Education Ronald E. McNair Post Baccalaureate Achievement Grant

References

[1] ASTM, Standard Practice for Statistical Analysis of Linear or Linearized Stress-Life (S-N) and Strain-Life (e-N) Fatigue Data, The American Society for Testing and Materials, 1998.

[2] A. Huang, W. Yao and F. Chen, "Analysis of Fatigue Life of PMMA at Different Frequencies," p. 8, 2014.

[3] J. L. Gilbert, D. S. Ney and E. P. Lautenschlager, "Self-reinforced composite poly(methy1methacrylate): static and fatigue properties," Elsevier Science Limited, vol. 16, no. 14, p. 13, 1995.

[4] D. Hoey and D. Taylor, "Comparison of the fatigue behaviour of two different forms of PMMA," p. 10, 2009.

Can't Touch This: Observations of Contact Between Belugas (Delphinapterus leucas)

Virianny I. Ortiz

Mentors: Heather M. Hill, Ph.D. and Michael Noonan, Ph.D.
St. Mary's University, San Antonio, TX

Physical contact has yet to be examined in large social groupings of captive belugas that are mixed in sex and age. The purpose of the current study was to examine the nature of contact between belugas housed at Marineland of Canada. Forty-seven mixed sex belugas, ranging in age from birth to estimated age of 30 years, were observed for rates of contact across multiple years. Data were extracted from archived electronic ethograms in which belugas were focal followed an average of 9 minutes approximately twice a week. Results indicated young belugas initiated contact significantly more with mothers than with other adults. Male belugas initiated contact more frequently than females. Adult belugas contacted other adult belugas more frequently than calves contacted other calves. These results support previous studies of contact examined in cetacean populations.

Social species engage in different forms of communication, such as touch, vocalizations, body movements, or physical displays. Among all forms of contact, touch may be one of the most common forms of communication in social species but the least studied. Asian elephants (Elephas maximus) (Makecha, Fad, & Kuczaj, 2012), orphaned chimpanzees (Pan troglodytes) (van Leeuwen, Mulenga, & Chidster, 2014), long finned pilot whale (Globicephala melas) (Aoki, Sakai, Miller, Visser, & Sato, 2013), and fish all use physical contact to communicate socially, including affiliative and aggressive needs. Lemon sharks (Negaprion bevirostris) show several social preferences, starting with which group the sharks join. Lemon sharks have more social interactions with familiar sharks than with unfamiliar sharks (Keller, Finger, Gruber, Abel, & Guttridge, 2017). Additionally,

juvenile lemon shark interactions are based on body length with younger sharks preferring to be in a group with similar sized sharks rather than larger sharks (Guttridge et al., 2011).

Contact has been observed among cetaceans such as humpback whales (Megaptera novaeangliae), bottlenose dolphins (Tursiops truncatus), and beluga whales (Delphinapterus leucas) in both their natural habitat and captivity (Dudzinski et al., 2012). Wild gray humpback whales (Eschrichtius robustu) remain close together in body contact for protection when attacked (Goley & Straley, 1994). Atlantic white-sided dolphins (Lagenorhynchus acutus) have been observed engaging in physical contact for 10% of their interaction time, which included rubbing, stroking, and conducting other body movements (Nelson & Lien, 1994). Belugas have been examined for various socio-sexual interactions leading to sexual behaviors being sequenced including pelvic thrusts, genital rubs, and mouthing (Hill et al., 2015). As social animals, tactile and behavioral signals are used to communicate with conspecifics. While sounds carry to conspecifics that are farther away, touch between body parts may communicate information without broadcasting it to others (Dudzinski et al., 2012). A variety of cetaceans use fins, flukes, head, back, and belly to contact one another, which may indicate different functions (Dudzinski et al ., 2012). However, most of the systematic research conducted on cetaceans has examined the function of pectoral fin contact in dolphins (Connor, Mann, & Watson-Capps, 2006; Dudzinski, 1998; Dudzinski, Gregg, Paulos, & Kuczaj, 2010; Dudzinski et al., 2012; Sakai, Hishii, Takeda, & Kohshima, 2006a).

Pectoral fin contact appears to serve two functions for dolphins: (1) as a means of communication and (2) as a form of social bonding (Dudzinski, Danaher-Garcia, & Greg, 2013). Lateralized behavior in pectoral fin use has been found within calves displaying a right fin preference, depending on age of other partners (Winship, Poelma, Kuzaj, & Eskelinen, 2017).

Adults dolphins also show this lateralized preference (Sakai, Hishii, Takeda, & Kohshima, 2006b). In contrast, killer whales use their fins to produce flipper strikes on the surface rather than on each other (Giljov, Karenina, Ivkovich, & Malashichev, 2016). The purpose of the water slaps is unknown, but the researchers speculated the pectoral fin strikes were forms of social interaction between individuals.

Tactile contact can be affiliative or aggressive, depending on the context (Paulos, Dudzinski, & Kuczaj, 2008). As a possible mediator for relationships, affiliative forms of touch are observed and appear to be essential during the early development of offspring (Hill, Dietrich, Guarino, Banda, & Lacy, 2018; Hill, Guarino, Geraci, Sigman, & Noonan, 2017). Mothers and offspring keep in close proximity with one another and touch may be a primary factor in their bond. Moreover, in many aquatic mammals touch is observed throughout life depending on the species. Male bottlenose dolphins will engage in contact swimming when courting females (Connor et al., 2006). Female dolphins will use their pectoral fins with unrelated females during social interactions. Adults and young animals engage in physical contact during social play or intense, aggressive interactions.

Belugas, another social cetacean, inhabit the icy waters of the Arctic circle and similar locations, and can be found in many different sized groups although many travel in groups of three to ten (Johnson & Moewe, 1999). Research focused on captive belugas primarily involved similar sized groups and has shown that the captive beluga behavior replicates wild beluga behavior (Hill et al., 2015). One pattern that has been observed for belugas is social interactions involving physical contact appear to be highly dependent upon the social composition (Hill et al., 2015). In a study observing the frequency of contact in beluga calf social interactions, physical contact was more common among calves and their mothers with calves initiating 98% of the interactions involving contact (Hill, Dietrich, Jantea, Garza, & Lacy, 2018).

Beluga calves positioned themselves in an infant position frequently, where the calf's head or mouth is near the mother's genitals. This position appears to provide calves safety, rest, nutrition, learning opportunities, and bonding.

In contrast to the frequent contact events between calves and their mothers, adult belugas do not seem to contact one another often, unless males are socializing with other males (Glabicky, DuBrava, & Noonan, 2010; Hill et al., 2015). However, when contact occurs between mothers and calves or between calves, social interactions lasted longer (Hill et al., 2015). Body length in belugas, like lemon sharks, may play a role in partner preference when engaging in contact. Knowledge of belugas being in proximity with other similar aged belugas may have to do with belugas preferring to be in closer proximity with other belugas based on similar body lengths. A good example of this might be a special mouth-to-mouth interaction that beluga calves engage in that looks like tug-a-war with their mouths (Hill, Dietrich, Guarino et al., 2018). Although belugas engage in this mouth interaction rarely, it does seem to involve a sex preference for partner and is more likely to occur early in development (Hill Dietrich, Guarino et al., 2018; Hill, De Oliveira Silva-Gruber, & Noonan, 2018), which mimics social interactions in later development (Mazikowski, Hill, & Noonan, 2018). Documented visually in the wild, this behavior has been speculated to be an attempt at dominance by young males (Krasnova, Chernetsky, Zheludkova, & Bel'kovich, 2014). More research is needed to better understand how contact influences calf development and other social interactions.

Socio-sexual interactions in wild and captive belugas have been found to show characteristics of sex segregation (Hill et al., 2018). Wild belugas show sex–segregated social groups and socio-sexual interactions vary with age (Hill et al., 2015). Adult male belugas are more frequently with other adult male belugas than with females (Hill et al., 2018) and the same results have

been observed in younger belugas (Mazikowski et al., 2018). Sex preference in various socio-sexual interactions could help explain relationships between belugas and future behaviors. These early preferences may also lead to more frequent contact if bond formation occurs early in development.

The purpose of the current study is to examine physical contact between belugas in a different captive population to determine if the same patterns of contact were observed as were previously established (Hill, Alvarez, Dietrich, & Lacy, 2016; Hill, Dietrich, Jantea et al., 2018). Observing the development of contact between belugas early in life could be compared to interactions observed in adulthood, leading to critical information on the type of contact interactions made on a daily basis. The presence and development of social interactions can demonstrate typical progression in development (Hill et al., 2017). Understanding the type and amount of tactile contact could be indicative of a milestone in the development of belugas.

For the current study, several hypotheses were tested. It was expected that mother-calf pairs would engage in the most contact compared to any other dyad. Calves were hypothesized to initiate more contact than adult belugas. Calves were also expected to engage in more occurrences of contact with other calves than adults would initiate contact with other adults. Sex was also seen as a variable that could influence the frequency of contact being observed. It was expected that male belugas would initiate more contact interactions than females. Adult male belugas were also expected to engage in male-to-male interaction more frequently than adult female-to-female interactions.

Method

Sample

Forty-nine belugas housed at Marineland of Canada were observed in the current study. The behaviors of 6 adult males, 21 adult females, 8 juvenile males, and 14 juvenile females were documented between 2006-2013 (Table 1).

The belugas were housed in one of two pools. The ACR pool held mother and calf social groups while the ACL pool housed adults. The social composition within each pool remained stable within a year, although some adults were added periodically to the two social grouping across years. Calf belugas ranging in 0 to 3 years of age were classified young belugas while any beluga that was sexually mature or white in coloration (approximately 8 years and older) were classified as adults.

Table 1
Date and Environmental Conditions

Year	Season	Pool	Composition	Total # belugas	#AF	#AM	#J	#MC pairs*
2006	Fall	ACR	Mother-calf	8	4	1	3	3
2007-2008	Fall-Spring	ACR	Adults	16	11	5	0	0
2010	Fall	ACR	Mother-calf	14	7	1	6	6
2011-2012	Fall-Spring	ACR	Mother-calf	9	5	1	3	3
2012	Summer	ACR	Mother-calf	12	6	1	5	5
2012-2013	Fall-Spring	ACL	Adults	14	9	3	2	2
2012-2013	Fall Spring	ACR	Mother-calf	13	6	1	6	6
2013	Fall	ACR	Mother-calf	10	6	0	4	4

Materials

Archived data, collected from real-time observations using electronic ethograms, were used to analyze all contact behavior between belugas. Data were organized in Excel and then transferred to SPSS 24 for analyses.

Procedure

All occurrence recording procedure was implemented to record individual behaviors of each focal followed whale. The majority of observations was made during early daylight hours in a given pool. Every interaction in which the focal beluga was engaged was recorded with electronic ethograms by the assigned research assistant for a nine-minute period. The number of whales recorded depended on the number of researchers available to record observations (up to 13 animals in a day). All focal follows of individual belugas were synchronized when possible but start and end times varied occasionally. The data collected from these focal follows were archived and processed to exclude all actions not involving contact.

The current study focused on all observed occurrences of contact initiated by a beluga. Relevant information included initiating beluga, age and sex identification, receiving beluga, age and sex identification, type of contact, and body part used in the interaction. Not all contact interactions included a whale receiver, as sometimes inanimate objects (e.g., toys, walls, gates, glass) were touched. When the receiver was a beluga whale, the body part touched by the initiator became the target.

Data Analyses

The data were collapsed across all animals and organized in correspondence to the type of contact used and by which animal. Ten to 15 observations made from each beluga were omitted due to incorrect or ambiguous coding during the initial data collection. Belugas were observed for different numbers of sessions (e.g., GEM observed 15 sessions, ISI observer 10 sessions) and sometimes for different session durations. To

accommodate these variations, frequency data were converted into rates based on the number of total seconds observed for each whale.

Table 2

Individual Observation Characteristics

Beluga	Season/Year	Age	Sex	Focal Follow observation time (sec)	Total Observation Time (hr)
GEM	Fall 2006	Adult	Female	23800	65894
	Fall 2010			25497	
	Summer 2012			0	
	Fall 2012 – Spring 2013 ACR			16597	
G2=BER	Fall 2006	0.5 Calf	Male	21097	21097
ISI	Fall 2006	Adult	Female	24341	58816
	Fall 2007 – 2008	Adult	Female	0	
	Fall 2010			34475	
I1=HOR	Fall 2006	0.5 Calf	Male	21097	21097
	Fall 2007 – Spring 2008			0	
OCE	Fall 2006	Adult	Female	19653	54264
	Fall 2007 – Spring 2008			2711	
	Fall 2010			31900	
O1=SEL	Fall 2006	0.5 Calf	Female	8654	8654
SIE	Fall 2006	Adult	Female	0	15459
	Summer 2012			0	
	Fall 2012- Spring 2013 ACR			15459	
ORI	Fall 2006	Adult	Male	0	20624
	Fall 2012-Spring 2013 ACL			20624	
BEY	Fall 2010	Adult	Male	10973	10973
	Fall 2011- Spring 2012 ACR			0	
	Summer 2012			0	
	Fall 2012- Spring2013 ACR			0	
G3=SAS	Fall 2010	0.5 Calf	Female	6632	6632
I2=QUI	Fall 2010	0.5 Calf	Female	33111	33662
	Fall 2012- Spring 2013 ACL	2.5 Calf		551	
O2=MIR	Fall 2010	1.5 Calf	Female	34474	34474
					(continued)

Beluga	Season/Year	Age	Sex	Focal Follow observation time (sec)	Total Observation Time (hr)
KEL	Fall2007-Spring 2008	Adult	Female	19634	78291
	Fall 2010			34473	
	Fall 2012-Spring 2013 ACL			11286	
	Fall 2013			12898	
K1=CLT	Fall 2010	1.5 Calf	Female	30265	30265
XEN	Fall 2007 – Spring 2008	Adult	Female	0	49777
	Fall 2010	Adult	Female	32630	
	Summer 2012			0	
	Fall 2012-Spring 2013 ACR			17147	
X3=EVE	Fall 2010	2.5 Calf	Female	32343	32243
CLE	Fall 2007 – Spring 2008	Adult	Female	19093	53569
	Fall 2010			34473	
C1=NEV	Fall 2010	1.5 Calf	Female	34473	34473
SKY	Fall 2007 – Spring 2008	Adult	Female	19273	85872
	Fall 2010			11762	
	Fall 2011-Spring 2010 ACR			38572	
	Fall 2012-Spring 2013 ACL			16265	
JUB	Fall 2011-Spring 2012 ACR	Adult	Female	40064	58961
	Summer 2012			0	
	Fall 2012-Spring 2013 ACR			18897	
J2=UBA	Fall 2011-Spring 2012 ACR	0.5 Calf	Female	39383	63021
	Summer 2012	1.5 Calf		1323	
	Fall 2012-Spring 2013 ACR	1.5 Juvenile		22115	
SK2	Fall 2011-Spring 2012 ACR	0.5 Calf	Female	50089	50089
	Fall 2012-Spring 2013 ACL			0	
ACD	Fall 2011-Spring 2012 ACR	Adult	Female	17806	31664
	Summer 2012			0	
	Fall 2012-Spring 2013 ACR			13858	
A1=TAN	Fall 2011-Spring 2012 ACR	0.5 Calf	Male	29901	51486
					(continued)

Beluga	Season/Year	Age	Sex	Focal Follow observation time (sec)	Total Observation Time (hr)
	Fall 2012-Spring 2013 ACR	1.5 Calf	Male	21585	
CAS	Fall 2007 – Spring 2008	Adult	Female	0	44347
	Fall 2011-Spring 2012 ACR	Adult	Female	30887	
	Fall 2012-Spring 2013 ACL			13460	
TAL	Fall 2011-Spring 2012 ACR	Adult	Female	15863	15863
G4	Summer 2012	0.5 Calf	Female	3273	27600
	FALL 2012-SPRING 2013 2013 ACR			24327	
LIL	Summer 2012	Adult	Female	0	14381
	Fall 2012-Spring 2013 ACR			14381	
L1	Summer 2012	0.5 Calf	Female	3624	24617
	Fall 2012-Spring 2013 ACR			20993	
S2	Summer 2012	0.5 Calf	Male	10052	34421
	Fall 2012-Spring 2013 ACR			24369	
X4	Summer 2012	0.5 Calf	Male	8442	31155
	Fall 2012-Spring 2013 ACR			22713	
AND	Fall 2007 – Spring 2008	Adult	Male	543	23416
	Fall 2012-Spring 2013 ACL			22873	
AUR	Fall 2012-Spring 2013 ACL	Adult	Female	18075	18075
KOD	Fall 2007 – 2008	Adult	Male	543	23781
	Fall 2012-Spring 2013 ACL			23238	
PEA	Fall 2012-Spring 2013 ACL	Adult	Female	16064	24469
	Fall 2013			8405	
PEE	Fall 2007 – Spring 2008	Adult	Female	0	25974
	Fall 2012-Spring 2013 ACL			13435	
	Fall 2013			12539	
SEC	Fall 2012-Spring 2013 ACL	Adult	Female	18101	18101
OSI	Fall 2007 – 2008	Adult	Female	0	15597
	Fall 2012			15597	
C2	Fall 2013	0.5 Calf	Female	30006	30006
					(continued)

Beluga	Season/Year	Age	Sex	Focal Follow observation time (sec)	Total Observation Time (hr)
K2	Fall 2013	0.5 Calf	Male	34866	34866
MEE	Fall 2013	Adult	Female	16146	16146
MI	Fall 2013	0.5 Calf	Female	34769	34769
PK1	Fall 2013	0.5 Calf	Female	35938	35938
CHR	Fall 2007 – Spring 2008	Adult	Female	3253	3253
TUK	Fall 2007 – Spring 2008	Adult	Male	0	0
TOF	Fall 2007 – Spring 2008	Adult	Male	0	0
MAP	Fall 2007 – Spring 2008	2 Calf	Female	0	0

Results

A two-way between subject ANOVA was conducted to compare the rate of contact between mother-calf pairs, adults, and calves. There was a significant interaction between initiator (adults and calves) and receiver partner based on age (mother-calf pairs, adults, and calves) on rate of contact, $F(2,214) = 168.60$, $p < .001$ $\eta^2_p = .612$. (Figure 1). Tukey HSD post hoc comparisons indicated that mother-calf pairs engaged in significantly more contact events with each other (calf initiated: M = .054 contacts/sec, SD = .021; adult initiated: (M = .004 contacts/sec, SD = .005) as compared to calf-initiated contacts with other calves (M =.001, SD = .002) or adults (M = .001 contacts/sec, SD = .001) and adult-initiated contacts with other adults (M = .002, SD = .009) or calves (M = .002 contacts/sec, SD = .006). Rates of contact initiated by calves to other calves or adults were similar to rates of contact initiated by adults to other adults or calves. Overall, calves (M = .012 contacts/sec, SD = .023) initiated significantly more contact than adults (M = .002 contacts/sec, SD = .006), $F(1,214) = 209.03$, $p < .001$ $\eta^2_p = .494$. In summary, mother-calf pairs received contact 27 times more often than calves with other belugas and 13.5 times more than adults with other belugas.

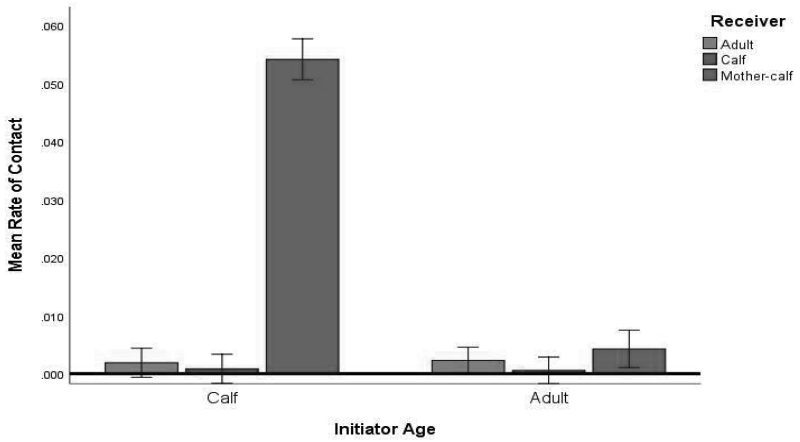

Figure 1. Interactions between initiator age and receiver age or mother-calf pairs. Error bars are 95% CI.

A 4-way factorial ANOVA was conducted to examine the effect of initiator age, initiator sex, receiver age, and receiver sex on rate of contact between adults and calves not including mother-calf pairs. The results indicated that the main effects for initiator and receiver sex were statistically significant. As expected, male belugas (M = .003, SD = .010) initiated contact more frequently than female belugas (M = 0.001, SD = .003), $F(1,160) = 10.62$, $p < .001$, $\eta^2_p = .062$ (Figure 2a). Female belugas received significantly more frequent contact than male belugas, $F(1,160) = 8.66$, $p = .004$ $\eta^2_p = .051$ (Figure 2b). Unexpectedly, adults (M = .002, SD = .008) initiated contact more frequently than calves (M = .001, SD = .002), $F(1,160) = 4.55$, $p = .034$, $\eta^2_p = .028$ (Figure 3). The 2-way interaction between initiator age and receiver age was statistically significant although weak in observed power (0.563), $F(1, 160) = 4.78$, $p = .030$, $\eta^2_p = .029$ (Figure 4). Unexpectedly, calf to calf contact (M = .001, SD = .002) was less frequent than adult to adult (M = .002, SD = .009). The 2-way interaction between initiator sex and initiator age was also statistically significant, as expected, $F(1, 160) = 9.28$, $p = .003$, $\eta^2_p = .055$. However, the results only

partially supported the expected outcome (Figure 5). Tukey HSD post hocs indicated that male adult-initiated contacts (M = .001, SD = .002) occurred significantly more than female adult-initiated contacts (M = .0003, SD = .0007). The female adult-initiated contacts were similar to the male calf- (M = .002, SD = .003) and to the female calf-initiated contacts (M = .004, SD = .001). Male calves initiated similar rates of contact as female calves.

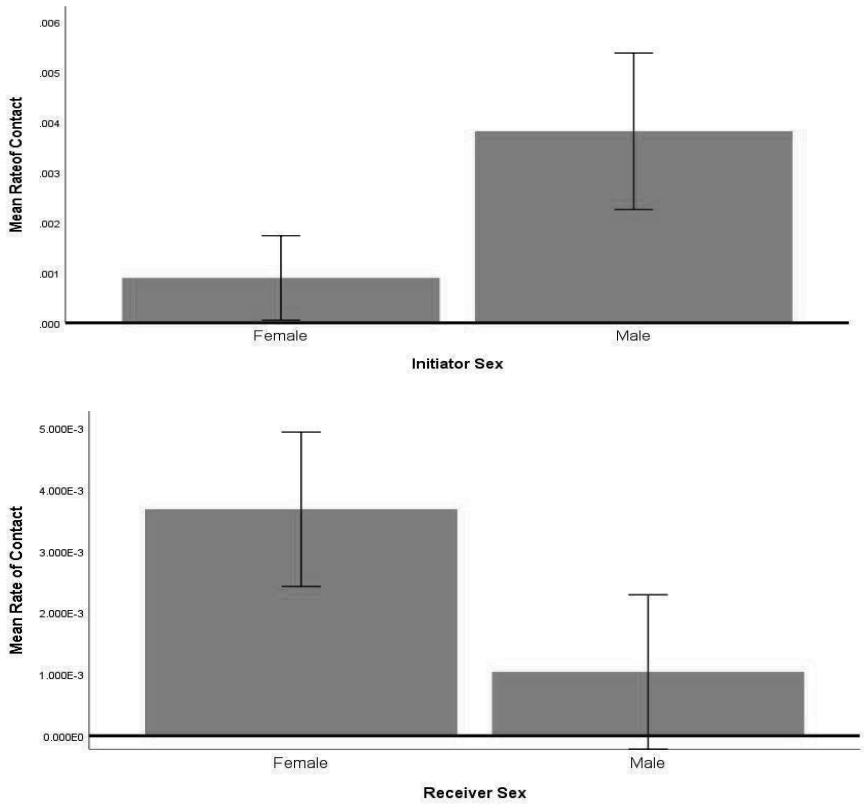

Figure 2. Mean rates of contact between initiator females and males are in the top panel. Mean rates of receiver females and males are in the bottom panel. Error bars are 95% CI.

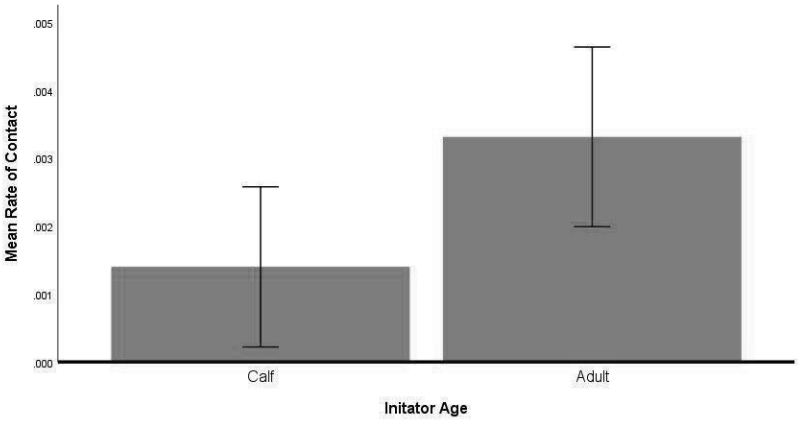

Figure 3. Mean rate of contact between initiator calves and adults. Error bars are 95% CI.

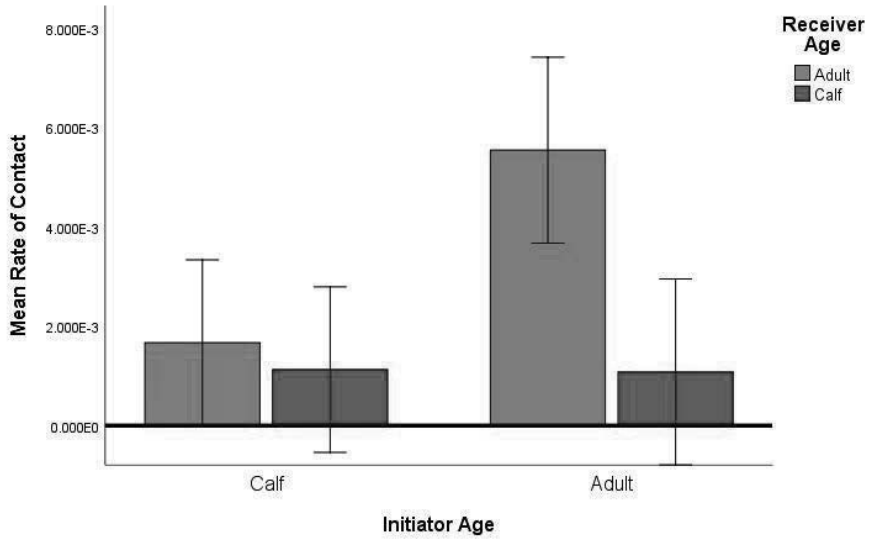

Figure 4. Mean rates of contact between initiator calves and adults with receiver calves and adults. Error bars are 95% CI.

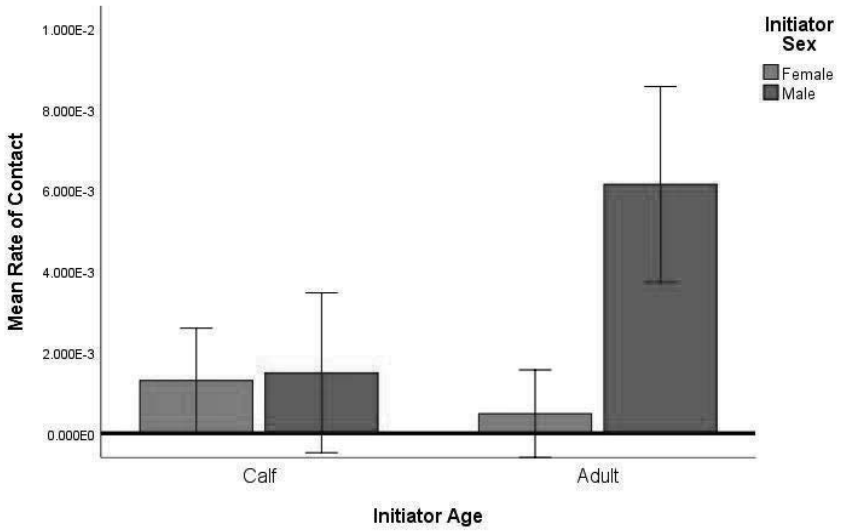

Figure 5. Mean rates of contact between initiator calves and adults with initiator females and males. Error bars are 95% CI.

Discussion

The current study examined the nature of contact between belugas housed at Marineland of Canada. Mother-calf pairs were expected to receive the greatest amount of touch than any other dyad. Mother-calf pairs did engage in majority of contact interactions with calves initiating the majority of the contacts as was found in a previous study on beluga calf contact (Hill, Dietrich, Jantea, et al., 2018). Mother-calf pairs initiated 1.62 contacts per minute making mother-calf pair the most to engage in contact. A closer examination of body part used for contact indicated that the amount of contact interaction between mother-calf pairs was produced most from nursing and infant position. This pattern is shared by all cetaceans studies conducted on mother-calf behaviors thus far, including small delphinids like bottlenose dolphins (Mann & Smuts, 1999; Reid, Mann, Weiner, & Hecker, 1995), large delphinds like killer whales (Asper,

Young, & Walsh, 1988; Guarino, Hill, & Sigman, 2017), and baleen whales like southern right whales (Eubalaena australis, Thomas & Taber, 1984).

Understanding that results of contact would be skewed toward mother-calf pairs, mother-calf pairs were excluded to examine the influence of sex and age on contact interactions with other belugas not involving mother-calf pairs. Past research has suggested that adult male beluga whales prefer to be in proximity with other males (adult and immature) rather than with females (Hill et al., 2018), and this same preference was expected to generalize to the contact between belugas. As expected, males initiated contact approximately four times as much as females-initiated contact. Females received contact more frequently in general.

Calves were expected to initiate contact more than adult belugas, although results showed otherwise and adult belugas initiated contact more often than calves. The outcome of adult belugas initiating contact more than calves was most likely because calves were less than three years old and generally remained close with mothers (Dudzinski, Gregg, Ribic, & Kuczaj, 2009). Calf-to-calf interactions were also expected to have more contact than other dyads like adult females or adult males based on previous research in which calf-calf contact was recorded (Hill, Alvarez, Dietrich, & Lacy, 2016; Hill, Dietrich, Jantea et al., 2018). Although mother-calf pairs were excluded, it was still expected for calves to initiate contact with other calves more than adults to initiate contact with other adults. However, adult-to-adult contact interaction occurred more frequently than calf-to-calf interactions. Adults initiated 0.12 contacts per minutes while calves initiated 0.06 contacts per minute. The calf contact was likely lower than previously reported contact rates due to the calves' ages in the current study. Most of the calves were relatively young and likely spent more time with their mothers rather than socializing with others with contact.

To better understand the unexpected finding that adults displayed more contact than calves, the interaction between sex and age of initiating was examined. The results of this analysis indicated that male adults preferred to contact other male adults more frequently than female adults contact other female adults. However, the rate of contact between female adults to other female adults was similar to the rate of contact male calves to male calves engaged in as well as female calves to female calves. This pattern of contact was different than reported by Hill, Dietrich, Jantea et al. (2018), most likely due to the different ages represented in each beluga population in the current study and the previous study. Calves were three and four years of age in the study conducted by Hill, Dietrich, Jantea et al.

The current study utilized an archived dataset, which limited the ability to assess interrater reliability. However, the data were collected by research assistants who were highly trained and completed reliability checks prior to data collection. When inconsistencies in the data occurred, the data were removed with no significant effects. The dataset was also biased toward mother-calf pairs with young calves, which may have influenced the patterns found in the current study. On average, calves spend between 60-80% of their time with their mothers, with solo swimming the next most frequent activity and social interactions occurring, but rarely (Hill, 2009; Hill & Campbell, 2014; Hill, Campbell, Dalton, & Osborn, 2013). Finally, some belugas that were not focal followed themselves were present in focal follow observations and contributed to interactions involving the focal followed belugas. These additional belugas may not have been represented accurately in the current sample.

Future research should examine the role of social composition on contact frequency. In the current study, the social groupings were controlled by the management of the facility, which created natural social groupings but limited opportunities for interactions with belugas of different ages and sexes. Overall,

the current study provided a more complete understanding of the nature of contact during social interactions between belugas in a captive setting. Comparing different social compositions separately in the future, could help evaluate the influence of different social interactions between belugas on contact, which may lead to a better understanding of contact with beluga populations.

References

Aoki, K., Sakai, M., Miller, P. J., Visser, F., & Sato, K. (2013). Body contact and synchronous diving in long-finned pilot whales. Behavioural Processes, 99, 12-20.

Asper, E. D., Young, W. G., & Walsh, M. T. (1988). Observations on the birth and development of a captive‐born Killer whale Orcinus orca. *International Zoo Yearbook*, *27*(1), 295-304.

Connor, R., Mann, J., & Watson‐Capps, J. (2006). A sex-specific affiliative contact behavior in indian ocean bottlenose dolphins, (*Tursiops sp*). *Ethology*, *112*(7), 631-638.

Dudzinski, K. M. (1998). Contact behavior and signal exchange in Atlantic spotted dolphins (*Stenella fimntalis*). *Aquatic Mammals*, *24*, 129-142.

Dudzinski, K. M., Danaher-Garcia, N., & Gregg, J. D. (2013). Pectoral fin contact between dolphin dyads at Zoo Duisburg, with comparison to other dolphin study populations. *Aquatic Mammals, 39*, 335–343. doi:10.1578/AM.39.4.2013.335

Dudzinski, K. M., Gregg, J., Melillo-Sweeting, K., Seay, B., Levengood, A., & Kuczaj, S. A. (2012). Tactile contact exchanges between dolphins: self-rubbing versus inter-individual contact in three species from three geographies. *International Journal of Comparative Psychology*, *25*(1).

Dudzinski, K. M., Gregg, J. D., Paulos, R. D., & Kuczaj II, S. A. (2010). A comparison of pectoral fin contact behaviour for three distinct dolphin populations. *Behavioural Processes*, *84*(2), 559-567.

Dudzinski, K. M., Gregg, J. D., Ribic, C. A., & Kuczaj, S. A. (2009). A comparison of pectoral fin contact between two different wild dolphin populations. *Behavioural Processes*, *80*(2), 182-190.

Giljov, A. N., Karenina, K. A., Ivkovich, T. V., & Malashichev, Y. B. (2016). Asymmetry ofpectoral flipper use in the orca Orcinus orca (Linnaeus, 1758) from the Avachinskii Bay (Eastern Kamchatka). *Russian Journal of Marine Biology, 42*, 196-198. doi:10.1134/S1063074016020048

Glabicky, N., DuBrava, A., & Noonan, M. (2010). Social–sexual behavior seasonality in captive beluga whales (*Delphinapterus leucas*). *Polar Biology*, *33*(8), 1145-1147.

Goley, P. D., & Straley, J. M. (1994). Attack on gray whales (*Eschrichtius robustus*) in Monterey Bay, California, by killer whales (*Orcinus orca*) previously identified in Glacier Bay, Alaska. *Canadian Journal of Zoology*, *72*(8), 1528-1530.

Guarino, S., Hill, H. M., & Sigman, J. (2017). Development of sociality and emergence of independence in a killer whale (*Orcinus orca*) calf from birth to 36 months. *Zoo Biology, 36(*1), 11-20.

Guttridge, T. L., Gruber, S. H., DiBattista, J. D., Feldheim, K. A., Croft, D. P., Krause, S., & Krause, J. (2011). Assortative interactions and leadership in a free-ranging population of juvenile lemon shark (*Negaprion brevirostris*). *Marine Ecology Progress Series*, *423*, 235-245.

Hill, H. M. (2009). The behavioral development of two beluga calves during the first year of life. *International Journal of Comparative Psychology*, *22*(4).

Hill, H. M., Alvarez, C. J., Dietrich, S., & Lacy, K. (2016). Preliminary findings in beluga (*Delphinapterus leucas*) tactile interactions. *Aquatic Mammals, 42*, 277-291. doi:10.1578/AM.42.3.2016.277

Hill, H. M., & Campbell, C. (2014). The frequency and nature of allocare by a group of belugas (*Delphinapterus leucas*) in human care. *International Journal of Comparative Psychology*, *27*(4).

Hill, H. M., Campbell, C., Dalton, L., & Osborn, S. (2013). The first year of behavioral development and maternal care of beluga (*Delphinapterus leucas*) calves in human care. *Zoo Biology*, *32*(5), 565-570.

Hill, H. M., De Oliveira Silva-Gruber, D. G., & Noonan, M. (2018). Sex-specific social affiliation in captive beluga whales *(Delphinapterus leucas*). *Aquatic Mammals,44*, 250–255. doi:10.1578/AM.44.3.2018.250

Hill, H., Dietrich, S., Guarino, S., Banda, M., & Lacy, K. (2018). Preliminary observations of an unusual mouth interaction between beluga calves (*Delphinapterus leucas*). *Zoo Biology*, 2018 1–8. doi:10.1002/zoo.21463

Hill, H., Dietrich, S., Jantea, R. F., Garza, S., & Lacy, K. (2018). The frequency of contact in beluga (*Delphinapterus leucas*) calf social interactions. *Aquatic Mammals, 44*, 62–75.doi:10.1578/AM.44.1.2018.62

Hill, H., Dietrich, S., Yeater, D., McKinnon, M., Miller, M., Aibel, S., & Dove, A. (2015). Developing an ethogram of sexual and socio-sexual behaviors of beluga whales in the care of humans. *Animal Behavior and Cognition*, *2*(2), 105-123

Hill, H. M., Guarino, S., Geraci, C., Sigman, J., & Noonan, M. (2017). Developmental changes in the resting strategies of killer whale mothers and their calves in managed care from birth to 36 months. *Behaviour, 154*(4), 435-466.

Johnson, C. M., & Moewe, K. (1999). Pectoral fin preference during contact in Commerson's dolphins (*Cephalorynchus commersoni*). *Aquatic Mammals,25*, 73-78.

Keller, B. A., Finger, J. S., Gruber, S. H., Abel, D. C., & Guttridge, T. L. (2017). The effects of familiarity on the social interactions of juvenile lemon sharks, *(Negaprion brevirostris*). *Journal of experimental marine biology and ecology*, *489*, 24-31.

Krasnova, V. V., Chernetsky, A. D., Zheludkova, A., & Bel'kovich, V. M. (2014). Parental behavior of the beluga whale (Delphinapterus leucas) in natural environment. *Biological and Bulletin 41,* 349–356.

Makecha, R., Fad, O., & Kuczaj, S. A. (2012). The role of touch in the social interactions of Asian elephants (*Elephas maximus*). *International Journal of Comparative Psychology*, *25*(1).

Mann, J., & Smuts, B. (1999). Behavioral development in wild bottlenose dolphin newborns (*Tursiops sp.). Behaviour*, *136*, 529-566.

Mazikowski, L., Hill, H. M., & Noonan, M. (2018). Young belugas (*Delphinapterus leucas*) exhibit sex-specific social affiliations. *Aquatic Mammals*, 44, 500–505. doi:10.1578/AM.44.5.2018.500

Nelson D. L. & Lien, J. (1994) Behavior patterns of two captive Atlantic white-sided dolphins, (*Lagenorhynchus acutus)*. *Aquatic Mammals 20*, 1-10

Paulos, R. D., Dudzinski, K. M., & Kuczaj, S. A. (2008). The role of touch in select social interactions of Atlantic spotted dolphin (*Stenella frontalis*) and Indo-Pacific bottlenose dolphin (*Tursiops aduncus*). *Journal of Ethology, 26*, 153-164. doi: 10.1007/s10164-007-0047-y

Reid, K., Mann, J., Weiner, J. R., & Hecker, N. (1995). Infant development in two aquarium bottlenose dolphins. *Zoo Biology*, *14*(2), 135-147.

Sakai, M., Hishii, T., Takeda, S., & Kohshima, S. (2006). Laterality of flipper rubbing behavior in wild bottlenose dolphins *(Tursiops aduncus): Caused by asymmetry of eye use? Behavioural Brain Research,170*, 204–2010.

Sakai, M., Hishii, T., Takeda, S., & Kohshima, S. (2006). Flipper rubbing behaviors in wild bottlenose dolphins *(Tursiops aduncus).Marine Mammal Science, 22*, 966-978.doi:10.1111/j.1748-7692.2006.00082.

Thomas, P. O., & Taber, S. M. (1984). Mother-infant interaction and behavioral development in southern right whales, (*Eubalaena australis*). *Behaviour*, 42-60.

Van Leeuwen, E. J., Mulenga, I. C., & Chidester, D. L. (2014). Early social deprivation negatively affects social skill acquisition in chimpanzees (*Pan troglodytes*). *Animal Cognition*, *17*(2), 407-414

Winship, K., Poelma, B., Kuczaj, S., & Eskelinen, H. (2017). Behavioral asymmetries of pectoral fin use during social interactions of bottlenose dolphins *(Tursiops truncatus). International Journal of Comparative Psychology,* 30, 1–13.